PHYSICS REPORTS (Section C of Physics Letters) 15, no. 4 (1975) 181–282. NORTH-HOLLAND PUBLISHING COMPANY

THE TWO-PHOTON PARTICLE PRODUCTION MECHANISM. PHYSICAL PROBLEMS. APPLICATIONS. EQUIVALENT PHOTON APPROXIMATION

V.M. BUDNEV, I.F. GINZBURG, G.V. MELEDIN and V.G. SERBO

USSR Academy of Science, Siberian Division, Institute for Mathematics, Novosibirsk, USSR

Received 25 April 1974
Revised version received 5 July 1974

Abstract:

This review deals with the physics of two-photon particle production and its applications. Two main problems are discussed first, what can one find out from the investigation of the two-photon production of hadrons and how, and second, how can the two-photon production of leptons be used?

The basic method for extracting information on the $\gamma\gamma \to$ h (hadrons) transition – the ee $\to$ eeh reaction – is discussed in detail. In particular, we discuss what information on the $\gamma\gamma \to$ h transition can be extracted from the related experiments and how it can be done. One examines which questions in hadrodynamics and photohadron interaction physics can be answered by such investigations. It is emphasized that their main peculiarity is the possibility of investigating dependence of the amplitude on the energy as well as on the masses of both colliding particles (photons).

The applications of two-photon lepton production in experimental high energy physics are discussed (the form factor investigation, the search for the real part of some forward scattering amplitudes, some auxiliary problems, etc.). Applications to the search for new (hypothetical) particles are considered.

A number of important differential distributions are given. Cross section estimations for different experimental set ups are obtained. A critical discussion of the equivalent photon approximation is given.

THE TWO-PHOTON PARTICLE PRODUCTION MECHANISM. PHYSICAL PROBLEMS. APPLICATIONS. EQUIVALENT PHOTON APPROXIMATION

V.M. BUDNEV, I.F. GINZBURG, G.V. MELEDIN and V.G. SERBO

USSR Academy of Science, Siberian Division, Institute for Mathematics, Novosibirsk, USSR

NORTH-HOLLAND PUBLISHING COMPANY – AMSTERDAM

Contents:

1. Introduction

Among the different electromagnetic processes of particle production much attention has been paid to two-photon production (fig. 1) in the last 3 years. In this process colliding particles 1 and 2 emit virtual photons. These photons produce some system f of particles. Thus two-photon particle production is connected directly with the process of light-light interaction – the condensation of light into matter ($\gamma\gamma \to f$).

The experimental study of two-photon production processes opens new ways towards the solutions of a number of physical problems. The present interest in the two-photon production is due, first of all, to the fact that a completely new region of investigations in high energy physics is thus

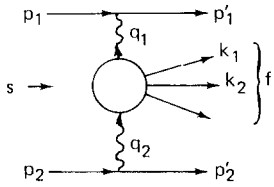

Fig. 1. The two-photon particle production.

discovered, i.e. the study of the reaction $\gamma\gamma \to$ h (hadrons). It is essential that in this case a study of the reaction dependence not only on the energy, but also on the "masses" of both colliding particles (photons) is possible. On the other hand, an experimental study of some two-photon production processes shows new ways to a solution of more traditional problems such as the investigation of π and K-meson form factors, a search for new particles etc. A comparatively large value of the cross section for two-photon e^+e^- pair production leads to a number of important effects in high energy processes (e.g. in cosmic ray physics). This allows to use this process as an instrument for solving some problems of experimental physics.

The above processes did not attract attention for a long time. In fact, they are of the fourth order in the electromagnetic interaction constant $\alpha = \frac{1}{137}$ and, at first glance, their cross sections seem to be very small. Nevertheless, in a number of cases these processes are dominant.

For example, for colliding $e^{\mp}e^-$ beams the two-photon channel of particle production should be already one of the main ones at not very high beam energies [1–3]. For illustration, the energy dependences of cross sections for different processes of particle production are plotted in fig. 2. These dependences have been calculated in QED (with no strong interaction effects taken into account). At low beam energy E the main channel for particle production is the annihilation one (fig. 3) that is a process of second order in α. Its cross section is determined by the virtual photon "mass", $\sigma \sim \alpha^2/q^2$. For example,

$$\sigma_{e^+e^- \to \mu^+\mu^-} = \frac{\pi\alpha^2}{3E^2} = \frac{8.7 \times 10^{-32}\,[\mathrm{cm}]^2}{s[\mathrm{GeV}]^2}. \tag{1.1}$$

The measured now total $e^+e^- \to$ h cross sections σ_h (fig. 12) have such values that $\sigma_h \leqslant 6\,\sigma_{e^+e^- \to \mu^+\mu^-}$ (at $2 < s < 25$ GeV^2).

In the two-photon production both photon "masses" can be simultaneously small and the cross section is not suppressed by photon propagators. Its value is determined by the $\gamma\gamma \to$ f cross section. An integration over each photon "mass" gives $\ln(E^2/m_e^2)$. An additional integration over each photon frequence also gives one or two $\ln E$, depending on the high energy behaviour of $\sigma_{\gamma\gamma \to f}$. For instance, at high energy the total cross section for two-photon production of lepton pair is given by the following formula [6]

$$\sigma_{e^\pm e^- \to e^\pm e^- l^+ l^-} = \frac{28\alpha^4}{27\pi m_l^2}\left(\ln\frac{s}{m_e^2}\right)^2 \ln\frac{s}{m_l^2}; \qquad l \equiv \mathrm{e}\ \text{or}\ \mu. \tag{1.2}$$

Therefore, the ee $\to$ ee$\mu^+\mu^-$-cross section at $\sqrt{s} = 4$ GeV is approximately 6 times as much (1.1) and is near to the $e^+e^- \to$ h cross section. In the same manner the total cross section for two-photon pro-

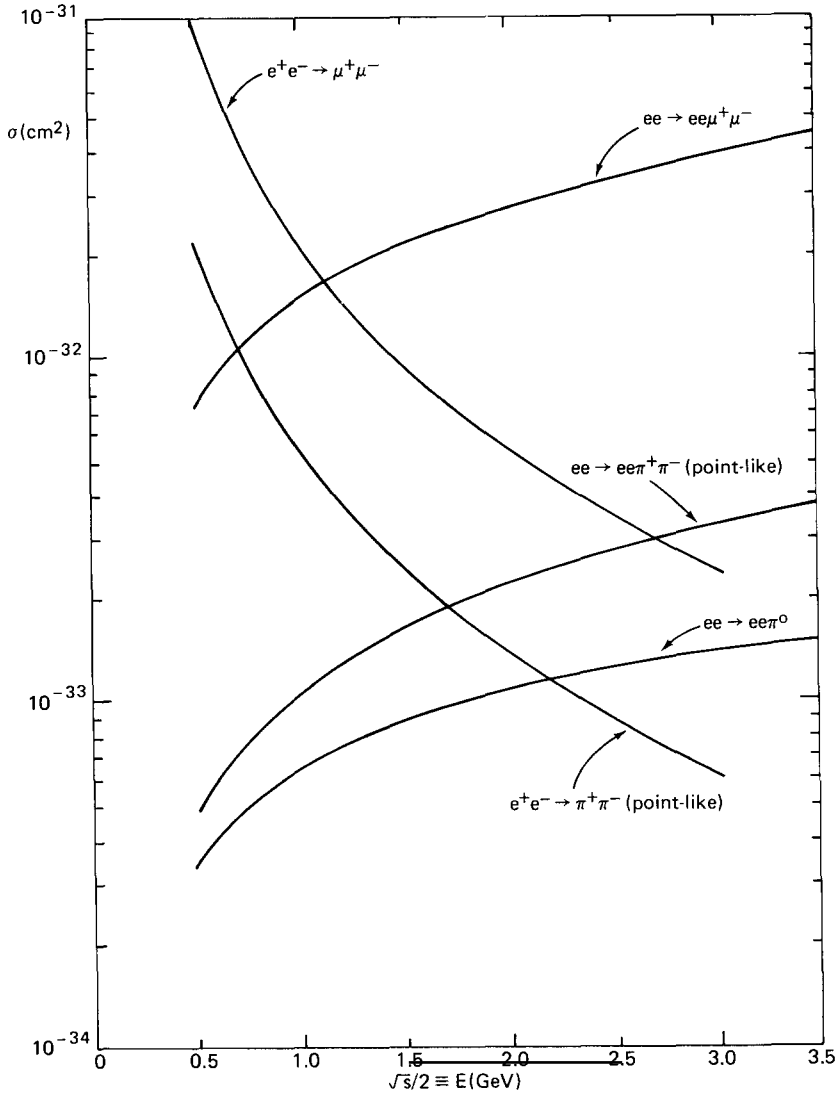

Fig. 2. Some production cross sections for colliding e^+e^--beams: $ee \to ee\ \pi^+\pi^-$, $ee \to ee\ \mu^+\mu^-$, $ee \to ee\ \pi^o$ (two-photon production) and $e^+e^- \to \pi^+\pi^-$, $e^+e^- \to \mu^+\mu^-$ (one-photon production). The $ee \to ee\ \pi^+\pi^-$ cross section (in neglecting a strong interaction) and the $ee \to ee\ \mu^+\mu^-$ cross section are the results of exact QED calculation [4], the $ee \to ee\ \pi^o$ cross section is the result of exact calculation with using the three-point vertex $\pi^o F^{\mu\nu}F^{\mu\nu}$ [5]. The $e^+e^- \to \mu^+\mu^-$ cross section is of the same order as the experimental $e^+e^- \to h$ cross section (cf. fig. 12).

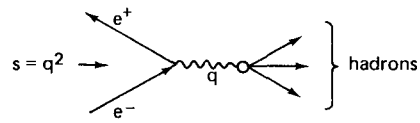

Fig. 3. The annihilation particle production ($q^2 = (p_1 + p_2)^2 = s = 4E^2$).

duction of hadrons is asymptotically (see [7])

$$\sigma_{e^{\pm}e^{-}\to e^{\pm}e^{-}h} = \frac{\alpha^4}{18\pi^2 m_\pi^2} \ln\frac{sm_\rho^2}{m_e^2 m_\pi^2} \ln\frac{sm_\rho^6}{m_e^6 m_\pi^2} \left(\ln\frac{s}{m_\pi^2}\right)^2 \tag{1.3}$$

$$\sigma_{\gamma\gamma\to h} \approx \frac{\alpha^2}{3m_\pi^2} \approx 0.3 \times 10^{-30}\ \text{cm}^2.$$

Therefore, in contrast to annihilation production, the two-photon production cross section increases logarithmically with energy.

The main possibilities for the experimental observation of such processes are due to progress of the accelerators with colliding $e^{\pm}e^{-}$ beams. The two-photon production has already been observed in experiments on such devices, firstly in Novosibirsk ($e^+e^- \to e^+e^-e^+e^-$) [9] and then in Frascati ($e^+e^- \to e^+e^-e^+e^-$ [10], $e^+e^- \to e^+e^-\mu^+\mu^-$ [11], $e^+e^- \to e^+e^-\pi^+\pi^-$ [201]). The feasibility of the experimental study of different processes with such devices is clear from a comparison of their cross sections (particularly shown in fig. 2) to the modern accelerator parameters (table 1). The counting rate (the number of observed events per time unit) for a process with cross section σ for a device with luminosity L is determined by the relation

$$\dot{N} = L\sigma. \tag{1.4}$$

For example, for a device with $L = 10^{31}\text{cm}^{-2}\text{sec}^{-1}$ at $\sqrt{s} = 2E = 7$ GeV the counting rate N for $ee \to ee\mu^+\mu^-$ and $ee \to ee\pi^+\pi^-$ observation should be 1600 and 140 events per hour, respectively. Thus, an investigation of the two-photon hadron production becomes quite a real problem.

Since 1970 many theoretical papers devoted to the two-photon production have been published. They are concerned with the four fundamental directions of investigation:

a) physics of the $\gamma\gamma \to h$ transition;

b) methods for extracting information on the $\gamma\gamma \to h$ transition from experimental data (e.g. from experiments with colliding beams) and the estimation of the related cross sections;

c) effects connected with the two-photon production of leptons;

d) search for new particles.

From our point of view, two problems are central here: what can be known while studying hadron production, and how lepton production can be used.

The following text of this section is, in essence, a brief description of the review structure. Each subsection corresponds to the section with the same title.

The structure of our review and the material selection correspond, to a considerable extent, to above classification of the problems. In particular, some results of exact quantum-electrodynamical calculations, e.g. the exact formulas for the electron energy spectrum in the $pp \to ppe^+e^-$ reaction [12] are not included. On the other hand, interesting questions such as photon decay into two photons in a nucleus Coulomb field [13], the role of the two-photon e^+e^- pair production at an early stage of evolution of the Universe and others are also not discussed here. However, "nobody can embrace the non-embraced" as Kozma Prutkoff said.*

*A review "Two-photon processes for particle production at high energies" by H. Terazawa [14] has been published recently. It seems useful to show what is the essential difference between this review and ref. [14]: 1) The treatment is intended for a general physicist audience. 2) The widest possible range of physical problems is discussed. 3) In the discussion of two-photon hadron production the main attention is paid to a problem (which is almost not treated in ref. [14]) namely, what information can be extracted from the related experiments and how. 4) In accordance with this, we give a more detailed discussion of various experimental feasibilities as well as a more detailed set of formulas. 5) There is a detailed discussion of the equivalent photon approximation with an indication of some specific mistakes and inaccuracies (some are encounted also in ref. [14]).

Table 1
The main parameters of e^+e^- and e^-e^- colliding beam accelerators (for details see ref. [8]).

Name and location	Type	Maximum total c.m.s. energy $\sqrt{s} = 2E$ GeV	The beginning of experiments	Luminosity L[cm^2 sec^{-1}]
VEP-1 (Novosibirsk)	e^-e^-	0.32	1965	10^{27} avear
(Stanford)	e^-e^-	1.1	1965	6×10^{27} peak
VEPP-2 (Novosibirsk)	e^+e^-	1.4	1967	3×10^{28} avear
ACO (Orsay)	e^+e^-	1.1	1968	6×10^{28} avear
ADONE (Frascati)	e^+e^-	3	1970	3×10^{29} avear
CEA Bypass (Cambridge, USA)	e^+e^-	5	1972	3×10^{28} peak
SPEAR (Stanford)	e^+e^-	4–9	1973	10^{31}
VEPP-2M (Novosibirsk)	e^+e^-	1.3	in preparation	10^{30}–10^{31}
VEPP-3 (Novosibirsk)	e^+e^-	6	in preparation	10^{31}
DORIS (Hamburg)	e^-e^- e^+e^-	6–9	in preparation	10^{32}
VEPP-4 (Novosibirsk)	e^+e^-	12–14	in preparation	

1.1. *Two-photon production of leptons and search for new particles*

An early interest in the two-photon processes has arisen after the discovery of the positron by Anderson (1932) and his experiments on fast particle interaction with matter. There appeared the necessity to find out the processes in which positrons are generated. Studying e^+e^- pair production in collision of fast charged particles, Landau and Lifshitz [6] have ascertained, that the two-photon channel of fig. 1 is dominant there. They have calculated the cross section of this process (1.2).

The two-photon channel is also of importance in present searches for new particles, whose main interaction with substance is through electromagnetic interaction (e.g. Dirac's monopoles, heavy leptons or W-bosons).

At present the processes of two-photon production of electrons, photons and muons are of special interest. Here one can hardly expect a discovery of new physical regularities. However,

these processes can give a large background contribution to the measurement of reactions of more physical interest. The importance of these processes is seen, e.g. from the following fact: in a proton collision with a nitrogen nucleus at $E_L = 10^{17}$ eV the cross section for the e^+e^- pair production reaches 350 mb, i.e. 25 mb per nucleon. This is comparable with the total pp-cross section ($\sigma_{pp} \approx 40$ mb) at energies of existing accelerators. The essential role of this process for charged particle deceleration in substance had already been discussed by Williams and Weizsäcker [15]. On the other hand, a comparatively large value of the cross section for two-photon e^+e^- pair production together with the possibility of its exact calculation within the QED frame allows one to use this process in a number of cases as an important instrument for investigation. Using this process one can, in principle, calibrate the luminosity of accelerators with colliding pp, $p\bar{p}$ and ep beams, study the pion and kaon form factors, measure the phase of the proton Compton-effect amplitude and high energy photon polarization, etc.

Finally, a relatively large value of the cross section for two-photon e^+e^- pair production allows one to observe radiative corrections to this process such as the two e^+e^- pair production, positronium production and production of the $e^+e^-\gamma$-system. All these problems are considered in section 2, where the main attention is given to the discussion of a qualitative part of their solution.

1.2. *Physics of hadron production by photons ($\gamma^* \to h$ and $\gamma\gamma \to h$)*

A wide range of interesting physical problems is connected with two-photon production. The problems associated with hadron annihilation production get into close contact with them. A study of hadron production by photons opens new, and often unique ways for solving a number of fundamental problems in strong interaction physics and also fundamental questions in QED.

The possibility of a direct investigation of the structure of strong interaction at short distances is a main advantage of processes of hadron production by virtual photons. Now progress in this direction is connected with the results of the SLAC-MIT-experiments on deep inelastic ep-scattering (i.e. on virtual photoabsorption by a proton).

A study of the $\gamma\gamma \to h$ reaction will permit an important further step in this direction because one may change here the "mass" of both projectile and "target". In particular, there exists such a domain of kinematical variables where the cross section for this reaction is due to short distance interaction only, while long distance effects are completely excluded. Only one-photon annihilation at high energy can be compared in this respect with the $\gamma\gamma \to h$ reaction.

In studying γp-scattering one has discovered that real, or almost real, photons interact with proton like hadrons. Simultaneously with an increase of photon "mass", i.e. with a transition to shorter distances, the photon-hadron interaction becomes pointlike. The study of $\gamma\gamma \to h$ transition together with other collisions involving hadrons such as pp and γp is of importance both for the test of the idea of a hadronlike photon and for understanding the character of changes in the collision process in the transition from structural hadrons (protons) to structureless ones (photons).

Moreover, experimental investigations of hadron production by photons permit testing some fundamental ideas of hadron physics such as current algebra and the partially conserved axial current (PCAC) hypothesis idea on the wide applicability of two-particle unitarity at low energies, etc. In these experiments one can also study a number of properties of the produced hadron systems, for example, the meson resonance parameters, S-wave scattering length in $\pi\pi$ scattering, etc.

This range of problems is discussed in section 3. Here we tried to show what new information can be obtained by the corresponding experiments for a solution of these problems. Particular reaction channels and related physical problems in two-photon and annihilation production are listed in tables 2 and 3, respectively.

1.3. *What can be investigated in the* $e^{\pm}e^{-} \to e^{\pm}e^{-}$ h *experiments and how*

Electron colliding beams (e^+e^- or e^-e^-) seem to be the main instrument for the study of the $\gamma\gamma \to$ h and $\gamma \to$ h processes. Preference for experiments on these accelerators is due to the fact that no difficult question associated with the genesis of the observed hadrons arises in this case. One can be sure that these hadrons are produced by one or two photons. In particular, while studying resonances no special hypotheses about the production mechanism which would be necessary for separating resonance from background are required as, e.g. in an analysis of πp collisions. The fact that there are no other hadrons but those produced by photons makes the interpretation of results easy.

When studying e^+e^- annihilation production of hadrons $e^+e^- \to \gamma^* \to$ h, a physically interesting quantity $M_{\gamma^* \to h}$ – the amplitude for the $\gamma^* \to$ h transition – is connected with the cross section by a simple relation $d\sigma_{e^+e^- \to h} \propto (\alpha/s)|M_{\gamma^* \to h}|^2$. On the contrary, for two-photon hadron production, the physically interesting amplitudes which correspond to $\gamma\gamma \to$ h transition are connected with the cross section of the observed process, ee $\to$ eeh, by rather complicated relations. They are of the type (1.8) given later.

Therefore, there arises in the first place, the question of what type of information on the $\gamma\gamma \to$ h process can be extracted from experimental data and how. On the other hand, and this for an estimate of the possibility of setting up for future experiments, the corresponding cross sections should be estimated taking into account experimental limitations. These very important problems are discussed in section 4. In order to provide estimations for the corresponding cross sections, we give simple and rather exact analytic formulas suitable for solving the numerous problems taking into account the various experimental limitations. (Let us note that in refs. [5, 16, 17] the tables and graphs have been calculated on a computer for some particular values of parameters. This clear and convenient representation of results suffers from the impossibility to be applied to other values of the parameters.)

1.4. *Kinematics and some differential distributions for the two-photon particle production*

In most cases interest in the two-photon production processes is stipulated by the possibility of the extraction of new information about still unknown amplitudes which they allow. Examples of such type are the study of amplitudes of the $\gamma\gamma \to$ h transition in the reaction ee $\to$ eeh and the pion form factor in the reaction $\pi Z \to \pi Z e^+e^-$, etc. For a solution of all these problems a special form for writing the differential distributions is useful, in which the contributions from vertices and transition amplitudes $\gamma\gamma \to$ f are factorized. Just such a description is contained in section 5 (which includes also much of the useful differential distributions).

Such writing allows one to apply the formulas obtained for a number of two-photon processes differing by the nature of the colliding particles or by the type of produced system f. These expressions are convenient not only for extracting information about the process $\gamma\gamma \to$ f but also for the calculation of the cross section when amplitudes for the process $\gamma\gamma \to$ f are known. Besides, such a

writing offers a basis for obtaining various approximations as well as estimation of their accuracy. Often these approximate formulas turn out to be formulas in an equivalent photon approximation.*

1.5. *Equivalent photon approximation*

An equivalent photon approximation (Weizsacker–Williams' method) is a convenient approximate method for calculating the cross sections of a large number of electromagnetic processes. As well known, it consists in describing the electromagnetic interaction of particles as the interaction of one of these particles with a flux of photons equivalent to the field of the second particle. This approximation is also widely applied to the description of two-photon particle production.

Section 6 contains a derivation of this approximation. Here we tried to give a description as complete as possible, which is similar in its style to a text-book. We have accompanied it by a criticism of the erroneous statement found in the literature. The necessity for such a description is due particularly to the fact that, in a number of papers using the equivalent photon approximation, one now meets erroneous or inaccurate statements together with superfluously lengthy formulas and calculations. We think that treating this approximation simply as a convenient method for the approximate calculation of some Feynman diagrams allows avoiding many such errors and inaccuracies. Such an approach has allowed to give a simple and accurate formulation of the approximation and also to estimate its accuracy and the range of its applicability to various physical problems.

1.6. *Some notations. Kinematics*

When using many-photon production processes the main research objects are the amplitudes for the $\gamma\gamma \to$ f process, both off mass shell and for almost real photons. Here the colliding photons with momenta q_1 and q_2 are space-like ($q_1^2 < 0$).** They may have both a transverse (T) polarization and a scalar (S) one. The produced system f is C-even and its mass is $W = \sqrt{(q_1 + q_2)^2}$. The observed ee $\to$ eef cross section is expressed in terms of the off mass shell $\gamma\gamma \to$ f cross sections for the corresponding photons σ_{TT}, σ_{TS}, σ_{ST}, σ_{SS}, e.g., σ_{TS} is the $\gamma\gamma \to$ f cross section for the collision of a transverse photon q_1 with a scalar one q_2. Besides, the result has four additional interfering terms τ_{TT}, τ_{TS}, τ^a_{TT} and τ^a_{TS}, e.g., the quantity τ_{TT} is the difference between cross sections for scattering transverse photons with the parallel ($\sigma_\parallel$) and orthogonal ($\sigma_\perp$) linear polarizations: $\tau_{TT} = \sigma_\parallel - \sigma_\perp$. Analogously, the quantity τ^a_{TT} is the difference between the cross sections for scattering of transverse photons in states with total helicity 0 (σ_0) and 2(σ_2)

$$\tau_{TT} = \sigma_\parallel - \sigma_\perp; \qquad \tau^a_{TT} = \sigma_0 - \sigma_2; \qquad \sigma_{TT} = \tfrac{1}{2}(\sigma_\parallel + \sigma_\perp) = \tfrac{1}{2}(\sigma_0 + \sigma_2). \tag{1.5}$$

The quantities τ_{TS} and τ^a_{TS} are connected with the interference terms of amplitudes for the transition $\gamma\gamma \to$ f where both transverse and scalar photons participate. All these quantities depend on W^2, q_1^2 and q_2^2 only.

The connection of these quantities with the absorptive part of the forward $\gamma\gamma$-scattering ampli-

*Cheng and Wu's [18] known statement on the nonapplicability of this approximation to a calculation of two-photon processes is merely a terminological misunderstanding connected with using a too limiting form of the approach (see in detail section 6.7).

**We use a standard practice of employing units where $\hbar = c = 1$. The metric is such that $p_1 p_2 = p_1^\mu p_2^\mu = p_1^0 p_2^0 - p_1 p_2$, so that a space like four-vector q have $q^2 < 0$. The fine structure constant $\alpha = e^2/4\pi \approx 1/137$. We use the spinor normalization $\bar{u}u = 2m$. The helicity of transverse (T) and scalar (S) photons equals ±1 and 0, respectively.

tude $W_{a'b',ab}$ and with the amplitudes M_{ab} for the $\gamma\gamma \to$ f transition is given in the helicity basis by the relations

$$W_{a'b',ab} = \tfrac{1}{2}\int M^*_{a'b'} M_{ab} (2\pi)^4 \delta(q_1 + q_2 - \textstyle\sum_i k_i) \mathrm{d}\Gamma; \tag{1.6}$$

$$\mathrm{d}\Gamma = \prod_i \frac{\mathrm{d}^3 k_i}{2\epsilon_i (2\pi)^3}; \qquad a, b, a', b' = \pm 1, 0.$$

$$2\sqrt{X}\,\sigma_{\mathrm{TT}} \equiv W_{\mathrm{TT}} = \tfrac{1}{2}(W_{++,++} + W_{+-,+-}); \qquad 2\sqrt{X}\,\sigma_{\mathrm{TS}} \equiv W_{\mathrm{TS}} = W_{+0,+0};$$

$$2\sqrt{X}\,\sigma_{\mathrm{ST}} \equiv W_{\mathrm{ST}} = W_{0+,0+}; \qquad 2\sqrt{X}\,\sigma_{\mathrm{SS}} \equiv W_{\mathrm{SS}} = W_{00,00};$$

$$2\sqrt{X}\,\tau_{\mathrm{TT}} \equiv W^{\tau}_{\mathrm{TT}} = W_{++,--}; \qquad 2\sqrt{X}\,\tau_{\mathrm{TS}} \equiv W^{\tau}_{\mathrm{TS}} = \tfrac{1}{2}(W_{++,00} + W_{0+,-0});$$

$$2\sqrt{X}\,\tau^{\mathrm{a}}_{\mathrm{TT}} \equiv W^{\mathrm{a}}_{\mathrm{TT}} = \tfrac{1}{2}(W_{++,++} - W_{+-,+-}); \qquad 2\sqrt{X}\,\tau^{\mathrm{a}}_{\mathrm{TS}} \equiv W^{\mathrm{a}}_{\mathrm{TS}} = \tfrac{1}{2}(W_{++,00} - W_{0+,-0}); \tag{1.7}$$

$$\sigma_{\mathrm{TS}}(W^2, q_1^2, q_2^2) = \sigma_{\mathrm{ST}}(W^2, q_2^2, q_1^2);$$

$$X = (q_1 q_2)^2 - q_1^2 q_2^2 = \tfrac{1}{4}[W^4 - 2W^2(q_1^2 + q_2^2) + (q_1^2 - q_2^2)^2].$$

The differential cross section for the two-photon production (fig. 1), summed over the final states of a system f, has the form (5.12) (one assumes that the initial and final particles are unpolarized)

$$\mathrm{d}\sigma = \frac{\alpha^2}{16\pi^4 q_1^2 q_2^2} \left[\frac{(q_1 q_2)^2 - q_1^2 q_2^2}{(p_1 p_2)^2 - m_1^2 m_2^2}\right]^{1/2} [4\rho_1^{++}\rho_2^{++}\sigma_{\mathrm{TT}} + 2|\rho_1^{+-}\rho_2^{+-}|\tau_{\mathrm{TT}}\cos 2\tilde{\varphi} + 2\rho_1^{++}\rho_2^{00}\sigma_{\mathrm{TS}}$$
$$+ 2\rho_1^{00}\rho_2^{++}\sigma_{\mathrm{ST}} + \rho_1^{00}\rho_2^{00}\sigma_{\mathrm{SS}} - 8|\rho_1^{+0}\rho_2^{+0}|\tau_{\mathrm{TS}}\cos\tilde{\varphi}] \frac{\mathrm{d}^3 p_1' \mathrm{d}^3 p_2'}{E_1 E_2}. \tag{1.8}$$

The quantities ρ_i^{ab} are expressed in a known way in terms of the momenta p_i and q_i and the particle form factors (cf. (5.13)). With the polarization of the colliding or scattered particles taken into account, the terms with $\tau^{\mathrm{a}}_{\mathrm{TT}}$ and $\tau^{\mathrm{a}}_{\mathrm{TS}}$ are added in (1.8).

Let us give some notations used below (see fig. 1):

p_i colliding particle momenta ($i = 1, 2$).

$s = (p_1 + p_2)^2$; $\sqrt{s} \equiv 2E$ the total c.m.s. energy.

p_i' scattered particle momenta.

$E_i \equiv p_i'^0$ scattered particle energies.

$m_i^2 = p_i^2 = p_i'^2$.

$q_i = p_i - p_i'$ virtual photon momenta, $q_i^2 < 0$.

k_j momentum of the jth produced particle.

$\epsilon_j \equiv k_j^0$ energy of the jth produced particle.

$k = \Sigma_j k_j = q_1 + q_2$ total momenta of produced system f.

$\epsilon = k^0 = \Sigma_j \epsilon_j$ total energy of produced system f.

$\boldsymbol{k}_{j\perp}$ transverse momentum of the jth produced particle in c.m.s. of colliding particles.

$\boldsymbol{k}_\perp = \Sigma_j \boldsymbol{k}_{j\perp} = \boldsymbol{q}_{1\perp} + q_{2\perp}$ total transverse momentum of system f.

$W = \sqrt{k^2}$ effective mass of system f.

$X = (q_1q_2)^2 - q_1^2q_2^2$. In the virtual photon c.m.s. X/W^2 is the squared three-momentum of a photon.

φ angle between the scattering planes of colliding particles in their c.m.s. (i.e. angle between $p'_{1\perp} = -q_{1\perp}$ and $p'_{2\perp} = -q_{2\perp}$).

$\tilde{\varphi}$ angle between the scattering planes of colliding particles in c.m.s. of virtual photons (see (A.4)).

ρ_i^{ab} elements of the photon density matrix for a photon produced by the ith particle; $a, b = \pm 1, 0$.

$\xi_i = |\rho_i^{+-}|/\rho_i^{++}$ polarization of the ith virtual photon.

Some words about terminology. We use for the processes under consideration (fig. 1) the term "two-photon particle production". In our opinion, this term describes more exactly the nature of the object, whose investigation is of great interest here. Though similar objects participate also in the two-photon annihilation production (fig. 30) and in the radiative one-photon annihilation processes $e^+e^- \to h\gamma$ (fig. 28), $e^+e^- \to h\mu^+\mu^-$ (fig. 29), we hope that using the above term for the processes of fig. 1 only causes no difficulty. It should also be noted that in some papers other terms are used for the fig. 1 process. They are based on the method for the observation of the process in the electron storage ring experiments; they are "symmetrical electroproduction", "double electroproduction" and "deep inelastic ee-scattering". (The last of these terms refers also to the analogy with the related process in deep inelastic ep-scattering.) These names are also not quite exact because they include both the process of fig. 1 and the bremsstrahlung production (fig. 27).

Acknowledgment

We are grateful to V.L. Chernyak, A.V. Efremov, A.T. Filippov, I.B. Khriplovich, V.V. Serebryakov, D.V. Shirkov, V.A. Sidorov and A.N. Skrinsky for useful discussions. We are also very grateful to M. Jacob for numerous remarks having led to an improvement of the review.

2. Two- photon production of leptons and search for new particles

2.1. *Production of* e^+e^- *and* $\mu^+\mu^-$*-pairs*

The two-photon production of lepton pairs has been the subject of a number of experimental investigations. The well-known investigations of the process $\gamma Z \to Z\, e^+e^-$ (Bethe–Heitler process) can be listed among them. Among the recent observations we mention only the electron storage ring ones ($e^+e^- \to e^+e^-e^+e^-$ [9, 10], $e^+e^- \to e^+e^-\mu^+\mu^-$ [11]).

Early calculations of the two-photon particle production were made already in 1934–1937. Naturally, at that time only e^+e^- pair production was discussed. In 1934 Landau and Lifshitz [6] calculated, in the main logarithmic approximation, the cross section for e^+e^--production in the collision of fast charged particles (with charges Z_1e, Z_2e and masses m_1, m_2)*

*Already ref. [6] contained many practically interesting differential distributions for the produced electrons in the region giving the main contribution to the cross section. Though they are written in the rest system of one of the colliding particles, a simple modification makes them suitable for colliding beams (see the end of section 5.6). Bhabha [19] has calculated such distributions in a wider energy range.

$$\sigma_{Z_1Z_2\to Z_1Z_2e^+e^-} = \frac{28\alpha^4}{27\pi m_e^2}(Z_1Z_2)^2 l^3 \approx 1.4\times 10^{-30}(Z_1Z_2)^2 l^3\ \mathrm{cm}^2;\quad l = \ln\frac{2(p_1p_2)}{m_1m_2}. \tag{2.1}$$

Already here we see the two characteristic features of this process:

A) Its cross section is slightly less than hadronic. In fact, $\alpha/m_e \approx 2/m_\pi$ and already at not too high energies $\alpha l^3 > 1$, i.e. $\sigma > (Z_1Z_2)^2\alpha/m_\pi^2$.

B) As the energy increases, the cross section increases rather rapidly $\propto l^3$.

At energies achieved now, the expression (2.1) provides only an order of magnitude for the cross section, since the first logarithmic correction proportional to l^2, has a large negative coefficient. Racah [12] has calculated this cross section for the collision of heavy particles up to terms of the order of s^{-1}

$$\sigma_{Z_1Z_2\to Z_1Z_2e^+e^-} = \frac{28\alpha^4}{27\pi m_e^2}[(l-2.12)^3 + 2.2(l-2.12) + 0.41]\,(Z_1Z_2)^2. \tag{2.2}$$

Appendix F contains more accurate expressions both for this cross section and for the cross sections for e^+e^- or $\mu^+\mu^-$ production in the collision of various particles. A review of modern calculations for lepton pair production can be found, for example, in [20].

We shall consider below only a number of physical effects associated with two-photon production of leptons.

1. *Energy losses of fast muons in matter.* When fast electron pass through matter they lose energy. This is mainly due to the bremsstrahlung. For muons such a mechanism is not alone. This is due to the fact that the bremsstrahlung cross section for muons ($\sim\alpha^3/m_\mu^2$) is essentially less than (2.1). However the mean energy loss in every act of two-photon e^+e^- production is m_μ/m_e times less than in bremsstrahlung. As a result both mechanisms play an approximately identical role in the energy losses of fast muons in matter (see e.g. [21, 22]).

2. *Contribution to the high-energy hadron cross sections.* The two-photon e^+e^- production gives an essential contribution (increasing with energy) to the interaction of cosmic ray protons with nuclei. Fig. 4 shows the dependence of the cross section for these processes on the laboratory energy calculated according to (2.2), (F. 1–3). In particular, for the energies investigated in cosmic rays

$$\sigma_{pZ\to pZe^+e^-} = \begin{cases} 0.7\,Z^2\mathrm{mb} & \text{at} \quad E_L = 10^4\ \mathrm{GeV} \\ 7\,Z^2\mathrm{mb} & \text{at} \quad E_L = 10^8\ \mathrm{GeV}. \end{cases} \tag{2.2a}$$

After the recalculation per proton for nitrogen nuclei ($Z = 7$) it gives $\sim 0.06\,\sigma_{pp}^{now}$ at $E_L = 10^4$ GeV and $\sim 0.6\,\sigma_{pp}^{now}$ at $E_L = 10^8$ GeV ($\sigma_{pp}^{now} = 40$ mb)*. As a result, this effect can be essential in the interpretation of the experimental results on total pp cross section.

Let us note also that at $E_L = 10^8$ GeV, the energy distribution of the pair produced has the form $d\epsilon/\epsilon$ in the range 1 MeV–10^5GeV. Hence, two-photon production of e^+e^- pairs can be essential in the evaluation of extended air showers with initial energy $E_L \geqslant 10^8$ GeV.

*In the calculation of the e^+e^- production off atoms (in air, in emulsion, etc.) one should take into account screening of nucleus by atomic electrons. This effect decreases slightly the cross section (2.2a).

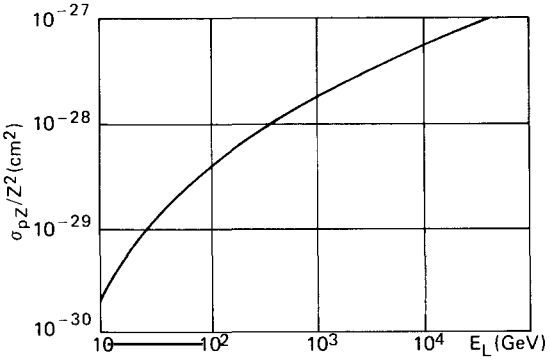

Fig. 4. The $pZ \to pZe^+e^-$ total cross section versus the proton lab-energy according to the Racah's formula (F.1–3).

3. Geshkenbein and Terentjev [23] have proposed to use the processes $\pi Z \to \pi Z e^+e^-$ and $KZ \to KZe^+e^-$ *for investigating the pion and kaon form factors* $F_\pi(q^2)$ and $F_K(q^2)$. In these processes at $(Z\alpha)^2/|q_2^2| > R^2$ (R is the nuclear radius) the two-photon contribution of fig. 5a dominates over the bremsstrahlung one of fig. 5b. This allows to determine the form factor of the π(K) from the known cross section $d\sigma/d\omega_1 dq_1^2 dq_2^2 dW^2$. The scattering on the nucleus is coherent and the nucleus form factor (the lower blob in fig. 5a) can be neglected at $|q_2^2| < R^{-2}$. For $Z\alpha \sim 1$ these both limitations coincide.

If lead is used as a target and $E_\pi \geqslant 60$ GeV, then for the determination of $F_\pi(q^2)$ in the region $-q^2 \sim 1$ GeV according to [23] the above conditions are fulfilled when the energy losses of the pions are not less than 30–50 GeV. One should measure here a cross section of the order of 10^{-34} cm^2 as well as a nuclear recoil momentum not exceeding 10–20 MeV.

4. *Possibility of calibration of accelerators with* pp, pp, ep-*colliding beams and with a gas target.* One of the main parameters of accelerators with colliding beams, the luminosity L, is defined by eq. (1.4). Let us consider a process with the following properties: 1) it is sufficiently exactly calculable; 2) it has not too small a cross section; 3) it is convenient for recording and is well separated from the other processes. Then its measurement allows one to determine the luminosity L in an independent way. In this case no detailed information on the distribution of the beams density in the interaction range, which is hard to measure, is required.

For the electron storage rings the problem of choosing such a (calibrating) process consists in

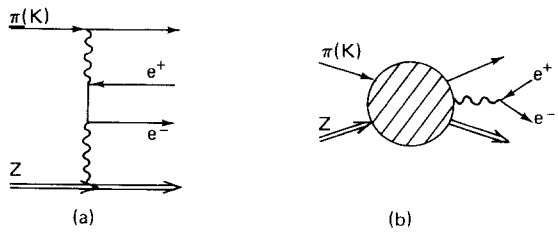

Fig. 5. The two-photon (a) and bremsstrahlung (b) e^+e^--pair production for π or K meson scattering on a nucleus.

selecting the most suitable process among many calculable ones in quantum electrodynamics. In accelerators with colliding pp-beams almost all the processes cannot be calculated without using models for strong interactions, i.e. no good accuracy is expected for the calculations. Such processes are not suitable for the calibration.

In our paper [24] it has been shown that with an accuracy not worse than 0.1%, the process $pp \to ppe^+e^-$ is completely calculable in the framework of quantum electrodynamics only provided that the energies $\epsilon_\pm$ and the escape angles of the $e^\pm$ in the c.m.s. of the protons are limited by the inequalities $\epsilon_\pm < 20\, m_e E/m_p$ and $|k_\perp|, W < 20\, m_e$. In this region the cross section is completely given by the diagram of fig. 1 together with the corresponding radiative corrections for it. Here the protons practically do not leave the beam and the behaviour of the proton form factors is not essential. The contribution of this region to the cross section is not less than 0.1 mb.

Due to these causes the process $pp \to ppe^+e^-$ was proposed to be used for determining the luminosity of accelerators with colliding pp-beams. Exactly, in the same manner, this process can be proposed for measuring the luminosity in experiments on a gas target in an ordinary accelerator. According to (2.2) its total cross section for 300 GeV protons equals 0.08 mb.

At present a project for a positron–electron–proton colliding beam system (PEP) with 15 GeV electrons and 72 GeV protons is being discussed [25]. At such energies e^+e^- production ($ep \to epe^+e^-$) turns out to be one of the main processes (its cross section is $\sigma \sim 3.4$ mb). Therefore, one may here propose the process $ep \to epe^+e^-$ for the calibration of such a device.

5. *Measurement of the forward amplitude phase for the processes* $\gamma p \to \gamma p$ *and* $\gamma p \to Vp$ (V is a vector meson). The process $\gamma p \to pe^+e^-$ is described by the two diagrams of fig. 6. The charge asymmetry in the differential distribution e^+ and e^- is only due to the interference of these two diagrams. The Bethe–Heitler amplitude of fig. 6a is completely known and real. Thus, the measurement of the charge asymmetry of the produced electrons gives the forward amplitude phase for the process $\gamma p \to \gamma p$. In the region of small effective masses of the e^+e^- pair the forward Compton amplitude phase has been found in such a way [26], and in the range of effective masses $\sim m_V$, the forward amplitude phase for the process $\gamma Z \to \rho Z$ has also been found [27]. It is clear that to study the forward amplitude phases of vector meson photoproduction one can also use the process $\gamma p \to p\mu^+\mu^-$.

6. *Measurement of high energy photon polarization.* The azimuthal asymmetry of the recoil electron in the reaction $\gamma e \to ee^+e^-$ is due to the photon polarization (cf. (5.48)). Therefore, one can use this reaction for finding the photon polarization (Boldishev, Peresun'ko [28], see also [29]). Already at the photon energy $\omega_L > 20\, m_e$ the cross section is described by the Bethe–Heitler diagram and has the form (5.48).

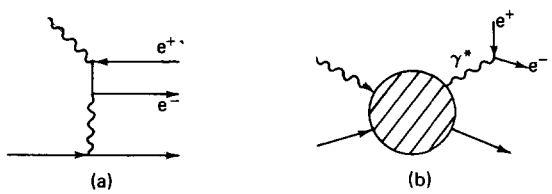

Fig. 6. The C-even (Bethe–Heitler's) (a) and C-odd (b) diagrams of the $\gamma p \to pe^+e^-$ process.

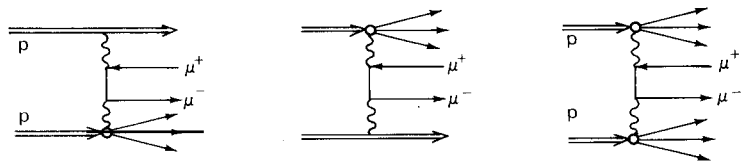

Fig. 7. The two-photon $\mu^+\mu^-$-pair production in pp-collision with the proton fragmentation (to the jet).

7. *The two-photon channel for production of the $\mu^+\mu^-$ pair with large invariant mass W in hadron collisions.* In the experiments of Christenson et al. at Brookhaven the production of massive $\mu^+\mu^-$ pairs ($W \sim 1-6$ GeV) in the collision of protons with an uranium target at the energy 20 to 30 GeV was studied. These experiments are expected to be continued at higher energies (at ISR and at NAL).

Such a process is of interest from two points of view. Firstly, in its investigation one hopes to find the W boson. Secondly, in the one-photon production of $\mu^+\mu^-$ pairs an additional possibility arises to investigate the hadron interaction at short distances. The two-photon channel of the $\mu^+\mu^-$ production can turn out a source of background in such investigations.

In these experiments [30] at not too high energies the one-photon channel dominates and the two-photon contribution is neglected. The one-photon $\mu^+\mu^-$ production can be imagined as the production of a hadron system with $J = 1$ and the further transition $\to \gamma^* \to \mu^+\mu^-$ (the simplest version of such a kind is a scheme of the vector dominance, see e.g. [31]). But then the cross section for the one-photon process should be constant like those for inclusive production of any hadron combinations with a fixed mass (except for the threshold growth at relatively small $s \sim W^2$).

The cross section for the two-photon process $pp \to pp\mu^+\mu^-$ grows rapidly with energy $d\sigma/dW^2 \propto \ln^3 s$. At $s = 2500$ GeV^2 and $W \gtrsim 2$ GeV it has the same order of magnitude [32–34] as the data [30] recalculated for pp-collisions (at $s \sim 50$ GeV^2), which are plotted in fig. 8.

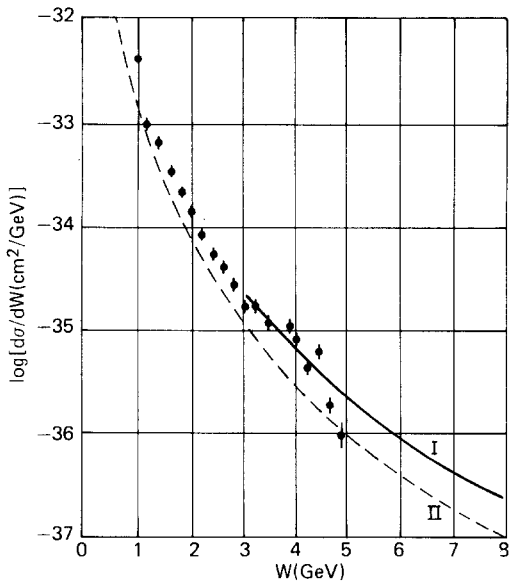

Fig. 8. The cross-section $d\sigma/dW$ for two-photon pair production in pp-collisions at $s = 2500$ GeV^2. Curve I is the cross section taking into account jets (fig. 1 and fig. 7) and curve II is the contribution of the fig. 1 diagram. The experimental points [30] at $s = 50$ GeV^2 are given for comparison.

Together with the usual two-photon mechanism (fig. 1) the process with jet formation (fig. 7) is of importance here. The contribution of the first of these mechanisms is easily calculated (for details see sect. 6.8) [34]. The total cross section, taking into account the jets shown in fig. 8, has been found by numerical integration in [35].

Thus, if the one-photon contribution does not grow with increasing s, then at $s \gtrsim 1000$ GeV^2 (in the experiments at the ISR) one needs to take into account the two-photon mechanism for $\mu^+\mu^-$ pair production.

2.2. *Some processes of high order in* α

With the increase of the energy of accelerators it now appears possible to measure processes of rather high order in α.

1. The cross section *for two* e^+e^- *pair production* is expressed in terms of the $\gamma\gamma \to e^+e^-e^+e^-$ cross section which is of special interest too.* The cross section of the process $\gamma\gamma \to e^+e^-e^+e^-$ is asymptotically constant and equals 6.45×10^{-30} cm^2 [36, 37]. The total cross section for the transition $ee \to eee^+e^-e^+e^-$ increases as $(\ln s)^4$ (Serbo [38], Lipatov and Frolov [37])

$$\sigma_{ee \to eee^+e^-e^+e^-} = \frac{\alpha^2}{6\pi^2}\,\sigma_{\gamma\gamma \to e^+e^-e^+e^-}\left(\ln\frac{s}{m_e^2}\right)^4. \tag{2.3}$$

At $\sqrt{s} = 7$ GeV this cross sections is $\sim 0.6 \times 10^{-31}$ cm^2 and of the same order as that for the process $ee \to ee\,\mu^+\mu^-$ (cf. fig. 2). This reaction can give a marked background in measuring the $\gamma\gamma \to h$ cross section. For hadron production on nuclei the role of the reaction $\gamma Z \to Ze^+e^-e^+e^-$ is discussed in refs. [39].

2. In the electron colliding beams the cross section *for positronium* Ps *production* in a free state appears to be not too small (Meledin, Serbo, Slivkov [41]) (we speak of the parapositronium, i.e. the e^+e^- bound state with a spin $S = 0$). Since, roughly speaking, it is necessary to hit in the momentum range $(\Delta p)^3 \sim (m_e\alpha)^3$, this cross section is α^3 times less than ones of the e^+e^- pair production:

$$\sigma_{ee \to eePs} = \frac{\alpha^7\zeta(3)}{3m_e^2}\left(\ln\frac{s}{m_e^2}\right)^3 = 6.6 \times 10^{-37}\left(\ln\frac{s}{m_e^2}\right)^3 \text{ cm}^2; \qquad \zeta(3) = 1.202. \tag{2.4}$$

We note that this cross section is of the same order as that for C-even hadron resonance production.

The produced positronium moves for some period of time in the accelerator magnetic field. This can lead to a new channel for its decay. In particular, the velocity of Ps may appear so high that already in the magnetic field of the accelerator it is converted into longer life orthopositronium or can decay into e^+ and e^-.

3. Fadin and Khose [42] have noted that in colliding ee-beams the two-photon production of the system $e^+e^-\gamma$ (fig. 9) is dominant *for producing the photons with the energy* $\omega > 1$ MeV *at large angles* $\theta_\gamma \sim 1$. This process is a radiative correction for the process of fig. 1, its cross section increases logarithmically with energy

*This interest is due to the fact that already at $W \sim 1$ GeV the $\gamma\gamma \to e^+e^-e^+e^-$ cross section is larger than the $\gamma\gamma \to e^+e^-$ cross section. The latter falls off with energy ($\sigma_{\gamma\gamma \to e^+e^-} \sim 4\pi\alpha^2/W^2$). Therefore, for cosmic photons with the energy $\omega_L \gtrsim 10^{22}$ eV just the process $\gamma\gamma \to e^+e^-e^+e^-$ determines a contribution into a mean free-path due to collisions with relic radiation [40].

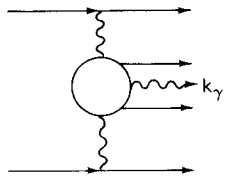

Fig. 9. The dominant diagram of $ee \to ee\,e^+e^-\gamma$ process. This process is a main source for low energy photons emitted at large angles.

$$d\sigma_{ee\to ee e^+e^-\gamma} = \frac{7\alpha^5}{3\pi^3\omega^4 \sin^4\theta_\gamma}\left(\ln\frac{s}{m_e^2}\right)^2\left(\ln\frac{\omega^2\sin^2\theta_\gamma}{m_e^2} - 0.06\right)\frac{d^3k_\gamma}{\omega}. \tag{2.5}$$

(The cross sections for both the usual and double bremsstrahlung radiations are negligibly small at $\omega^2 \lesssim \alpha^2 s$, since they fall as α^3/s and α^4/s.)

The above process can give a marked background for the physically very interesting reaction $e^+e^- \to \nu\bar{\nu}\gamma$.

2.3. *Production of new (hypothetical) particles*

Searches for certain new particles have been carried out already for a long time. We want to emphasize that, in some cases, the two-photon channel can give new ways for their search.

1. In 1931 Dirac pointed out that some particle which would have an *elementary magnetic charge g (monopole)* ($g = n/2e$; $n = 1, 2, 3, \ldots$) can exist. Result of searches for monopoles now consists in the fact that for $m_g \lesssim 5$ GeV the cross section for monopole production is less than 10^{-43} cm^2 (see, e.g. review [43]).

The magnitude of the cross section for monopole production in electromagnetic interactions should not be determined in terms of order α since the small constant e enters such a cross section only when multiplied by a large constant g. For that reason the two-photon channel is not here, at least, less significant than the one-photon channel. The importance of the two-photon channel was pointed out by Cabibbo and Ferrari [44].

Because of the strong interaction of monopoles with light their production should be suppressed as long as the relative momenta g and $\bar{g}$ are not very large, i.e. at $W \sim 2m_g$ (Ruderman and Zwanziger [45]). It is very probably that at $W > 2m_g$ a large part of the energy is realised in electromagnetic radiation [45].

In addition to this, one can expect, by analogy with hadrons, that the cross section for the two-photon production of n photons (through the virtual $g\bar{g}$ state) is already $\sigma_{\gamma\gamma\to n\gamma} \sim m_g^{-2}$ already at $W \lesssim 2m_g$. Therefore, if Dirac monopoles exist, then at $s > 16m_g^2$ nearly isotropic background of photons (and perhaps e^+e^-, $\mu^+\mu^-$) can be observed with the cross section $\gtrsim m_g^{-2}$ and specific effective mass $\sim 2m_g$ in pp-scattering. The characteristics of the spectrum of such photons is discussed by Newmeyer and Trefil [46].

2. One cannot exclude that besides $e^\pm$ and $\mu^\pm$ *other charged heavy leptons* $L^\pm$ can exist (see, e.g. review [47]).

As Gerstein, Landsberg and Folomeshkin have pointed out [48], if the spin of the $L^\pm$ is more

than $\frac{1}{2}$, then the cross section for the process $\gamma\gamma \to L^+L^-$ can grow with energy. The two-photon mechanism should then dominate already at not too high energies.

3. Topical problems deal with *the two-photon production of an intermediate vector boson* W *in* ee-*collisions* ($ee \to ee\,W^+W^-$). The cross sections expected here depend essentially on the W-boson gyromagnetic ratio g. In the Weinberg renormalizable theory of weak and electromagnetic interactions $g = 2$.

In this theory Sushkov, Flambaum and Khriplovich [49a] have investigated the W-boson production. At $W^2 \gg m_W^2$ the $\gamma\gamma \to W^+W^-$ cross section is asymptotically constant, $\sigma \approx 8\pi\alpha^2/m_W^2$. As a result, the total $ee \to eeW^+W^-$ cross section grows as $\ln^4 s$ (like for $ee \to eeh$). At $(s/m_e^2) \gg \ln(s/m_W^2)$:

$$\sigma_{ee \to eeW^+W^-} = \frac{4\alpha^4}{\pi m_W^2}\left(\ln\frac{s}{m_e^2}\right)^2\left[\left(\ln\frac{s}{m_W^2}\right)^2 - \tfrac{41}{6}\ln\frac{s}{m_W^2} + \tfrac{215}{12} - \tfrac{1}{3}\pi^2\right]. \tag{2.6}$$

This cross section begins to dominate over the annihilation ($e^+e^- \to W^+W^-$) production cross section at $\sqrt{s} \approx 14 m_W$.

If $g \neq 2$ (nonrenormalizable theory), then the $\gamma\gamma \to W^+W^-$ cross section increases as $\alpha^2 W^2/m_W^4$ when W^2 increases. As a result, at $g = 1$ one has $\sigma_{ee \to eeW^+W^-} \approx (5\alpha^4 s/54\pi m_W^4)\{\ln(s/m_e^2)\}^2$ [49b].

Let us note in conclusion that in the Weinberg theory $m_W \geqslant 37$ GeV/c^2. The present experimental lower bound of m_W is 10 GeV/c^2.

3. Physics of hadron production by photons

In this section we shall discuss the physical problems connected with hadron production by photons in the $\gamma\gamma \to h$ and $e^+e^- \to \gamma^* \to h$ reactions. We restrict ourselves to a discussion of problems, which are of great interest from our point of view.

We begin with a brief review of experimental results obtained for these reactions (sub-section 3.1). The following sub-sections are devoted to a description of a number of physical problems whose understanding can advance by means of experiments on hadron production by photons. We attempt to construct our description in order to show what new information for solving these problems can be obtained from such experiments*. A summary for a number of possible experiments is given in tables 2, 3.

The $\gamma^*\gamma^* \to h$ transition is studied in experiments on two-photon hadron production (fig. 1)

$$e^\pm e^- \to e^\pm e^- \gamma^*\gamma^* \to e^\pm e^- h. \tag{3.1}$$

Here the main object for an investigation is the $\gamma\gamma \to h$ amplitudes, both off mass shell and for almost real photons. In this reaction the colliding photons are space-like ($q_i^2 < 0$). The produced hadron system is C-even and its total mass is $W = \sqrt{(q_1 + q_2)^2}$.

The $\gamma^* \to h$ transition is studied in experiments on annihilation hadron production (fig. 3)

$$e^+e^- \to \gamma^* \to h. \tag{3.2}$$

Here the main object under study is the vertex $\gamma^* \to h$. The produced hadron system has the quan-

*A discussion of a number of such problems from a similar point of view is contained in refs. [7, 50, 34, 14].

tum number of a γ, i.e. it is C-odd, its total angular momentum $J = 1$, and its effective mass is $\sqrt{q^2} = \sqrt{s} = 2E$.

3.1. *Experimental results*

The main experimental data on hadron production by photons have been obtained from experiments on electron colliding beams ($e^{\pm}e^{-}$). The energies of the first generation of such accelerators were comparatively low. Therefore, in experiments which had been carried out up to now, mainly annihilation production (3.2) was studied.

First of all vector mesons with the photon quantum numbers ρ, ω, φ have been investigated. These experiments have provided an important extra information on their parameters (masses, widthes, decay modes and mixing angles), see e.g. [51].

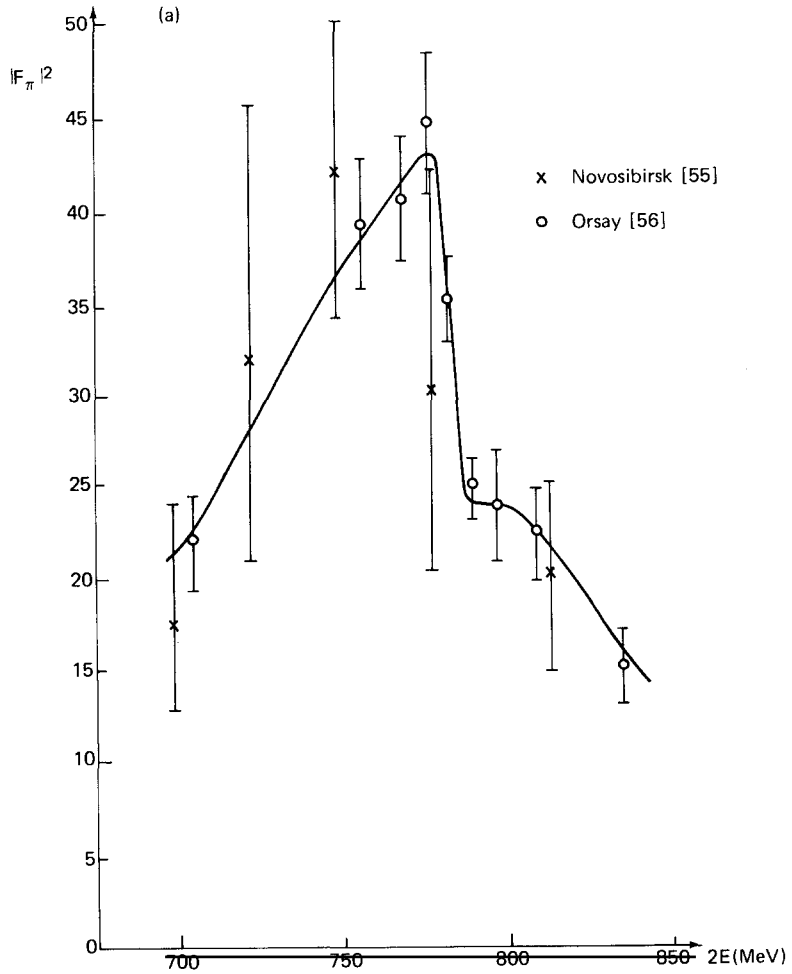

Fig. 10a

The broad peak in the energy dependence of the cross section for production of four charged pions in e^+e^--annihilation [52] has been interpreted [52–53] as evidence for the existence of a new vector meson resonance, ρ', of mass $m_{\rho'} \approx 1.6$ GeV and with $\Gamma_{\rho'} \approx 0.35$ GeV, having the same quantum numbers as the ρ-meson ($J^{PC} = 1^{--}$, $I^G = 1^+$). The same resonance was observed also in photoproduction off a proton [54].

In colliding e^+e^- beams, π, K and p form factors have been investigated firstly in the range of time-like photon momenta. To extract e.g. the pion form factor $F_\pi(s)$ one uses the relation:

$$\sigma_{e^+e^- \to \pi^+\pi^-} = \frac{\pi\alpha^2}{3s}\left(1 - \frac{4m_\pi^2}{s}\right)^{3/2} |F_\pi(s)|^2 . \tag{3.3}$$

The experimental values of $F_\pi(s)$ are plotted in fig. 10. The ρ-peak ($|F_\pi(s = m_\rho^2)|^2 \approx 42$) and the shoulder at $\sqrt{s} \approx 780$ MeV due to $\rho-\omega$ mixing are seen clearly. The experimental values of the

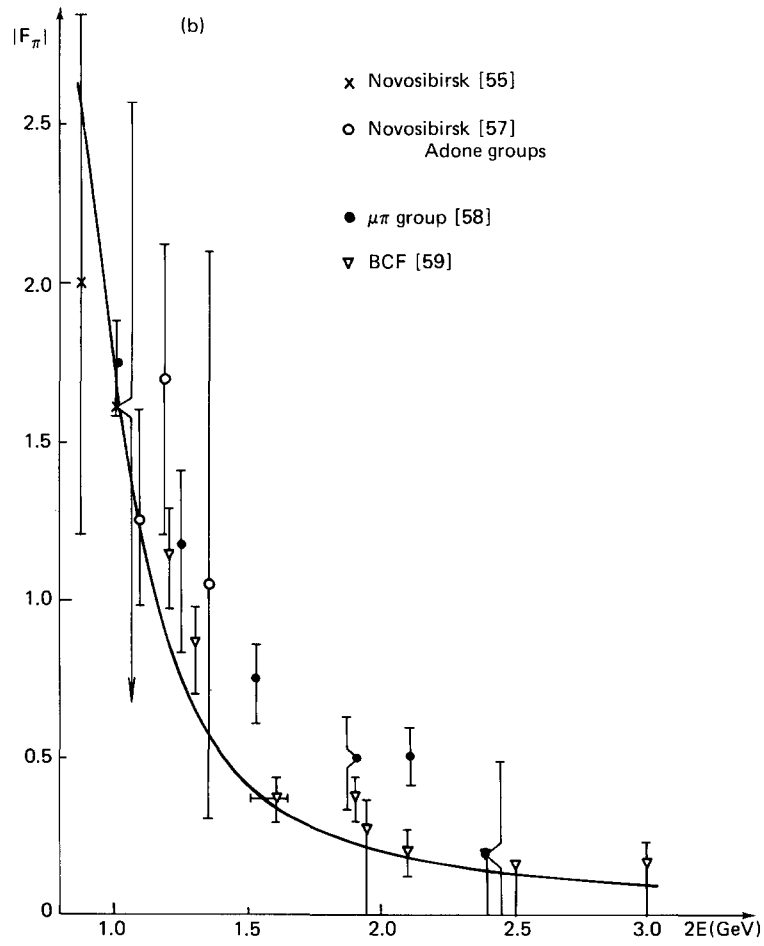

Fig. 10b.

Fig. 10a, b. The pion form factor versus $\sqrt{s} = 2E$. The solid line is the best fit on the ρ-range in which the Gounaris–Sakurai approximation [60] was used, and $\rho-\omega$-mixing was taken into account.

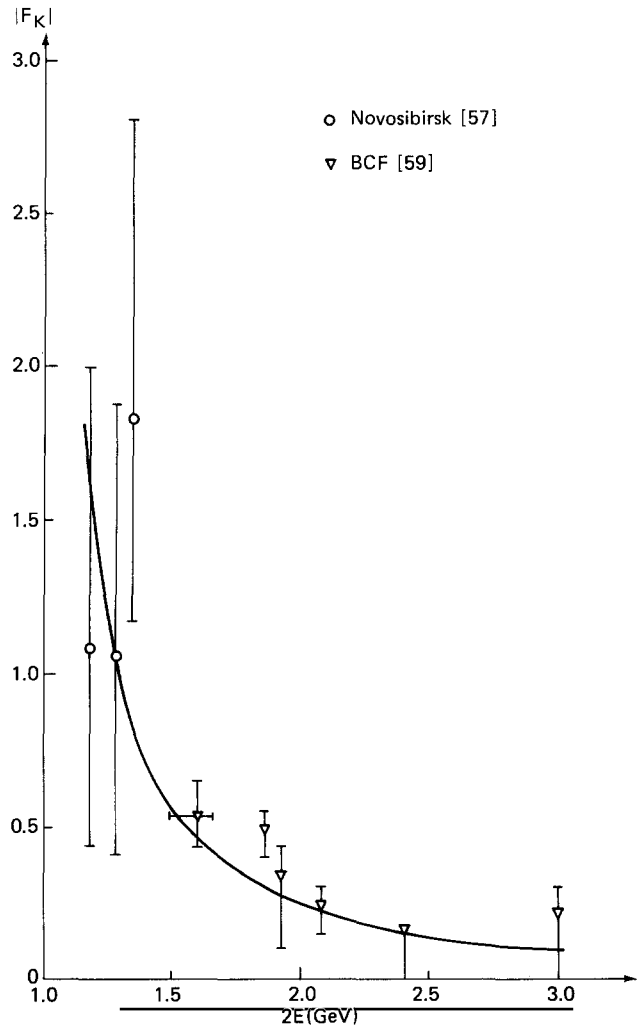

Fig. 11. The kaon form factor versus $\sqrt{s} = 2E$. The solid line is the theoretical expectation based on the ρ, ω, φ tails.

kaon form factor at $s > m_\varphi^2$ are plotted in fig. 11 ($|F_K(s = m_\varphi^2)| \approx 85$). The $e^+e^- \to \bar{p}p$ cross section is measured now at a unique value $\sqrt{s} = 2.1$ GeV only [61]. Assuming $|G_E| = |G_M|$ the authors of ref. [61] have found $|G_E| = |G_M| = 0.27 \pm 0.04$ at $q^2 = 4.4$ GeV^2. This value is considerably greater compared to what is obtained by a simple extrapolation from a space-like region (dipole approximation).

One of the most interesting trends in electron colliding beams is an investigation of the total cross section $\sigma_{e^+e^- \to h}$ of the annihilation hadron production. As it is seen from fig. 12 the cross section $\sigma_{e^+e^- \to h}$ is of the same order or even larger than that of the annihilation of point-like particles (1.1). Such a relatively large cross section is mainly due to multihadron ($n_h \geqslant 3$) production.

These various enumerated results are discussed in more detail in a number of reviews (see e.g. [51, 68, 70]).

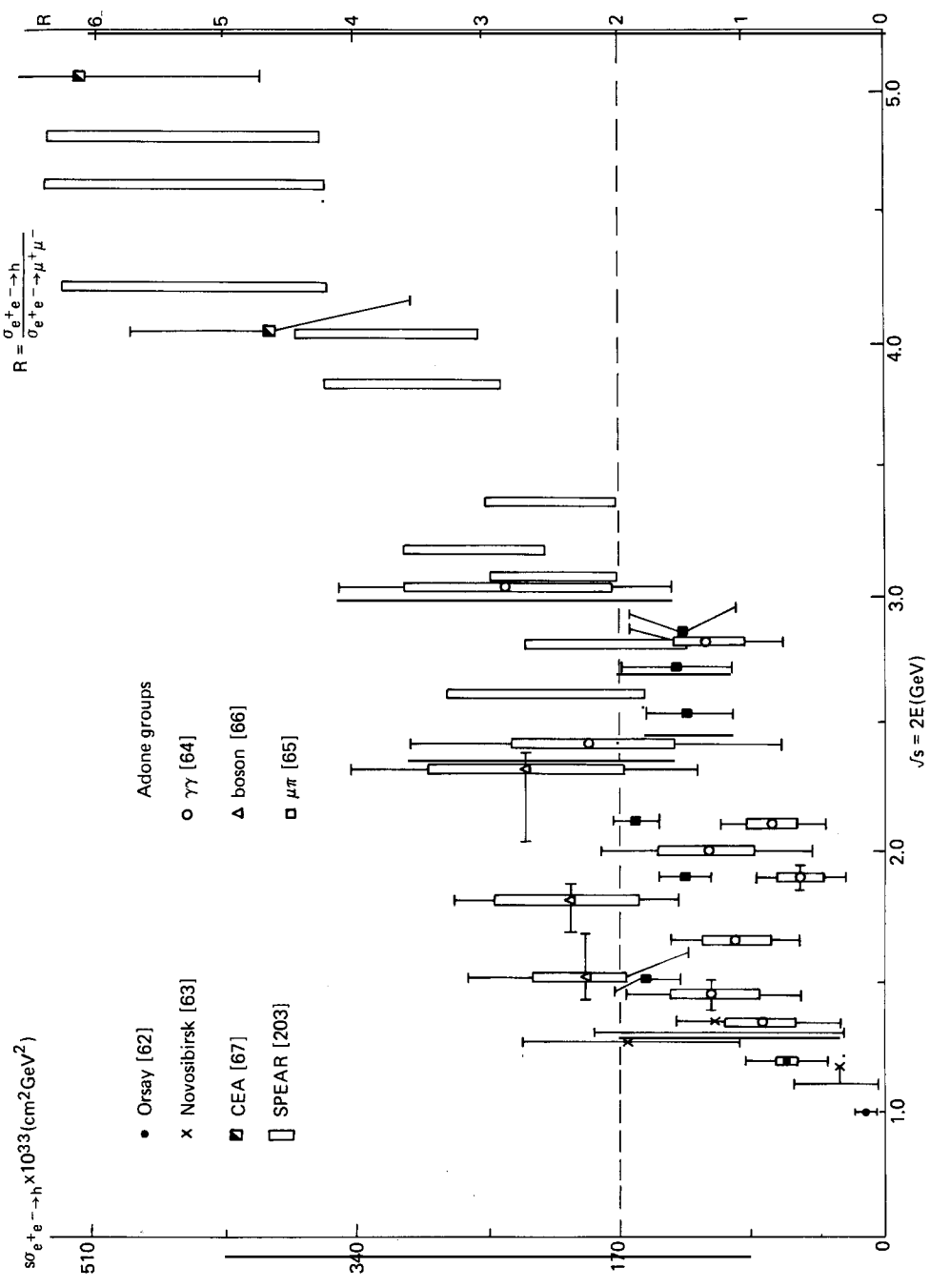

Fig. 12. The $s\sigma_{e^+e^-\to h}$ versus $\sqrt{s} = 2E$. For the every events the open box indicates the systematical error. The dotted line is the prediction for coloured quark model ($R = 2$).

At last, $\gamma\gamma \to$ h transition was investigated so far mainly in experiments on the photoproduction of π^0 and η off a nucleus only (Primakoff effect, cf. [69]). In such a way, the most precise value of the π^0 life-time has been obtained. In colliding e^+e^- beams the process $e^+e^- \to e^+e^-\pi^+\pi^-$, i.e. $\gamma\gamma \to \pi^+\pi^-$ transition, has been observed recently [201].

3.2. *The hadron-like properties of the photon. The reaction* $\gamma\gamma \to$ h *near the mass shell*

From the present point of view, the interaction of a real, or almost real, photon with a hadron is similar to that of hadrons with an other hadron. Such an approach allows one to use a number of ideas of hadron physics for a description of the $\gamma\gamma \to$ h reaction also. Experimental study allows one to test the correctness of this approach and as long as this is the case one then finds only some peculiarities for the $\gamma\gamma$-interaction when compared to other hadron collisions.

1. The idea of the hadronlikeness of the photon allows one to predict a number of specific features for the $\gamma\gamma \to$ h reaction. Some of these predictions seem reliable enough.

In the first place they are concerned with the *energy dependence of the total cross section* $\sigma_{\gamma\gamma}$ [7]. This dependence should be found to be as shown in fig. 13. A distinction between $\sigma_{\gamma\gamma}$ and hadron cross sections is primarily determined by the factor α^2. This gives the characteristic value of $\sigma_{\gamma\gamma} \sim \alpha^2/m_\pi^2$.

Near threshold $W^2 = 4m_\pi^2$ the cross section should be close to the $\gamma\gamma \to \pi^+\pi^-$ one calculated in QED (Born approximation) $\sigma_{\gamma\gamma\to\pi^+\pi^-\mathrm{QED}} \approx (\pi\alpha^2/2m_\pi^2)\sqrt{1 - 4m_\pi^2/W^2}$. As W^2 increases strong interaction becomes dominant. At first the main contribution to the cross section is due to the production of a $\pi\pi$-system. Further $\sigma_{\gamma\gamma}$ shows a set of overlapping peaks corresponding to the production of C-even boson resonances. With further increase of W^2, the cross section gradually approaches a constant $\sigma_{\gamma\gamma}(\infty) \sim \alpha^2/m_\pi^2$ just as in other hadron processes.

Inclusive reactions of the type $\gamma\gamma \to \pi +$ ... will be apparently the first to be studied experimentally. At intermediate energies a usual missing-mass method allows one to obtain from them a new information on resonances.

At high energies one can expect that the Feynman scaling law [71] will be fulfilled. And the question now is what energies for $\gamma\gamma$-collisions are large enough, i.e. beyond what energies the scaling law, if any, takes place. A peculiarity of $\gamma\gamma$-collisions can result in a noticeable distinction for the composition of secondaries at high energies as against that found in pure hadron collisions.

The distribution in *transverse momentum* also should have the same characteristics as in hadron collisions. It is natural to expect a mean transverse momentum $\langle p_\perp \rangle$ of the same order as that found in all hadron processes (300–500 MeV). But in the range $|p_\perp| < 300$–500 MeV the distribution in $p_\perp$ is probably flatter than in usual hadron collisions (see sect. 4.3). The $\gamma\gamma \to$ h reaction can turn out to be the most convenient one for a study of the $\langle p_\perp \rangle$ dependence, if any, on energy.

2. Let us describe now more specific predictions concerned with particular models of hadron interaction.

For a description of the cross section $\sigma_{\gamma\gamma}$ in analogy with hadron cross sections, one can apply a Regge analysis. If the Pomeranchuk singularity is dominant, then according to the factorization theorem [72]

$$\sigma_{\gamma\gamma}(W^2, q_1^2, q_2^2) = \sigma_{\gamma p}(W^2, q_1^2)\sigma_{\gamma p}(W^2, q_2^2)/\sigma_{pp}(W^2). \tag{3.4}$$

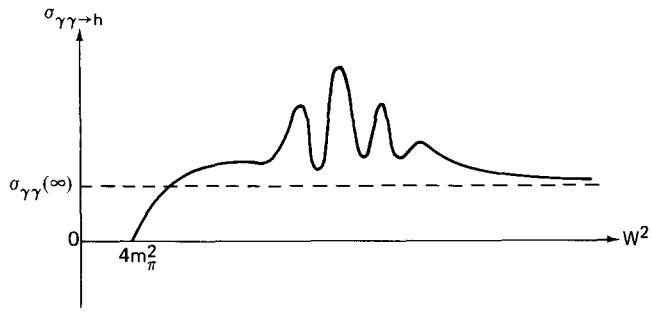

Fig. 13. The near-mass-shell $\gamma\gamma \to$ h cross section versus squared center-of-mass energy W^2 in assumption of hadronlikeness of photon.

From there we have the asymptotic behaviour of the total cross section on mass shell [7]

$$\sigma_{\gamma\gamma}(\infty, 0, 0) = \sigma_{\gamma\gamma}(\infty) = (0.11)^2/38 \text{ mb} \approx 3 \times 10^{-31} \text{ cm}^2 \approx \alpha^2/3\, m_\pi^2. \tag{3.5}$$

One can expect that the total contribution of all resonances is large. If this is so then, due to duality at finite values of $W^2 \gtrsim 5$ GeV^2, the value $\sigma_{\gamma\gamma}(W^2)$ should markedly exceed $\sigma_{\gamma\gamma}(\infty)$. This difference should decrease as $a\, W^{-1}$ (contributions of P′ and A_2 trajectories). Taking account of the f-resonance in direct channel only, we have $a \gtrsim \sigma_{\gamma\gamma}(\infty)$ GeV.

At $W^2 \gg 1$ GeV^2 a large contribution to the cross section should result *from diffractive photon excitation*, i.e. processes $\gamma\gamma \to V_1V_2$ ($V_{1,2} = \rho, \varphi, \omega, \ldots$) [2]. The total cross section for these processes can be calculated either by means of the factorization theorem (with known cross sections $\gamma p \to Vp$ and $pp \to pp$) or by means of a vector dominance model. Both these methods give close results. For instance [73, 74, 5]

$$\sigma_{\gamma\gamma\to\rho^0\rho^0} \approx (2-5) \times 10^{-32} \text{ cm}^2 \sim 0.1\, \sigma_{\gamma\gamma}(\infty). \tag{3.6}$$

Comparing (3.5) and (3.6), one sees that the fraction of diffractive photon excitation in the total $\gamma\gamma$ cross section is to be of the same order as the fraction of elastic hadron scattering in the total cross section.

An important characteristic of these processes is the slope parameter of a diffractive peak b. Using the usual approximation $d\sigma/dt = Ae^{bt}$ for a contribution of the Pomeranchuk singularity P and with the aid of the factorization theorem, we obtain

$$b_{\gamma\gamma\to V_1V_2} = b_{\gamma p\to V_1 p} + b_{\gamma p\to V_2 p} - b_{pp\to pp}. \tag{3.7}$$

There is here the interesting possibility of an anomalous small value of $b_{\gamma\gamma\to V_1V_2}$, i.e. the weak t-dependence of the vertex γVp [74]. So, choosing experimental values for the Pomeranchon (i.e. neglecting contributions except p) $b_{\gamma p\to\varphi p} = 5.4 \pm 0.3$ [75] and $b_{pp\to pp} = 10$ GeV^{-2} we obtain $b_{\gamma\gamma\to\varphi\varphi} = 0.8 \pm 0.3$ GeV^{-2}.

In the resonance range the $\gamma\gamma \to$ h cross section may be estimated with the help of *finite energy sum rules*. The two-photon widths of ϵ, f, A_2 were obtained in refs. [76] just in the same manner.

One can study also *the quantity* $\tau_{\gamma\gamma}$. There is a difference between the cross sections for scattering of a transverse photon with parallel linear polarization ($\sigma_\parallel$) and orthogonal linear polarization ($\sigma_\perp$), $\tau_{\gamma\gamma} = \sigma_\parallel - \sigma_\perp$ (1.5). At small W the value of $\tau_{\gamma\gamma}$ is of the same order as of $\sigma_{\gamma\gamma}$. So, in the production of a hadron system with $J^P = 0^\pm$ (e.g. some resonances)

$$\tau_{\gamma\gamma} = \pm 2\sigma_{\gamma\gamma}. \tag{3.8}$$

In ref. [77] a Regge analysis of all $\gamma\gamma$-forward amplitudes has been carried out and this analysis has shown that singularities with the negative P-parity (and positive signature) only contribute to $\tau_{\gamma\gamma}$. For such Regge trajectories $\alpha(0) < 0$. The leading singularity of such type corresponds to the exchange by three Pomeranchons. Their contribution decreases as $(\ln W^2)^{-2}$ only. If such relatively large contribution to $\tau_{\gamma\gamma}$ will not be observed, then this will come to large doubts about the validity of models with the Regge cuts. If in $\tau_{\gamma\gamma}$ there are no fixed singularities with $\mathrm{Re}\, j \geqslant 0$ and such Regge cuts are unessential, then in this case the superconvergent sum rule is applied [74]

$$\int \tau_{\gamma\gamma}(W^2)\mathrm{d}W^2 = 0. \tag{3.9}$$

3. The near-mass shell region. The whole preceding description was applied to processes in which participate both real photons and photons with a small virtuality ($|q_i^2| \lesssim m_\rho^2$). (An evident modification for virtual photons is the inclusion of processes with the participation of scalar photons.)

In particular, the energy dependence of the cross sections σ_{ab} should be qualitatively the same as in fig. 13. But with increasing $|q^2|$ the typical value for these cross sections changes. By analogy with deep inelastic ep scattering one can expect with sufficient confidence here that with the increasing of $-q_i^2$ the cross section σ_{TT} decreases while σ_{TS}, σ_{ST}, σ_{SS} first increase but later decrease. A specific scale for these changes is, apparently, $\sim m_\rho^2$. Such a behaviour seems also natural from the point of view of the vector dominance model.

In the asymptotic region ($W^2 \to \infty$) the relative value of the cross sections of scalar photon scattering can be found by using the data on γ^*p-scattering [78] with the help of the factorization theorem (3.4). This theorem may be applied separately to both the scalar and transverse photons. This results in [7]

$$\frac{\sigma_{SS}(\gamma^*\gamma^* \to \mathrm{h})}{\sigma_{TS}(\gamma^*\gamma^* \to \mathrm{h})} = \frac{\sigma_{ST}(\gamma^*\gamma^* \to \mathrm{h})}{\sigma_{TT}(\gamma^*\gamma^* \to \mathrm{h})} = \frac{\sigma_S(\gamma^*\mathrm{p} \to \mathrm{h})}{\sigma_T(\gamma^*\mathrm{p} \to \mathrm{h})} = R \approx 0.18. \tag{3.10}$$

According to the SLAC data [79] the relative Pomeranchukon contribution to the γp-cross section decreases with decreasing $-s/q^2$. Hence the estimation (3.10) becomes less accurate with decreasing $-W^2/q_i^2$.

It is also very interesting to study the q_i^2 dependence for such quantities as the multiplicity, the transverse momentum distribution, the composition of secondaries, the relative role of diffraction, the character of inclusive spectra etc. The SLAC-MIT experiments show us that for γp scattering the above features change qualitatively already at not too high $|q_i^2| \sim 1$ GeV^2 (see e.g. [79]). This fact is interpreted as a transition to a domain where the photon interacts as a point particle probing the internal structure of the hadron. Does a similar phenomena take place in $\gamma\gamma$ scattering? And if it is the case then, for what q_i^2 such a change in the q^2 behaviour takes place?

Finally, at still higher values of $|q_i^2|$ we reach a region, where the short distance interaction becomes dominant.

3.3. *The short distance interaction*

The nature of strong interactions at short distances is a fundamental problem of elementary particle physics. The conventional point of view is such that at short distances the hadron mass spectrum details are negligible and the strong interaction has a high symmetry and universality.

The highly virtual photons can probe in detail the internal particle structure. Then a study of hadron production in processes with highly virtual photons is one of the few direct ways of studying strong interaction at short distances.

1. Let us describe briefly some basic theoretical approaches which are used in the investigation of phenomena at short distances.

One of the most transparent models is the *parton* one [80–82]. In this model hadron consists of pointlike constituents – partons, and the short distance parton–parton interaction is negligibly small. Then the interaction of highly virtual photons with hadron is reduced to noncoherent interactions with pointlike partons.

In other words, the hadron is supposed to consist of partons in much the same way as nuclei consist of nucleons. But in contrast to nucleons the free partons are not identified up to now.

Another widely discussed possibility is the hypothesis that short-distance strong interaction is *scale invariant* [83–85]. This means that in case of a coordinate dilatation (scale transformation) the vacuum expectation of a product of any number of field operators, which are taken at near-by points, changes by a numerical factor only. In a renormalizable theory the scale symmetry leads to the conformal one additionally (see cf. [84]). Such a model also corresponds to the description of hadron as composite particle. Here, however, the hadron constituents strongly interact with each other by such a way that the dimensional parameters of the theory (masses and coupling constants) are not essential.

Still another method of approach is in terms of *light cone commutators.* The measurable cross sections with high virtual photons are expressed via the commutators of the electromagnetic currents $J^\mu(x)$ (cf. (3.11), (3.16)), e.g. the main subject investigated in the experiments on deep inelastic ep scattering, fig. 14 (the absorptive part of the forward Compton amplitude) is

$$\tfrac{1}{2}\int d^4x \langle p|[J^\mu(x), J^\nu(0)]|p\rangle \cdot \exp\{iqx\}$$

$$= 8\pi^2 \alpha m_p \left\{-\left(g^{\mu\nu} - \frac{q^\mu q^\nu}{q^2}\right) W_1(qP, q^2) + \left(P^\mu - q^\mu \frac{qP}{q^2}\right)\left(P^\nu - q^\nu \frac{qP}{q^2}\right)\frac{W_2(qP, q^2)}{m_p^2}\right\} . \qquad (3.11)$$

In a very natural assumption one can show that as $|q^2| \to \infty$ and a fixed $\omega = 2Pq/(-q^2)$ the main contribution to this integral is due to the short distance region $x^2 \sim 1/q^2$. Therefore, phenomena at $|q^2| \to \infty$ are determined by the character of the light cone current commutator singularity [86].

The approaches based on *quantum field theory* models are often used as well. Here theories of the φ^3-type [87] and the ladder γ^5-model with transverse momentum cut-off [80] correspond to the parton model. A similar picture appears also in the non-Abelian gauge theories of strong interactions which have the property of becoming a free-field theory at short distances (asymptotic freedom) [97]. The short distance interaction is scale invariant in the renormalizable theories if

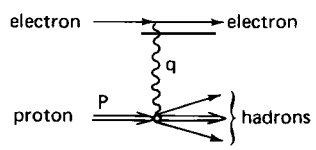

Fig. 14. The deep inelastic ep-scattering.

the dimensionless coupling constant renormalization is finite (see e.g. [88]). In particular, the short distance scale invariance take place in theories of the type (see in detail [89]):

$$L_{\text{int}} = g_{\text{S}}\bar{\psi}\psi\varphi_{\text{S}} + g_{\text{PS}}\bar{\psi}\gamma^5\psi\varphi_{\text{PS}} + h\varphi^c . \tag{3.12}$$

2. Most models and approaches considered were called into being by the SLAC-MIT experimental results on deep inelastic ep-scattering. In these experiments the structural function W_1 and qPW_2 (3.11) were found to depend practically on the dimensionless ratio $\omega = 2Pq/(-q^2)$ but not on the quantities q^2 and Pq separately (if $|q^2|$ and Pq are large enough). This quite nontrivial property predicted by Bjorken [90] is called a scaling law (or an automodelity). Before describing the applications of the considered models to $\gamma\gamma$-scattering, it is useful to note that all they do at least not contradict to these data.

This scaling law is naturally explained by the parton model [80–82]. Just in the same manner this scaling law is obtained under the assumption that the light-cone current-commutator singularity is just the same as that for free fields [91].*

In the models with scale invariance at short distances the scaling law can be broken by strong interaction at short distances. In such models the products of field operators on the light cone are in general more singular than that for free fields [84]. For the structure functions W_i the Polyakov sum rules take place only here [85], e.g.

$$\int_1^\infty (qP)W_2(\omega, q^2)\frac{\mathrm{d}\omega}{\omega^j} = B(j)(-q^2)^{-\gamma(j)}; \qquad j \geqslant 2; \quad \gamma(2) = 0. \tag{3.13}$$

Here B and γ are independent on q^2. The scaling law for W_1 and qPW_2 is valid only if $\gamma(j) \equiv 0$. In particular, in the ladder γ^5-model $\gamma(j) \neq 0$ and the scaling law is broken. This breaking can be numerically small [93] and could not contradict the experimental data.

Thus, the known results of experiments on deep inelastic ep-scattering do not contradict the above models. To choose between them it is necessary to investigate both this and other processes (e.g. $\gamma\gamma$-scattering).

Annihilation hadron production ($e^+e^- \to \gamma^* \to h$):

1. When studying the total cross section for one-photon-annihilation hadron production $\sigma_{\text{h}}(s)$ a fundamental problem is whether a quantity $s\sigma_{\text{h}}(s)$ is asymptotically constant as it is in the electrodynamics of point-like particles (1.1). Such a dependence is obtained from sufficiently general suggestions in a wide class of models [80–82, 85, 94–96, 31, 97].

A. In the simplest variant of the parton model (see e.g. [80, 95]) an annihilation production develops according to the scheme of fig. 15, namely, a photon decays into a parton–antiparton pair followed by the further conversion of these partons into real hadrons. Since the electromagnetic transition vertex is point-like, then $s\sigma_{\text{h}}(s) \to$ const. The value of this constant is determined by the charge and the spin of the partons only. In this case [94, 95]

$$\lim_{s\to\infty}\frac{\sigma(e^+e^- \to \gamma^* \to h)}{\sigma(e^+e^- \to \gamma^* \to \mu^+\mu^-)} = R = \sum|Q_{\text{f}}^2 + \tfrac{1}{4}\sum|Q_{\text{b}}^2. \tag{3.14a}$$

*The restrictions on spectral functions of the Jost–Lehman–Dyson representation due to the scaling law are obtained in refs. [92].

Here $Q_f e$ and $Q_b e$ are the charges of the parton with spin $\frac{1}{2}$ and 0 respectively. In the usual quark model $R = \frac{2}{3}$. In the coloured quark model $R = 2$ as well and if meson and baryon octets are elementary then $R = \frac{9}{2}$. The experimental s-dependence of R is plotted in fig. 12.

B. In theories with scale invariance at short distances the electromagnetic current has a normal dimension due to gauge invariance. Because of this the quantity $s\sigma_h(s)$ is also asymptotically constant [85] but the quantity R has no simple meaning (3.14a).

Crewther [139], Chanowitz and Ellis [152] have considered the photon form factor for the trace of the stress-energy tensor $\langle\gamma(k_1\mu)|\theta^\lambda_\lambda(0)|\gamma(k_2\nu)\rangle = -(g^{\mu\nu}(k_1k_2) - k_2^\mu k_1^\nu)F[(k_1-k_2)^2]$ in the model of partially conserved dilatation current (PCDC). They have shown that this form factor is connected with R through a simple relation

$$R = \frac{6\pi^2}{e^2}F(0) = \frac{3\pi}{2\alpha}F(0). \tag{3.14b}$$

Using VDM and the hypothesis that the electromagnetic current is U-spin singlet, Terazawa [202] has obtained from here the result which is in agreement with data (cf. fig. 12)

$$R = 16\pi^2/f_p^2 \approx 5.7 \pm 0.9. \tag{3.14c}$$

C. A different approach to the problem of asymptotic behaviour for $s\sigma_h(s)$ based on the ideas of the vector dominance model is discussed in section 3.4.

D. The recent SPEAR and CEA data (see fig. 12) show that the cross section $\sigma_h(s)$ itself is approximately constant, $\sigma_h(s) \approx 15-25$ nb in the interval $4\ \text{GeV}^2 \leqslant s \leqslant 25\ \text{GeV}^2$. Such a behaviour is impossible to understand in the framework of the known models.* If $\sigma_h(s)$ will not decrease as s will increase, then there arises a contradiction to the present ideas about the nature of the strong and electromagnetic interactions which appears, probably, to be too serious. This seems to us to be impossible, i.e. we suppose that $\sigma_h(s)$ will *decrease not slower than* s^{-1} *beginning from some values of* s.

2. *The shape of the angular and energy distribution of secondaries and multiplicity* depends essentially on the feature of the pure hadron interaction also.

A. In a parton model, as well as in models with scale invariance a photon decays into a parton–antiparton pair (figs. 15, 16). But further the process may develop in different ways.

In a version of the parton model [80] hadron production from a primary parton is like bremsstrahlung (fig. 15). In this case produced hadron form two jets. The transverse momentum spread within the limits of these jets is small and a distribution in $\log \epsilon_j$ is, roughly speaking, uniform. Depending on average mass of the primary virtual parton, the number of produced hadrons (multiplicity) is either finite [98] or growing as $\ln s$ [80].

B. In a model with scale invariance [85] a parton or stream decay is a cascade process (fig. 16). At each step a heavy stream is transformed into a small number of lighter streams with masses comparable to that of the stream that has produced them. The fission process goes on until the mass decreases and is a real hadron mass. As a result, the produced hadrons form a few jets inside which one can extract more small jet structures with large transverse momenta. For such a mechanism the multiplicity $\langle n\rangle$ increases as s^δ $(\delta < \frac{1}{2})$.

*Note, however, that for the minimal (nonrenormalizable) electromagnetic interaction of vector mesons the quantity $s\sigma_h$ should increase with s [158].

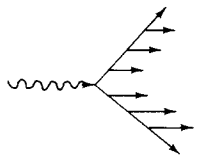

Fig. 15. The hadron production in a timelike photon decay according to models [80, 95]. The photon decays into parton–anti-parton pair, the hadron production off the initial parton is similar to bremsstrahlung.

C. A special group is formed by statistical and hydrodynamical models in which a photon decay is like a point explosion. These models predict angular and momentum distributions and also multiplicity but no value for the cross section. In the statistical model [99] one suggests that, after the explosion, the interaction is switched off immediately and the mean energy does not depend on s. In this case the hadron decay is isotropic and the multiplity grows as $\sqrt{s}$ ($\langle n\rangle \sim \sqrt{s}/\langle E_n\rangle$). If strong interactions among a large number of hadrons after the explosion are taken into account, in the spirit of the hydrodynamical Landau theory [100], then the decay is altogether isotropic but some secondaries are high energetic ones*. For multiplicity estimation, it is sufficient here to use the thermodynamical relations for the entropy S and energy Q: $S \propto VT^3$, $Q \propto VT^4$ (V is the volume, T is the temperature, $Q = \sqrt{s} = \sqrt{q^2}$). The multiplicity $\langle n\rangle$ is proportional to the entropy at the moment of decay for fragments when $V \sim m_\pi^{-3}$. As a result, in such a model $\langle n\rangle \propto Q^{3/4} = s^{3/8}$.

3. A specific information can be obtained by studying the *inclusive cross sections* $e^+e^- \to p + ...$, $e^+e^- \to \pi + ...$ etc. (fig. 17). The corresponding distribution in energy $\epsilon = qP/\sqrt{s}$ and in escape angle θ of the labelled hadron has the form [80]:

$$\frac{d\sigma}{d\epsilon d\cos\theta} = \frac{4\pi\alpha^2}{q^4} m_p \sqrt{\epsilon^2 - m_p^2} \left[2\bar{W}_1 + \left(\frac{\epsilon^2}{m_p^2} - 1\right)\bar{W}_2 \sin^2\theta\right].$$

The $e^+e^- \to p + ...$ structure functions $\bar{W}_1$ and $qP\bar{W}_2$ are specific analytic continuations to the domain $q^2 > 2qP > 0$ of the functions W_1 and W_2 (3.11) defined for $q^2 < 0$ (see e.g. [102]). Is the scaling law fulfilled for $\bar{W}_1$ and $qP\bar{W}_2$ in the timelike region? Are there any simple relations between $\bar{W}_i$ and W_i? The relation

$$\bar{W}_2(1/\omega, q^2) = -\frac{1}{\omega} W_2(\omega, -q^2)$$

is an example of such a relation, obtained in ref. [101].

A comparison of inclusive spectra of different particles will be an important *test of short-distance-interaction internal symmetry*. For example, according to SU(3) and the hypothesis that the electromagnetic current is a U-spin singlet, the differential cross section labelled by the detected baryon, and observed at identical values of q^2 and qP, should satisfy the relations [80]:

*Let us note that in this point the preliminary data of SPEAR [203] are close to the predictions of the hydrodynamical model [100, 204].

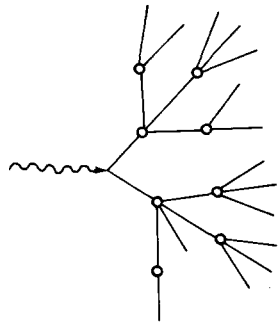

Fig. 16. The hadron production for a timelike-photon decay according to scale invariance model [85].

$$\sigma_{\pi^-} = \sigma_{\pi^+} = \sigma_{K^\pm}, \qquad \sigma_{K^0} = \tfrac{1}{2}(3\sigma_\eta - \sigma_{\pi^0}),$$
$$\sigma_{\Xi^-} = \sigma_{\Sigma^-}, \qquad \sigma_{\Sigma^+} = \sigma_p, \qquad \sigma_{\Xi^0} = \sigma_n = \tfrac{1}{2}(3\sigma_\Lambda - \sigma_{\Sigma^0}). \tag{3.15}$$

If at short distances there is no SU(3) breaking then at large q^2 and qP these relations should be exact. As a possible criterion for passage to the short distance region one can use e.g. the fulfillment of scaling law for W_1 and qPW_2.

From a somewhat different point of view some of the above questions are discussed in the excellent review [70].

Two-photon hadron production

$\gamma\gamma$-scattering is a unique example of a reaction in which the masses of both colliding particles can be changed in a wide range.

Deep virtual $\gamma\gamma$-scattering is less studied theoretically than γp-scattering. Also in a majority of papers only the total $\gamma\gamma$-cross sections are described. One usually proposes that these cross sections should depend not on three invariants W^2, q_1^2, and q_2^2 but on the smallest number of parameters, namely, on one or two combinations of these invariants. These combinations depend both on a used model and on the relation between W^2, q_1^2, q_2^2 and $m_0^2 \sim 1$ GeV^2 (m_0 is the inherent mass parameter of strong interactions). In particular, W^2/q_i^2 is no good scaling variable in $\gamma\gamma$-scattering usually.

The $\gamma\gamma$-cross sections are connected with the absorptive part of the forward $\gamma\gamma$-amplitude

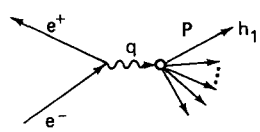

Fig. 17. Inclusive process $e^+e^- \to \gamma^* \to h$ + anything.

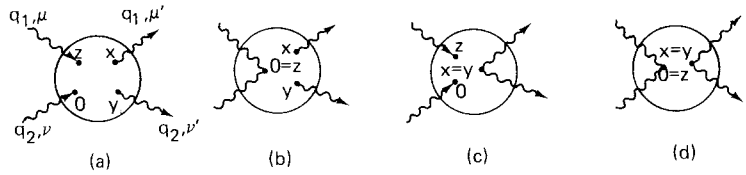

Fig. 18. The virtual forward $\gamma\gamma$-scattering.

$W^{\mu'\nu',\mu\nu}$ (cf. (5.7)). This amplitude is in turn connected with a commutator of four currents by the equation* (see fig. 18)

$$W^{\mu'\nu',\mu\nu} = \tfrac{1}{2}\int d^4x\, d^4y\, d^4z \exp[iq_1(x-z) + iq_2y]\langle 0|[T^*\{J^{\mu'}(x)J^{\nu'}(y)\}^+, T^*\{J^{\mu}(z)J^{\nu}(0)\}]_-|0\rangle. \quad (3.16)$$

In γp-scattering one squared distance x^2 only can be small (the distance between the space-time points x and 0 in (3.11)). Then e.g. in the parton model [81] this process is represented by the diagram of fig. 19 in which the straight line between x and 0 corresponds to a free parton, and the dashed blob describes the (large-distance) parton–proton scattering. Therefore, in the measurable cross section both short and large distances effects are essential. Such a property applies to almost all the other known processes.

Unlike in γp-scattering, in $\gamma\gamma$-scattering there are values of the kinematic variables W^2, q_1^2 and q_2^2 such that simultaneously small values for some distances x^2, $(x-y)^2$, z^2 etc. are essential. The essential supremacy of $\gamma\gamma$-scattering over the other processes is that such a domain of W^2, q_1^2, q_2^2 exists, in which all six distances in fig. 18 are small. In it large distance interactions is inessential. That domain is of the most principal interest.

1. *Short distance region.* In accordance with ref. [103], a main contribution to (3.16) is due to the domain where all six distances between the vertices of fig. 18, have small values if**

$$m_0^2 \ll W^2 \ll q_1^2q_2^2/m_0^2; \qquad |q_i^2| \gg m_0^2; \qquad m_0 \sim 1\ \text{GeV}. \quad (3.17)$$

A. Here one can test most directly the short distance scale invariance hypothesis [200]. According to this hypothesis the $\gamma\gamma$-amplitude is a non-trivial function of two dimensionless variables. In the absence of quasilocal terms of fig. 18b–d it has the form

$$f(q_1^2/W^2,\ q_2^2/W^2). \quad (3.18)$$

The usual additional factor $(W^2)^{-2\epsilon_\gamma}$ is absent here because of the photon anomal dimension $\epsilon_\gamma = 0$ (cf. e.g. [85]). If the quasilocal terms are essential then the terms which grow as $(W^2)^\eta$ can appear (η is the anomal dimension of the (scalar or tensor) quasilocal operator $[\delta S/\delta A^\mu(x)\delta A^\nu(x)]S^+$ (cf. [200])).

B. Let us discuss now this domain in terms of light cone algebra. The existence of a large number

*The designation T^* corresponds to the necessity of taking account of quasilocal terms (corresponding to interactions of the type $\pi\pi A_\mu A_\mu$, $\pi^0 F\mu\nu\tilde{F}\mu\nu$ etc.). With their being taken into account a direct reduction to the usual commutator of four currents is impossible. As a result, the measurable absorptive part in W^2 is described by diagrams of fig. 18. Usually, only the first of them (fig. 18a) is taken into account.

**In this case (at $q_1^2 \sim q_2^2$)

$$(x-y)^2 \sim z^2 \lesssim q_1q_2/q_1^2q_2^2; \qquad (x-z)^2 \lesssim q_1q_2/W^2q_1^2; \qquad y^2 \lesssim q_1q_2/W^2q_2^2; \quad (3.17a)$$

$$x^2 \lesssim q_1q_2(W^2-q_2^2)/W^2q_1^2q_2^2; \qquad (y-z)^2 \lesssim q_1q_2(W^2-q_1^2)/W^2q_1^2q_2^2; \qquad 2q_1q_2 = W^2-q_1^2-q_2^2.$$

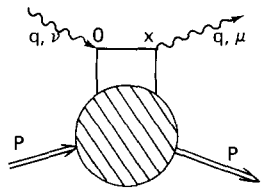

Fig. 19. The γp-scattering diagram giving the main contribution at small x^2 according to the parton model. The straight lines correspond to free partons the dashed blob describes parton–proton scattering.

of short distances demands here new assumptions. The usual assumption on the singularity of a simple commutator of two electromagnetic currents near the light cone [91] (which gives the result for the γp-scattering) reduces the matrix element (3.16) to the commutator of two bilocal operators near the light cone. Further, it is necessary to make an assumption about the character of the singularity of this commutator.

Such an assumption is contained e.g. in a hypothesis on the bilocal operator algebra as made in ref. [104]. According to this hypothesis, the singularity of this commutator is the same as that for free fields. These assumptions determine the asymptotic behaviour of $W^{\mu'\nu',\mu\nu}$ in the domain (3.17) completely. This asymptotic behaviour is just the same as that of the box-diagram contribution of fig. 20 [105–109] *.

C. Finally, in the parton model the amplitude is also determined by the box-diagram contribution of fig. 20, in which the lines between the vertices x, y, z, 0 correspond to free partons [109–111]. The choice of a definite set of fundamental partons determines the result exactly. (This corresponds to the fact that at short distances, strong interactions are switched off and only the usual electromagnetic parton-light interactions are conserved.) The corresponding contributions of scalar and spinor partons to the γγ-amplitude are computed e.g. in ref. [108]. They are listed in appendix E.

Sometimes the scalar and spinor contributions are fully separated. For example, scalar partons do not contribute to a transverse photon cross section at $W^2 \gg |q_i^2|$:

$$\sigma_{TT}(\gamma^*\gamma^* \to h) = \sigma_{TT}(\gamma^*\gamma^* \to \mu^+\mu^-) \cdot \sum Q_f^4. \tag{3.19a}$$

Spinor partons do not contribute to a scalar photon cross section at $W^2 \ll |q_1^2 - q_2^2|$:

$$\sigma_{SS}(\gamma^*\gamma^* \to h) = \frac{2\pi\alpha^2}{|q_1^2 - q_2^2|}\left[1 + \frac{2q_1^2 q_2^2}{q_1^4 - q_2^4} \ln\frac{q_1^2}{q_2^2}\right] \cdot \sum |Q_b^4|. \tag{3.19b}$$

Here eQ_f and eQ_b are the charges of the spinor and scalar partons, respectively. In the quark model $\Sigma Q_f^4 = \frac{2}{9}$, $\Sigma Q_b^4 = 0$, in the coloured quark model $\Sigma Q_f^4 = \frac{2}{3}$, $\Sigma Q_b^4 = 0$, if partons form meson and baryon octets, $\Sigma Q_f^4 = 4$, $\Sigma Q_b^4 = 2$.

Equations (3.19) and (3.14a) (for the $\gamma^* \to h$ transition) will give an important knowledge on the parton charge and spin.

*In ref. [105] another channel $\gamma \to h\gamma^*$ was considered (for timelike photons). In refs. [106–108] the results of ref. [105] were extended to a $\gamma^*\gamma^* \to h$ transition for space-like photons in the domain $W^2 \ll -q_i^2$; $|q_i^2| \gg m_0^2$. In refs. [103, 109] one has shown that, for $q_i^2 < 0$, the box-contribution is dominant in a wider domain (3.17).

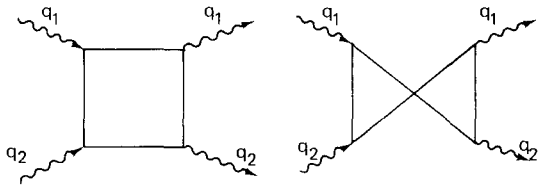

Fig. 20. The box-diagrams for $\gamma\gamma$-scattering.

2. With our going out of the region (3.17) the large distance strong interaction effects become essential.

The first example of such a kind is the *Regge region* at large photon "masses":

$$W^2 \gg q_1^2 q_2^2/m_0^2; \qquad |q_i^2| \gg m_0^2. \tag{3.20}$$

Here the main contribution to the integral (3.16) is due to small values of $(x-z)^2 \sim 1/q_1^2$ and $y^2 \sim 1/q_2^2$ and due to a larger domain in the other distances: x^2, z^2, $(x-y)^2$, $(y-z)^2 \lesssim W^2/q_1^2 q_2^2$ [109]. Therefore, the usual methods of the hadrodynamics may be used here.

A. In particular, one can expect that in the region (3.20) the factorization theorem (3.4) is valid for each Regge-trajectory contribution. For the trajectory α in pp-scattering $W^2\sigma_{pp} \sim (W^2/m_0^2)^{\alpha_P}$. In much the same way as in γp-scattering $W^2\sigma_{\gamma p} \sim (W^2/q^2)^{\alpha_P}$ (if the scaling law is fulfilled in the Regge-region also).

As a result $W^2\sigma_{\gamma\gamma} \sim (W^2\sigma_{\gamma p})^2 (W^2\sigma_{pp})^{-1} \sim (W^2 m_0^2/q_1^2 q_2^2)^{\alpha_P}$. Since this conclusion is valid for a contribution of any Regge-trajectory, the total amplitude has then the form [93, 112]:

$$W^2\sigma_{\gamma\gamma} = f(W^2 m_0^2/q_1^2 q_2^2), \tag{3.21}$$

i.e. it depends on the only (dimensional) parameter $W^2/q_1^2 q_2^2$.

B. The result (3.21) is also obtainable in the parton model [113] as well as with usual assumptions about light cone commutator algebra[109]*. Of course, in all these descriptions it is necessary to take into account the box-contribution of fig. 20. The amplitude has the form (3.21) only if the quantity (3.21) is dominant over the box-contribution [111].

The application of the factorization theorem (3.4) both for transverse and scalar photons permits to conclude that the ratio R (3.10) of the cross sections for scalar and transverse photons scattering is independent of the type of target. In the parton model R gives an estimate of the relative significance of spinor and spinless partons in the corresponding processes. The universality of R means that the composition of partons with which the "heavy" photons interact is independent of the type of target. Data on deep inelastic ep-scattering show a small value of R (≈ 0.18) i.e. a dominant role of spinor partons.

C. For a model with short distance scale invariance in the region (3.20) the amplitude depends both on $W^2/q_1^2 q_2^2$ and on the other dimensional parameter $q_1^2 q_2^2$. Here sum rules like (3.13) take place. In a very rough approximation, the contribution of every Regge trajectory α is multiplied by $(q_1^2 q_2^2/m_0^4)^{c(\alpha)}$ [89].

*This is easily understood with the help of the arguments of ref. [113]: If photon q_2 is treated as a target then it is clear (by analogy with the γp-scattering) that the amplitude is some function $\varphi_1(W^2/q_1^2; q_2^2/m_0^2)$. But if photon q_1 is treated as a target, then this amplitude is $\varphi_2(W^2/q_2^2; q_1^2/m_0^2)$. Since φ_1 and φ_2 are the same function, then it should depend on $W^2/q_1^2 q_2^2$ only.

D. Using the automodelity hypothesis [31] (or dimensional analysis) the result should take a form independent of the relations between W^2, q_1^2 and q_2^2. Here no amplitude should depend on dimensional variables, i.e. it should depend on q_1^2/W^2 and q_2^2/W^2 only, either in the region (3.17), or in a Regge region (3.20). In the last case this prediction obviously differs from that of other models.

3. An other example is the *resonance region*

$$W^2 \sim m_0^2; \quad |q_i^2| \gg m_0^2. \tag{3.22}$$

Here the main contribution to the integral (3.16) comes from small values of $(x-y)^2 \sim z^2 \sim 1/(q_1 - q_2)^2$ [105].

The usual assumption is that the light-cone current-commutator singularity is the same as that for free fields. It is used here in the same manner as when obtaining the scaling law for γp-scattering. It now follows that amplitudes depend on two parameters only [105–107]

$$f(W^2/m_0^2;\ (q_1^2 - q_2^2)/(q_1^2 + q_2^2)). \tag{3.23}$$

(This conclusion is also reproduced in the parton model [107–109] and in models of the φ^3-type [103].)

At $-q_1^2$ changes from zero up to values much greater than m_0^2 at fixed $|q_2^2| \gg m_0^2$, the values of the amplitudes and the relative contributions of resonances and background can be noticeably changed. However, from (3.23) one can see that with a further $-q_1^2$ growth, at q_2^2 fixed, the amplitudes do not change, since a second argument of (3.23) is transformed to unity. Using an additional assumption about the fast decrease of the one photon–hadron vertices with the increase of the photon mass [114], authors of ref. [109] obtained that this conclusion is valid also if the second photon is not too "heavy", i.e. $-q_2^2 \lesssim m_0^2$.* Such a behaviour is in strong contrast with the well known fact that there is rapid decrease of resonance contributions in γ^*p-scattering. This difference is due to the special nature of the targets: in γ^*p-scattering the target is structural but in the $\gamma^*\gamma^*$-scattering the target is a structureless one.

3.4. *Resonances*

The meson resonances were the first to be studied in colliding beam experiments. In such experiments the most precise investigation of meson resonance properties (masses, widths, decay modes etc.) is, in principle, possible. A prominent advantage of their study in colliding beams experiments follows from the fact that the abovementioned properties can be extracted without special hypotheses about the resonance production mechanism (such hypotheses are necessary e.g. in an analysis of πp-scattering).

1. *The annihilation production.* The investigation of the *C-odd vector mesons* ρ, φ, ω [51] is a well known example. Indication for the existence of the ρ' meson [52] puts a number of new questions. In particular, whether ω and φ-mesons have similar analoges, ω' and φ' [116], and then, whether the set of vector mesons is finite. To answer these questions is of course of importance

*In a number of papers [115] for the description of the region $-q_1^2 \gtrsim m_0^2$; $q_2^2 \approx 0$ another assumption was used that the $\gamma^*\gamma$ structural functions are distinguished only by a factor from the well known γ^*p-structural functions.

for particle systematics. This allows also a deeper understanding on the applicability range of models of the vector dominance (VDM) type. In an extended VDM [117, 118] one assumes that the annihilation production takes place through vector mesons only. One calls here for a Veneziano-like spectrum of vector mesons, with properties $M_n^2 = M_\rho^2(2n+1)$, $M_n/f_n = M_\rho/f_\rho$, and adds up all their contributions (assuming their Breit–Wigner form at q^2 far from m_V^2 also). To provide the convergence of the series, a hard enough restriction on the resonance widths is necessary (e.g. in the variant [117] $\Gamma_n \to 0$ is necessary and in the variant [118] $\Gamma_n/M_n \to 0$). As a result, it turned out that the ratio $R = \sigma_h/\sigma_{e^+e^- \to \mu^+\mu^-}$ is constant on the average, $R = 8\pi^2/f_\rho^2 \approx 2.5-3$. (With the modification of the mass spectrum and M_n/f_n, one obviously can get any suitable value for R.) Unfortunately, a direct test of such a construction is at least difficult. This is due to strong overlap between resonances and also to the competitions between different effects.

In the investigation of hadron production in an inclusive set up (s is not too large) a main interest is in the study of *quasi-two-particle final states* ($e^+e^- \to \gamma \to \pi R$, $e^+e^- \to \gamma^* \to R_1R_2$) [124, 125]. These final states contribute essentially to $\sigma_h(s)$ at $\sqrt{s} \sim 1-1.5$ GeV (cf. [52b]). Such processes are the two-particle decays of a motionless massive photon (with secondaries moving collinearly). Therefore, their study allows to test directly the relations followed from collinear symmetry groups e.g. $(SU6)_w$ [126].

A study of A_1 production is of special interest due to its production in hadron collisions and is often suppressed (because of this fact one doubts in the A_1 existance). There is a hypothesis [127] that in the $\gamma^* \to \pi A_1$ reaction this suppression disappears.

2. *Two-photon production of C-even resonances. Resonances with spin $J \neq 1$* can be produced by almost real photons [119, 120, 1]. If such a resonance is narrow ($\Gamma \ll m_R$) then its production cross section is expressed through its two-photon decay width $\Gamma^{\gamma\gamma}$ (with an accuracy of the order of Γ/m_R):

$$\sigma_{\gamma\gamma \to R} \approx 8\pi(2J+1)\frac{\Gamma^{\gamma\gamma}\Gamma}{(W^2 - m_R^2)^2 + \Gamma^2 m_R^2} \approx 8\pi^2(2J+1)\frac{\Gamma^{\gamma\gamma}}{m_R}\delta(W^2 - m_R^2). \tag{3.24}$$

For most (but not all!) of the resonances one may restrict oneself now to the rough estimation

$$\Gamma^{\gamma\gamma} \approx \alpha^2\Gamma \tag{3.25}$$

which is often the average value of different theoretical estimations obtained by means of, either finite energy sum rules [76], or the tensor dominance model [121], or the quark model [122] etc.

For the production of *resonance with $J = 1^+$*, like the $A_1(1070)$, though one photon should have an essentially nonzero mass. The cross sections for such resonance production must then be markedly smaller than for resonances with $J \neq 1$.

In connection with the *pseudoscalar nonet problem* it is interesting to study X° and E production (their spins are not yet known well enough [69]). Here one can expect additional information on the X°-spin, since according to [123] a ratio $\Gamma^{\gamma\gamma}(J=2)/\Gamma^{\gamma\gamma}(J=0) \approx 10^{-3}$ is obtained for two permissible values of $J(X^\circ)$. The observation of many events of the two-photon type E(1422) production would eliminate the possibility $J^P = 1^+$ for this meson which is discussed now.

3.5. *Current algebra, PCAC, etc.*

The hypothesis of a partially conserved axial current (PCAC) and current algebra allow a global description of a number of phenomena of low energy pion physics. Such an approach also permits to establish a number of relations for pion production by photons, some of them having a high accuracy. Some of the features of such amplitudes reflect the essential dynamical properties of strong interactions. On the other hand in studying pion production by photons one can directly investigate quantities which are basic for this approach such as spectral densities of axial and vector currents.

1. Pais and Treiman [128] have noted that the spectral *density of the isovector axial and vector currents** can be defined from the differential cross section of the reactions (fig. 17):

$$e^+e^- \to 1 \text{ soft pion} + \text{anything} \tag{3.26}$$

$$e^+e^- \to 2 \text{ soft pions} + \text{anything}. \tag{3.27}$$

Let us consider e.g. the reactions (3.26). A soft pion with a zero four-momentum $P \to 0$ takes away a parity and one unit of isospin only. Therefore, the system "anything" is produced by the isovector axial current A^i_μ. As a result, the differential cross section of the process (3.26) summed over all the possible states standing for "anything" is proportional to the axial current spectral density $\rho_A(q^2)$ (3.28). With the aid of PCAC and current algebra Pais and Treiman have obtained that this relation has the form (at $q^2 < 4m_\rho^2$)

$$8\pi f_\pi^2 q^2 \lim_{qP \to 0} \left\{ [(qP)^2 - q^2 m_\pi^2]^{-1/2} \frac{d\sigma}{d(qP)} \right\} = \begin{cases} \sigma_A(q^2) = \dfrac{16\pi^3\alpha^2}{q^4} \rho_A(q^2) & \text{for } \pi^\pm \\ 0 \quad \text{for } \pi^0. \end{cases} \tag{3.29}$$

(The possibility of studying the spectral density $\rho_A(q^2)$ is here complicated by the large extrapolation range from $qP = \epsilon\sqrt{s} \geqslant m_\pi\sqrt{s}$ to $qP = 0$. In this connection the accuracy of the approximation is controlled only by testing π^0-production suppression, i.e. a theoretical estimation of the accuracy in the measurement of ρ_A is $d\sigma^0/d\sigma^\pm$.)

The current algebra and PCAC hypothesis give a number of predictions for *a pion production by one or two photons near a threshold.* These predictions are discussed in details e.g. in the reviews [129, 14]. We limit ourselves here to a short survey of some of the most important results.

2. *The production of an even number of pions near a threshold.* Terentjev [129] has obtained the next expression for the $\gamma\gamma \to \pi^+\pi^-$ amplitude on mass shell

$$M^{\mu\nu} = M^{\mu\nu\text{Born}} + e^2\beta W^2(g^{\mu\nu} - q_2^\mu q_1^\nu / q_1 q_2). \tag{3.30a}$$

*These densities are introduced by analogy with the electromagnetic current spectral density, e.g.

$$(2\pi)^3 \sum_n \langle 0|A^i_\mu|n\rangle\langle n|A^i_\nu|0\rangle \delta(q - p_n) = -\delta^{ij}\left\{\left(g_{\mu\nu} - \frac{q_\mu q_\nu}{q^2}\right)\rho_A(q^2) + \frac{q_\mu q_\nu}{q^2}\rho_{PS}(q^2)\right\}. \tag{3.28}$$

Using the first Weinberg sum rule ($\int(\rho_V - \rho_A)d\mu^2/\mu^2 = f_\pi^2$) [133], he has obtained*

$$\beta = \tfrac{1}{3}\langle r^2\rangle + \frac{1}{f_\pi^2}\int \frac{\rho_A(\mu^2) - \rho_V(\mu^2)}{\mu^4}\, d\mu^2 \sim \frac{1}{2m_\rho^2}. \tag{3.30b}$$

Here $\langle r^2\rangle$ is the squared pion radius. Therefore, the amplitude is described by the simple Born diagram with the high accuracy of order of $(W/m_\rho)^2$. In the same manner the $\gamma\gamma \to \pi^0\pi^0$ amplitude is of the order of $(W/m_\rho)^4$ [129]. For the large photon masses the $\gamma\gamma \to \pi^+\pi^-$ amplitude is [130, 131]

$$\frac{8\pi\alpha}{f_\pi^2}\left(g^{\mu\nu} - \frac{q_2^\mu q_1^\nu}{q_1 q_2}\right)\int \frac{\rho_V(\mu^2) - \rho_A(\mu^2)}{\mu^2 + q_1 q_2}\, d\mu^2. \tag{3.30c}$$

With a subsequent use of PCAC and reduction formulas it follows that the $\gamma\gamma \to n(\pi^+\pi^-)$ amplitude near a threshold equals the $\gamma\gamma \to \pi^+\pi^-$ amplitude multiplied by kinematic factors only [132].

3. In the description of the production of an odd number of soft pions a new parameter F^{π^0} appears, which is the coupling constant for $\pi^0 \to \gamma\gamma$ decay (π^0 life-time $\tau = 64\,\pi\,(F^{\pi^0})^{-2} m_\pi^{-3}$). Let us explain its origin.

In a naive use of the standard PCAC procedure, the two-photon decay of a massless pion is forbidden. In this connection Adler [134] has shown that with regard to electromagnetic interaction the basic PCAC relationship between the pion field π^i and the axial current $A_\mu^i(x)$ for the neutral component ($i = 0$) should be modified as follows (anomalous PCAC condition)

$$\partial_\mu A_\mu^0(x) = m_\pi^2 f_\pi \pi^0(x) + \frac{\alpha S}{4\pi}\,\epsilon^{\mu\nu\rho\sigma} F^{\mu\nu}(x) F^{\rho\sigma}(x). \tag{3.31}$$

Here $F^{\mu\nu}(x)$ is the electromagnetic field tensor and Adler's anomaly S is a certain number. In this case F^{π^0} for the massless pion is expressed through S

$$F^{\pi^0}(m_\pi^2 = 0) = -\frac{2\alpha}{\pi f_\pi} S. \tag{3.32}$$

One supposes usually that this quantity differs slightly from the physical constant F^{π^0}, i.e.

$$F^{\pi^0} \equiv F^{\pi^0}(m_\pi^2) \approx F^{\pi^0}(0). \tag{3.32b}$$

The observed π^0 life-time ($\tau = 0.84 \times 10^{-16}$ sec) corresponds to $S = 0.54$.

A true role for the Adler's anomaly can be found in the first place by studying the $\pi^0 \to \gamma\gamma$, $\gamma^* \to 3\pi$ and $\gamma\gamma \to 3\pi$ reactions. Using the general assumptions of PCAC and current algebra only, Terentjev [135] and Adler et al. [136] have obtained an important relationship between F^{π^0} and the constant $F^{3\pi}$ of the $\gamma^* \to 3\pi$ reaction:

$$eF^{3\pi} = F^{\pi^0} f_\pi^{-2}. \tag{3.33}$$

This equation determines the connection between the values of the observed processes only if

*The formula for β obtained in ref. [132] does not contain the term $\langle r^2\rangle/3$ (cf. in details [129]).

they are due to the anomal term (3.31) only. If it is not the case, equation (3.33) becomes meaningful. Thus *the experimental verification* of (3.33) will be an essential test for the determination of the true role of the Adler's anomaly.

The $\gamma\gamma \to 3\pi$ amplitude is determined through the constant F^{π^0} and the parameter γ, connected with the $\pi\pi$-scattering length [135, 136]. One can express through the same parameters the $\gamma^* \to (2n+1)\pi$ and $\gamma\gamma \to (2n+1)\pi$ amplitudes near the threshold (see e.g. [129]). Such expressions are obtained also for $\gamma = 0$ by means of a phenomenological Lagrangian technique [137].

The $\gamma\gamma \to n\pi^0$ amplitudes vanish near threshold $P_{\pi^0} \to 0$ at least as $(P_{\pi^0})^{n+1}$ [138, 134].

4. *Adler's anomaly and short distance interaction.* Wilson has shown that Adler's anomaly is entirely due to short distance interaction (i.e. the large distance interaction does not contribute in the value of S) [84]. It has allowed a determination of S e.g. in different variants of the quark parton model (see e.g. [129])

$$S = \tfrac{1}{2} \sum_i \lambda_{ii}^3 Q_i^2 = \bar{Q} = \tfrac{1}{2}(Q_p + Q_n). \tag{3.34}$$

Here $e\bar{Q}$ is the average charge of the fundamental isotopic multiplet. In the usual quark model $\bar{Q} = \frac{1}{6}$, in the coloured quark model $\bar{Q} = \frac{1}{2}$. The last value permits to explain a visible lifetime under the assumption that it is due to Adler's anomaly only.

In the assumption of short distance scale invariance, Crewther [139] has shown that

$$S = \tfrac{1}{4} RK. \tag{3.35}$$

Here $R = \lim_{s\to\infty} [\sigma_{e^+e^- \to \gamma^* \to h}(s)/\sigma_{e^+e^- \to \mu^+\mu^-}(s)]$ (cf. fig. 12) and K is the axial current contribution to a Wilson operator product expansion for the product of two electromagnetic currents. The quantity K^2 can be measured from the $e^+e^- \to \mu^+\mu^-\pi^0$ cross section at large s and p_{π^0} fixed [140]. In ref. [141] the connection between S and the $\gamma\gamma \to h$ cross section at large $|q_i^2|$ and W^2 is discussed.

The fact that the quantity S is independent on large distance interaction makes the investigation of the q_i^2 dependence of S especially interesting. For this purpose one should compare the q_i^2-dependence on the π^0 two-photon production amplitude and the spectral density of the axial current. One may attempt to extract the latter, in particular, from experiments on the A_1 two-photon production.

3.6. *The reactions* $\gamma^* \to \pi\pi(KK)$ *and* $\gamma\gamma \to \pi\pi(KK)$ *on mass shell, low energy* $\pi\pi$*-scattering,* ϵ *and* S*-mesons

In the reactions $\gamma^* \to \pi\pi$, $\gamma^* \to K\bar{K}$, ... the π, K, ... form factors are obtained (3.3). As the form factors describe directly the space electromagnetic structure of the particles their further investigation is of unquestionable interest.

At not too high energies pion pair production ($\gamma\gamma \to \pi^+\pi^-$) should be the most important $\gamma\gamma \to h$ channel. A study of reactions $\gamma\gamma \to \pi\pi$ and $\gamma\gamma \to KK$ will allow to test a wide range of fundamental ideas for the low energy physics (see e.g. [142]) both for $\pi\pi$ scattering and for the transitions $\gamma\gamma \to \pi\pi$, $\gamma^* \to \pi\pi$. The test of these ideas involves in particular the following questions: 1) with what accuracy are threshold theorems valid and what is the range of their applicability? 2) what is the domain of applicability of the two-particle unitarity approximation? 3) how do

resonances in $\pi\pi$ and $K\bar{K}$ system influence the character of the $\gamma\gamma \to \pi\pi$ ($K\bar{K}$) amplitudes? 4) how do crossing-channel processes have an influence on these reactions? 5) what are the main parameters of $\pi\pi$-scattering?

The $\gamma\gamma \to \pi^+\pi^-$ amplitude at threshold must be close to the Thomson limit. Current algebra and PCAC determine the accuracy of this approximation. According to (3.30), a description of the $\gamma\gamma \to \pi^+\pi^-$ reaction by means of QED formulas (for pointlike pions) is valid with an accuracy $\sim(W/m_\rho)^2$. The $\gamma\gamma \to \pi^0\pi^0$ amplitude is determined in the same approximation by means of an effective Lagrangian including the $\gamma\pi\rho$ and $\gamma\pi\omega$ interactions. This amplitude near the threshold is of the order of

$$\sim \alpha\, W^2(W^2 - 2m_\pi^2)/m_\rho^4.$$

In the low energy domain two-particle unitarity is valid for the $\gamma\gamma \to \pi\pi$ amplitude, namely

$$\operatorname{Im} M^{JI}(\gamma\gamma \to \pi\pi) \propto M^{*JI}(\gamma\gamma \to \pi\pi) M^{JI}(\pi\pi \to \pi\pi). \tag{3.36}$$

At $W < 4m_\pi$ this equation is exact. An assumption of approximative validity for such equations up to $W \sim 1$ GeV is one of the fundamental hypothesis of the low-energy physics. From the equation (3.36) it follows directly, that the $\gamma\gamma \to \pi\pi$ phases coincide with the $\pi\pi$ phases δ_J. Let us note, that this relation does not determine directly the $\gamma\gamma \to \pi\pi$ partial amplitude values. For elastic scattering the amplitude is simply $e^{i\delta}\sin\delta$, i.e. the amplitude modulus is unambiguously determined by the phase δ. In contrast to this for an inelastic reaction, such as $\gamma\gamma \to \pi\pi$ the amplitude is $|f|e^{i\delta}$ with $|f|$ not directly connected with δ. In particular, a small value of the phase δ does not lead, generally speaking, to a small value of $|f|$.

For $\pi\pi$-scattering at $W \lesssim 1$ GeV the higher partial amplitudes (with $J \geqslant 2$) are small ($\delta_J \ll 1$). Due to (3.36) it follows that the related $\gamma\gamma \to \pi\pi$ phases are small. However, the related partial amplitude modules at not too high W are determined by the Born diagrams (due to the threshold conditions). Therefore, one may say that, in accordance with ideas of present low energy physics, the Born approximation should describe these waves with a good accuracy at $W \lesssim 1$ GeV. It is of interest to elucidate up to what energies such a description is valid.

A special question is the behaviour of an isoscalar S-wave amplitude M^{00} [143–149]. For the calculation of the M^{00} a dispersion approach was often used. In this approach the result is ambiguous. The ambiguity can, however, be removed using certain normalizations for the amplitude: at $W \to \infty$ [146], on the amplitude value either at $W \sim m_\epsilon$ (which is being unknown now) [147], or at the threshold (using the low-energy expansion (3.30)) [144, 145]. The last variant (with using (3.30)) seems to us to be most suitable. The amplitude M^{00} resulting in this case has a wide maximum connected with the ϵ-meson. The position of this maximum (at $W < m_\epsilon$) significantly differs from $m_\epsilon \sim 750$ MeV (due to the high ϵ-meson width, ~ 400 MeV), and the value of M^{00} in this maximum can be expressed through the parameter β from (3.30). At $W \approx 400$–700 MeV the quantities M^{00} obtained at the reasonable values of the β are of the same order of magnitude as M^{00}_{Born}. Namely, at $W = 600$ MeV the ratios $(M^{00}/M^{00}_{\text{Born}})$ equal 1; 2 and 3 for $\beta = 1/2m_\rho^2$; $1/m_\rho^2$ and $-3/2m_\rho^2$, respectively [144]. In order to imagine ourselves the real significance of the S-wave in the cross-section $d\sigma_{\gamma\gamma \to \pi\pi}/d\cos\theta \propto (|M_{+-}|^2 + |M_{++}|^2)$ we list a few numbers: at $\theta \approx \frac{1}{2}\pi$ and $W = 660$ MeV the amplitude M_{++} coincides practically with M^{00} and $|M_{++}/M_{+-}| \approx 0.5$ for $\beta = 1/m_\rho^2$, but the cross section differs from the Born one very slightly for $\beta = 1/2m_\rho^2$.

The experimental investigation of the $\gamma\gamma \to \pi\pi$ reaction permits us to answer some questions which appear in other problems of low energy physics.

Table 2
The physical problems for the $\gamma\gamma \to h$ reaction

Measured quantity or reaction	Studied physical object or investigated problem	The ee → eeh cross section (cm^2) to be measured (at $\sqrt{s} \sim 5$–10 GeV)
$\gamma\gamma \to \pi^+\pi^-$	Threshold theorems, Born term.	10^{-33}
$\pi^0\pi^0$	PCAC, current algebra.	10^{-35}–10^{-36}
	Two-particle unitarity approximation.	10^{-34}–10^{-35}
	(Range of validity.)	
	The number of essential partial waves.	
	$\pi\pi$-phases and scattering lengths.	10^{-35}–10^{-36}
	Going out of mass shell.	10^{-35}–10^{-36}
	The first Weinberg sum rule [132, 133].	
	ϵ, f, S*, inelasticity.	10^{-33}–10^{-34}
$\gamma\gamma \to K\bar{K}$	Connection with the trace of energy-momentum tensor.	
	FESR	
$\gamma\gamma \to n\pi;\ n > 2$	PCAC, chiral Lagrangians.	10^{-36}–10^{-37}
$\gamma\gamma \to \pi^0(\eta)$	π^0-lifetime.	10^{33}
	Triangle anomaly, q^2-dependence [157].	
$\gamma\gamma \to R$	Resonance parameters (ϵ, f, A_2, etc.).	10^{-33}–10^{-35}
(resonance)	Spin of X^0, E.	10^{-33}–10^{-34}
	FESR, symmetries.	
	Parameters of A_1, etc.	$\lesssim 10^{-35}$
High energy behaviour of $\sigma_{\gamma\gamma}(W^2)$	Validity of Regge analysis.	10^{-34}
	Factorization theorem.	
	Duality.	
$\gamma\gamma \to V_1V_2$	Diffractive excitation of photons.	3×10^{-35}–10^{-36}
	b_p, α'_p, q^2-dependence.	
($V_i = \rho, \omega, \varphi, \ldots$)	q^2-dependence for the relative contribution of diffraction.	
	Vector dominance.	
$\tau_{TT} = \sigma_\parallel - \sigma_\perp$	P-parity of resonances.	10^{-35}–10^{-36}
(1.5)	Superconvergent sum rule (3.9).	
Distribution in transverse momentum, multiplicity, secondaries composition, $p_\perp^2$-dependences, large $p_\perp$, q^2-dependence	Transition from structural particles to pointlike ones.	10^{-34}–10^{-37}
	Short distance interaction.	
	Dependence on large $p_\perp$ behaviour, on the nature and masses of the colliding particles.	
	Parton model [153].	
Inclusive reactions $\gamma\gamma \to \pi + \ldots$; $\gamma\gamma \to p + \ldots$	Feynman's scaling law.	10^{-34}
$\gamma\gamma \to$ soft pion + anything	$\langle\gamma\|VV + AA\|\gamma\rangle$ [154]	
the $\gamma\gamma \to h$ cross-section at large q_i^2	Short distance interaction.	10^{-37}–10^{-39}
	Parton model.	
	Bilocal operator algebra.	
	Scale invariance.	
	The number of independent variables in $\sigma_{\gamma\gamma}$.	
$W^2 \gtrsim \frac{q_1^2 q_2^2}{m_0^2} \gg m_0^2$	Super-scaling.	
	Applicability of Regge analysis.	
$m_0^2 \ll W^2 \ll \frac{q_1^2 q_2^2}{m_0^2}$; $\|q_i^2\| \gg m_0^2$	Direct test of scale invariance.	
	Charge and spin composition of partons.	
$m_0^2 \sim W^2 \ll \|q_i^2\|$	Relationship between resonances and background at large q_i^2.	

Table 3
The physical problems for the $e^+e^- \to \gamma^* \to h$ reaction

Measured quantity or reaction	Studied physical object or investigated problems	Cross-section to be measured (cm^2)
Asymptotic behaviour of the total cross section $\sigma(e^+e^- \to \gamma^* \to h) \equiv \sigma_h$	Short distance electromagnetic interaction. Test of pointlikeness. Composition of partons. Connection with triangle anomaly. Character of renormalization in QED.	$\frac{10^{-31}}{s(\mathrm{GeV}^2)}$
High energy angular and energy distributions, multiplicity	What is short distance hadron interaction? (Variants: it is inessential, it is scale invariant, thermodynamic, etc.)	$\frac{10^{-31}}{s(\mathrm{GeV}^2)}$
High energy inclusive reactions $e^+e^- \to p + ...$, Comparison of different reactions	Comparison with ep-scattering. Scaling law. Light cone commutator algebra. Short distance interaction symmetry. Electromagnetic splitting of particle masses.	$\frac{10^{-32}}{s(\mathrm{GeV}^2)}$
$e^+e^- \to R$ (resonance)	Vector meson parameters (ρ, ω, φ). Number of vector mesons (ρ' etc.). Role of resonances for σ_h at $s \to \infty$. Extended VDM. Role of vector mesons in strong interactions.	10^{-30} $10^{-32}-10^{-33}$
Final states	Decay modes of vector mesons and their off-shell coupling constants. Comparison with $p\bar{p}$-annihilation.	$10^{-32}-10^{-33}$
Quasi-two-particle final states $e^+e^- \to \pi R$, R_1R_2 ($R = \omega, \rho, \epsilon, A_1, ...$)	Contribution to σ_h. Investigation of A_1, B, ... Test of $SU_W(6)$.	$10^{-33}-10^{-34}$
$e^+e^- \to \gamma^* \to \pi^+\pi^-$ $\to K\bar{K}$ $\to p\bar{p}$	π, K, p, ... -form factors	2×10^{-31} at $s = 6\, m_\pi^2$ 10^{-34} at $s = 8\ \mathrm{GeV}^2$
$\frac{\sigma(e^+e^- \to K^0\bar{K}^0)}{\sigma(e^+e^- \to \pi^+\pi^-)}$ $\frac{\sigma(e^+e^- \to K^+K^-)}{\sigma(e^+e^- \to \pi^+\pi^-)}$ at large s	Test of short distance SU(3)	
$e^+e^- \to \gamma^* \to \pi + ...$ $e^+e^- \to \gamma^* \to \pi\pi + ...$ (soft pions)	Isovector axial and vector currents. Test of isotensor current absence [155].	
$e^+e^- \to \gamma^* \to n\pi$ $n > 2$	PCAC	10^{-35}
$e^+e^- \to \gamma^* \to 3\pi$	Triangle anomaly.	10^{-35}
$\frac{\sigma(e^+e^- \to \gamma^* \to \bar{p} + ...)}{\sigma(e^+e^- \to \gamma^* \to p + ...)}$ $\frac{\sigma(e^+e^- \to \gamma^* \to K^- + ..)}{\sigma(e^+e^- \to \gamma^* \to K^+ + ...)}$	Test of *C*-invariance [155].	
$e^+e^- \to K_L^0K_S^0$ at $\sqrt{s} \approx m_\varphi$ Correlations in decays	Test of *CP*-invariance [156].	

For example, the observation of interference quantities $\mathrm{Re}(M_{+-}^{*}M_{++})$ and $\mathrm{Re}(F_{\pi}^{*}M_{++})$ (4.6) near threshold permits, in principle, to determine in this range the S and P-waves $\pi\pi$ scattering phases δ_0 and δ_1 ($\mathrm{Re}(M_{+-}^{*}M_{++}) \approx M_{+-}^{B}M_{++}^{B}\cos(\delta_0-\delta_2)$, $\mathrm{Re}(F_{\pi}^{*}M_{++}) \approx |F_{\pi}|M_{++}^{B}\cos(\delta_0-\delta_1)$, M_{ab}^{B} are Born amplitudes with helicities a, b). From here one can determine the S-*wave* $\pi\pi$ *scattering lengths* (as $\delta_2/\delta_1 \to 0$; $\delta_1/\delta_0 \to 0$).

A very interesting features of $\pi\pi$ scattering is the sharp variation of S-wave phase at $W \sim 950$ MeV [151] which is interpreted as due to the influence of the $K\bar{K}$ bound state (S*-resonance [150]). The investigation of $\gamma\gamma \to \pi\pi$ and $\gamma\gamma \to K\bar{K}$ in this range should give additional information on this effect. In this region one should, apparently, find out the $\gamma\gamma \to \pi\pi$ and $\gamma\gamma \to K\bar{K}$ amplitudes simultaneously with taking account of the $\pi\pi$ and $K\bar{K}$ intermediate states in the unitarity relation.

An investigation of the $\gamma\gamma \to \pi\pi$ and $\gamma\gamma \to KK$ S-wave amplitude energy dependence is of interest also in connection with the determination of *the two-photon widths of the* ϵ *and of the* S^*.[‡] These two-photon widths are obtained in an independent way with the help of FESR [76]. From another point of view, such a piece of formation is essential for an approach in which ϵ (and S^*) are connected with the trace of the momentum-energy tensor θ_{μ}^{μ} in a broken scale invariance model where $\langle 0|\theta_{\mu}^{\mu}|\epsilon\rangle = m_{\epsilon}^2 F_{\epsilon}$. For the coupling constant of ϵ with two photons $g_{\epsilon\gamma\gamma}$, one obtains here the relation [139, 152]:

$$12\pi^2 F_{\epsilon} g_{\epsilon\gamma\gamma} = R = \lim_{s\to\infty} \frac{\sigma(e^+e^- \to \gamma^* \to h)}{\sigma(e^+e^- \to \mu^+\mu^-)} . \tag{3.37}$$

If one chooses $F_{\epsilon} \sim 150$ MeV ($\Gamma_{\epsilon\to\pi\pi} \sim 400$ MeV) and $m_{\epsilon} \sim 700$ MeV then, according to [152] and (3.37), it follows that the width for two-photon ϵ decay $\Gamma_{\epsilon\gamma\gamma} \approx 0.2R^2$ keV (cf. fig. 12). This does not contradict the data of ref. [201].

4. What can be investigated in $e^{\pm}e^- \to e^{\pm}e^-h$ experiments and how

When studying two-photon hadron production the $\gamma\gamma \to h$ amplitudes are of main interest. They are connected with the observed ee → eeh cross section by means of rather complicated relations of the type (1.8). The related differential distributions are obtained in section 5. Here we take them as a basis and discuss what information about the $\gamma\gamma \to h$ transition can be extracted from colliding beam experiments and how it can be done. The cross section estimations given below show to what degree the above experiments are realistic.

Hadron production by two photons was considered for the first time by Primakoff [160] who suggested to measure the π^0 life-time in the reaction $\gamma Z \to Z\pi^0$. In 1960 Low [119] has drawn attention to the fact that the π^0 life-time can be measured also in $e^{\pm}e^-$ collisions in the reaction ee → ee π^0 (fig. 1). Simultaneously Calogero and Zemach [161] have considered the two-photon reaction ee → ee $\pi^+\pi^-$. However, the rates involved seemed unmeasurable at that time and no further work was done.

Since 1969 in view of the increase of accelerator energy a wide streem of papers devoted to the two-photon particle production appeared. In the early papers of this generation, production of $\pi\pi$

[‡] The direct determination of these quantities through their production cross sections is impossible since ϵ is a very wide resonance and since S^* lies near threshold.

and KK systems, π^0 and η-mesons was considered (De Celles and Goehl [162], Arteaga-Romero, Jaccarini, Kessler, Parisi [1]).

These authors have pointed out the possibility to study some problems of hadron physics in these experiments. In the papers [2, 163, 7] Balakin, Budnev and Ginzburg have shown that from the colliding beam experiments one could extract information on a new fundamental process namely $\gamma\gamma \to$ h. They have also given the necessary formulas and estimations. Almost simultaneously with ref. [2] the paper of Brodsky, Kinoshita and Terazawa [3] appeared, in which the conclusion for a dominant role of the two-photon channel was made on the basis of the study of the reaction $ee \to ee\pi^+\pi^-$ within the frame of QED.

Later on similar problems were widely discussed by various authors, which considered a new domain of variables (e.g. Choban and Shechter [164], Kunszt [108], Terazawa [106]) or new experimental set-ups (e.g. Carlson and Tung [143], Cheng and Wu [18], Baier and Fadin [165], Chernyak and Serbo [166]), as well as the influence of some experimental limitations (e.g. Kessler with collaborators [16], Slivkov and Schwartzman [17], Brodsky et al. [5]) etc. A number of papers devoted to $\gamma\gamma \to$ h physics have also appeared (cf. section 3).

As a result many physicists reached the definite point of view about the two photon processes. To all appearances correct statements coexist often with the erroneous ones in the corresponding literature.* We hope that the consideration given in this section will allow particularly to dissipate similar mistakes.

This section is intended to focus the readers attention on the results only. The basic kinematical information which is necessary to read this section is contained in sub-section 1.6. If the reader will desire to retrace the derivations of the formulas of this section he should read section 5 before section 4.

4.1. *Ways of extracting information about the* $\gamma\gamma \to$ h *process*

1. An accurate separation of the two-photon channel demands *measuring the momenta of the scattered electrons.* In this case the procedure of extracting information about the $\gamma\gamma \to$ h transition is quite similar to that used in experiments on deep inelastic ep-scattering. The parameters of the hadron system on the whole (W^2, q_1^2, q_2^2) are fixed in full from the known electron momenta. Such an approach seems very attractive from a theoretical point of view since here it is possible to investigate the $\gamma\gamma \to$ h transition both on mass shell and far away from it.

In the considered set-up the relations (5.12), (5.13) solve completely the problem of extracting the information on the $\gamma\gamma \to$ h transition from experimental data. We shall consider in details in the next sub-section how and what information can be extracted in some important kinematical domains in such a set-up. We follow below, in the main, the papers of Balakin, Budnev and Ginzburg [2, 7, 163], where this set-up has been suggested and analysed in details. (A discussion of such a set-up is contained also in refs. [143, 164, 168].)

Note that for the elimination of background due to pure electromagnetic processes such as $ee \to ee\gamma\gamma$, $ee \to eee^+e^-$, ..., one should record the scattered electrons in coincidence with a produced hadron. This requirement gives a rise to very complicated problems due to limited effi-

*Two typical mistakes are wide-spread: 1) For the estimations one uses often the wrong equivalent photon spectra from [119, 3]. 2) The opinion disseminate that the total cross section decreases as W_{min}^{-2} with rising the threshold W_{min} of the recorded effective hadron mass (cf. [167]). The first of these mistakes is discussed in details in section 6.7, and the second one in section 4.3.

ciency of recording this hadron, when the produced hadron momentum distribution is unknown. At present such a problem is solved only for the production of resonances, which decay into two particles [5, 16, 17], and also for pion (kaon) pair production [5, 16]. (The analysis of kaon and pion pair production [5, 16] was made neglecting strong interactions. Such a description is probably valid near threshold (cf. sections 3.5–6). An extension of these results to a domain of large effective masses $W \gtrsim 1$ GeV can result in errors.)

The problem on the efficiency of hadron recording was not yet discussed in full. We discuss below (at the end of section 4.3) only the effect of the distribution over hadron tranverse momentum which is important at solving this problem.

For studying inclusive cross section (e.g. $e^{\pm}e^{-} \to e^{\pm}e^{-}\pi + ...$) the problem of the efficiency of hadron recording becomes however purely technical. Here one can use the relation (5.12), (5.13) and formulas of section 4.2 with the trivial substitution $\sigma_{ab} \to d\sigma_{ab}/d^3k_{\pi}$. Taking into account the hadron azimuthal asymmetry one can use here Karlson and Tung's results [143].

Provided the electrons and one hadron are recorded, the only background process is the bremsstrahlung hadron production (fig. 27). We discussed it in section 4.6 (but irrespectively of the problem of the efficiency of hadron recording).

2. Another experimental set-up is also widely discussed where only hadron moments are measured (like the wide-angle experiments of the type discussed in [9]). In these experiments using the hadron distributions one can define, in principle, the on-shell $\gamma\gamma \to h$ helicity amplitudes only.

In this case for obtaining any complete information on the $\gamma\gamma \to h$ transition, in $e^{+}e^{-}$ collisions it is necessary to measure the momenta of all the produced hadrons. (This is difficult because of the neutral hadrons and those emitted at small angles.) Therefore, it is useful here to know the specific features of the two-photon mechanism.

For the production of an arbitrary hadron system in the two-photon channel, the distribution in the total transverse momentum $k_{\perp}$ is very distinctive. At $k_{\perp}^2 < m_{\pi}^2$ it has the form (5.31) $(dk_{\perp}^2/k_{\perp}^2)\ln k_{\perp}^2$. (If one hadron is not recorded, then the distribution in the total transverse momentum of the visible hadrons which are left becomes more smooth.) This allows one to test the recording efficiency of the entire hadron system produced and its two-photon origin.

The two-photon particle pair production is characterized also by a sharp distribution (5.46) in the non-coplanarity angle ψ (between $\boldsymbol{k}_{1\perp}$ and $-\boldsymbol{k}_{2\perp}$)

$$d\sigma \propto \frac{d\psi}{\psi} \ln\left(\psi \frac{E}{m_e}\right) \quad \text{at} \quad \frac{m_e}{E} \ll \psi < 1. \tag{4.1}$$

The sharpness of this distribution has already been used for the identification of two-photon production of $e^{+}e^{-}$ pairs [9] and $\mu^{+}\mu^{-}$ pairs [11]. In this experimental set-up an investigation of the π and K pair production at not very large values of their summary effective mass $W \lesssim 1$ GeV seems the most realistic. In the next sub-section we discuss, what information can be extracted from such experiments.

The background problem for colliding $e^{-}e^{-}$ beams should be solved in a similar way as in the previous experimental set-up. In the colliding $e^{+}e^{-}$ beams the separation from the annihilation channel may make good use of the record of the presence of though one scattered electron. At the same time, even rather rough energy measurement for both scattered electrons permits to control the absence of hadrons which would be not-recorded in the given event.

4.2. *What can be measured and how*

1. In such a set-up, when *the momenta of the scattered electrons are measured,* equations (1.8) or (5.12), (5.13) solve completely the problem of extracting information on $\gamma\gamma \to$ h transition from the experimental data. Measuring the angular and energy distributions of these electrons by means of (1.8) or (5.12) one can, in principle, find six $\gamma\gamma \to$ h amplitudes σ_{TT}, σ_{TS}, σ_{ST}, σ_{SS}, τ_{TT}, τ_{TS} depending on W^2, q_1^2, and q_2^2.* The coefficients ρ_i^{ab} of (1.8) in front of these functions depend only on the electron momenta and in this sense are completely defined by (5.13). In a number of regions of importance these relations are simplified and become more clear.

A. The main contribution to the cross section is given by the region of small angles of electron scattering θ_i (these electrons can be extracted e.g. by means of a magnetic field in the interaction domain). From (5.12), (5.13) at $m_e^2 \ll |q_i^2| \ll W^2$ with the accuracy limited only by $|q_i^2|/W^2 \lesssim \theta_i^2 s/W^2$ we obtain [2] (see notations in fig. 21)

$$\frac{d\sigma}{dE_1 dE_2 d\Omega_1 d\Omega_2} = \left(\frac{\alpha}{8\pi^2}\right)^2 \frac{(E^2+E_1^2)(E^2+E_2^2)}{E^4(E-E_1)(E-E_2)\sin^2\frac{1}{2}\theta_1 \sin^2\frac{1}{2}\theta_2}\, \sigma^{exp}_{\gamma\gamma\to h}; \tag{4.2}$$

$$\sigma^{exp}_{\gamma\gamma\to h} = \sigma_{TT} + \xi_2\sigma_{TS} + \xi_1\sigma_{ST} + \xi_1\xi_2(\sigma_{SS} + \tfrac{1}{2}\tau_{TT}\cos 2\varphi) - \delta\cdot\tau_{TS}\cos\varphi.$$

In this approximation

$$W^2 = 4(E-E_1)(E-E_2), \qquad q_i^2 = -4EE_i\sin^2\tfrac{1}{2}\theta_i;$$

$$\xi_i = \frac{2EE_i}{E^2+E_i^2}, \qquad \delta = 4\frac{E\sqrt{E_1E_2}(E+E_1)(E+E_2)}{(E^2+E_1^2)(E^2+E_2^2)}. \tag{4.3}$$

Here φ is the (azimuthal) angle between the electron scattering planes.

It is seen from here that one can find τ_{TT} and τ_{TS} measuring the azimuthal asymmetry of the scattered electrons. To measure σ_{ab} separately it is necessary to study the dependence of $\sigma^{exp}_{\gamma\gamma\to h}$ on ξ_i. In the main region $E \approx E_i \gg \omega_i$, where the quantities ξ_i are close to 1, one can measure only a combination $\sigma_{TT} + \sigma_{TS} + \sigma_{ST} + \sigma_{SS}$.

A similar study of the region of deep virtuality for both photons $|q_i^2| \sim W^2 \ll s$ has been carried out by Choban and Shechter [164].

B. If the scattering angle of one of the electrons (e.g. of the second one) is very small, then the information only on *real photon collision with the virtual* one can be extracted [1, 163]. Such a set-up is indeed more natural when the energies of both scattered electrons and scattering angle of the first electron are all measured. (The scattering angle of the second electron which is inside the interval $\theta_2 \leqslant \theta_m \ll m_\rho/E$ is not measured.) The corresponding cross section obtained with accuracy $\eta \sim \max\{|q_1^2|/W^2; (\theta_m^2 EE_2)m_\rho^{-2}\ln^{-1}(E^2\theta_m^2 m_e^{-2})\}$ has the form

*From polarized electron experiments one can, in principle, define the remaining two functions τ^a_{TT} and τ^a_{TS} by means of (5.12), (5.13a). However, such measurements are hardly possible in the near future, since in the main region covered by the kinematic variable the coefficients A and B (5.13a) appearing in front of τ^a_{TT} and τ^a_{TS} are very small. After azimuthal averaging their relative values are of order of m_e^2/s (in comparison with that in front of σ_{TT}). The terms in A and B connected with the azimuthal asymmetry in the main region are also small. But in the region of very small $|q_i^2|$ where such terms are of order of 1, measuring the azimuthal asymmetry is doubtful.

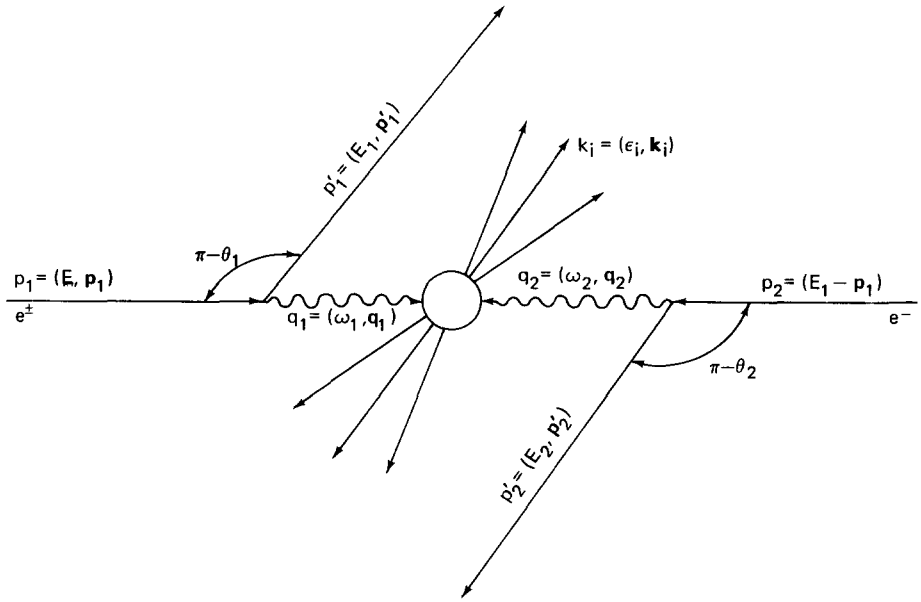

Fig. 21. The kinematics of the two-photon particle production for colliding $e^{\pm}e^{-}$-beams.

$$\frac{d\sigma}{dE_1 dE_2 d\cos\theta_1} = \frac{\alpha}{4\pi} \frac{(E^2 + E_1^2)N(E_2, \theta_m)}{E^2(E - E_1)(E - E_2)\sin^2 \frac{1}{2}\theta_1} (\sigma_{TT} + \xi_1 \sigma_{ST}); \tag{4.4}$$

$$N(E_2, \theta_m) = \frac{\alpha}{\pi}\left[\frac{E^2 + E_2^2}{E^2} \ln \frac{EE_2\theta_m}{m_e(E - E_2)} - \frac{E_2}{E}\right]; \qquad EE_2\theta_m \ll m_\rho^2.$$

It is seen from this relation that, in this set-up, only σ_{TT} and σ_{ST} at $q_2^2 = 0$ can be determined.*

C. If both scattering angles are small, then information only on *the real photon interaction* can be extracted (i.e. on the W^2 dependence of σ_{TT} on mass shell). It is necessary then to record all the electrons scattered within the angular range $\theta_{1,2} \leqslant \theta_m \ll m_\rho/E$. It is sufficient to measure the energies E_1, E_2 of these electrons but their scattering angles $\theta_{1,2}$ themselves are unnecessary to measure. Then and with the relative inaccuracy $EE_i\theta_m^2[m_\rho^2 \ln(E^2\theta_m^2/m_e^2)]^{-1}$ we have

$$\frac{d\sigma}{dE_1 dE_2} = \frac{1}{(E - E_1)(E - E_2)} N(E_1, \theta_m)N(E_2, \theta_m)\sigma_{TT}(W^2). \tag{4.5}$$

In such a set-up one can, in particular, investigate *the C-even resonances with spin* $J \neq 1$. The position of the maximum and the width of the $d\sigma/dW^2$ curve give the value $(2J + 1)\Gamma^{\gamma\gamma}$ (cf. (3.24)). The resonance spin can be found from (4.13) if $\sigma_{\gamma\gamma \to R}$ and $\Gamma^{\gamma\gamma}$ are known, as well as from the details of the angular distribution (Budnev, Slivkov [120]). Measuring the sign of the quantity τ_{TT} should allow the determination of the resonance parity (cf. (3.8)) [50].

*For this set-up a term "deep inelastic scattering of electron on the photon target" [115] was suggested in a number of papers. We note that in the above papers the wrong spectrum $N(E_2, \theta_m)$ is used (for details see section 6.7).

D. More detailed information can be extracted by measuring both the distribution of the electrons and that of the produced hadrons (not necessary all). Carlson and Tung [143] have obtained the differential distribution for an inclusive reaction with one or two detected hadrons. This distribution $d\sigma$ involves 20 independent combinations of the helicity amplitudes $M^*_{a'b'}M_{ab} \equiv T_i$. When averaging over azimuthal directions the $d\sigma$ has the same form as (5.12); the $d\sigma$ involves 6 terms T_i with $a-b = a'-b'$. The azimuthal asymmetry of the produced hadrons is due to the 14 rest T_i (with $a-b \neq a'-b'$). Thus, measuring the corresponding cross sections with the help of these formulas, one can find not only the differential cross sections but also density matrix elements for the given $\gamma\gamma \to$ h channel.

2. In a set-up where *hadron momenta only* are measured the pion (kaon) pair production was the only case investigated in details.* The two photon origin of these hadrons may be tested by an inherent sharp distribution over the total transverse momentum $k_\perp$ or acoplanarity angle ψ (between the hadron production planes).

We consider here separately three regions for the total transverse momentum of the pion pair, namely: a) $k_\perp^2 \gtrsim \lambda^2$, b) $k_\perp^2 \lesssim m_e^2$, c) $m_e^2 \ll k_\perp^2 < \lambda^2$. (Here λ^2 is a specific parameter for the variation of amplitudes M_{ab} as a function of t and q_i^2.)

In a first case the dependence of the amplitudes M_{ab} on q_i^2 cannot be neglected. It is essential since the cross section $d\sigma/d^3k_1 d^3k_2$ is expressed in terms of integrals over q_i^2 of the amplitudes M_{ab} multiplied by nontrivial weight functions (ρ_i^{ab}). Therefore, extracting interesting information on the transition $\gamma\gamma \to \pi\pi$ in this region is rather difficult to say at least.

Using Cheng and Wu's [18] formulas one can, in principle, find M_{++} and M_{+-} and the relative phase of M_{++} and M_{+-} on the mass shell in the range $k_\perp^2 \lesssim m_e^2$. However, the measurement of such a small $k_\perp$ is a complicated experimental problem. One should measure the pion momenta with very high accuracy so that the corresponding inaccuracy $\Delta k_{i\perp}$ is rather less than m_e.

More information on the amplitudes M_{ab} can be extracted from the range $(m_e\omega_i/E)^2 \ll k_\perp^2 \ll \lambda^2$ which gives the main contribution to the cross section. In this range the pion differential distribution $d\sigma/d^3k_1 d^3k_2$ depends on six combinations of three helicity amplitudes M_{ab} and on the pion form factor F_π (5.40). If the pion momenta are measured rather accurately, the study of the angular and energy correlations between pions allows, in principle, to extract from experiment all the six combinations (Cernyak, Serbo [166])** by means of (5.40)

$$\begin{aligned} &\tfrac{1}{2}(|M_{++}|^2 + |M_{+-}|^2) \propto d\sigma_{\gamma\gamma\to\pi\pi}/dt; \qquad \mathrm{Re}(M^*_{-+}M_{++}); \qquad |M_{+-}|^2 \\ &\mathrm{Re}[(M^*_{-+}M_{0+} + M^*_{--}M_{0-})/i\sqrt{-q_1^2}]; \qquad \mathrm{Re}(F^*_\pi M_{++}); \qquad \mathrm{Re}(F^*_\pi M_{+-}). \end{aligned} \tag{4.6}$$

The measurement of the first three quantities allows to extract the module and relative phase of the on-shell amplitudes M_{++} and M_{+-}. The fourth combination describes the relative value of amplitudes with scalar photon participating as compared to those with a purely transverse photon. A measurement of the charge asymmetry among pions allows to extract the last two combinations, i.e. the relative phases F_π and amplitudes M_{++} and M_{+-} ($|F_\pi|$ is found from experiment in the annihilation channel).

*For calibration of hadronic events it is useful together with the hadron production to measure also in the same set up the $\mu^+\mu^-$ pair production (the related formulas for the $\mu^+\mu^-$ pair production are given in sections 5.5–6 and appendix E.

**A relative order of the neglected terms in (5.40) is $\sim k_\perp^2/\lambda^2$. The accuracy of defining the first two combinations (4.6) is of the same order and for the rest the accuracy is not worse than $\sim k_\perp/\lambda$, ($\lambda \gtrsim m_\pi$).

As it was discussed in section 3.6 for a wide range of $W \lesssim 1$ GeV while describing the $\gamma\gamma \to \pi\pi$ process one can restrict himself to the approximation of two-particle unitarity (3.36). In this approximation the phases of the partial amplitudes of the $\gamma\gamma \to \pi\pi$ and $\gamma^* \to \pi\pi$ processes are equal to those of $\pi\pi$-scattering. Since the form factor F_π depends only on W^2, the phase analysis of the two latter quantities in (4.6) is simpler than that of the first four ones. For example, the quantity $|M^J_{++}| \cos(\delta_J - \delta_1)$ can be defined from the relation

$$\int_{-1}^{1} \mathrm{Re}(F^*_\pi M_{++}) P_J(\cos\theta)\, \mathrm{d}\cos\theta \propto |F_\pi| \cdot |M^J_{++}| \cos(\delta_J - \delta_1). \tag{4.7}$$

Here M^J_{++} is a partial amplitude with momentum J, and δ_J is the related $\pi\pi$ phase (we remind that unlike the $\pi\pi$-amplitudes, the amplitudes M^J_{++} with $J \geqslant 2$, are not small to all appearances when compared to M^0_{++} and this already at $W^2 \gtrsim 5m_\pi^2$ [143]). At threshold values of W the measurement of the interference contributions $\mathrm{Re}(M^*_{++}M_{+-})$ and of $\mathrm{Re}(F^*_\pi M_{++})$ permits to find directly the phases $\delta_0 - \delta_2$ and $\delta_0 - \delta_1$, i.e. the $\pi\pi$ scattering lengths.

All the combinations (4.6) except the first one (proportional to the cross section for real unpolarized photon scattering $\mathrm{d}\sigma_{\gamma\gamma}/\mathrm{d}t$) are included into the cross section (5.40) with factors depending on the azimuthal angle χ (between $\boldsymbol{k}_\perp$ and $\boldsymbol{k}_{1\perp} - \boldsymbol{k}_{2\perp}$). Therefore, it is necessary for their determination to measure pion momenta $k_{i\perp}$ with error $\Delta k_{i\perp}$, essentially smaller than $k_\perp$. Otherwise, an effective averaging over angle χ (as in (5.45a)) takes place:

$$\langle \mathrm{d}\sigma \rangle_\chi = \frac{2\alpha^2}{\pi^4 k_\perp^2} \frac{\mathrm{d}\sigma_{\gamma\gamma\to\pi\pi}}{\mathrm{d}t} \left[g_1 \left(\ln \frac{k_\perp^2 s}{m_e^2 W^2} - 1 \right) + g_2 \right] \frac{\mathrm{d}^3 k_1 \mathrm{d}^3 k_2}{\epsilon_1 \epsilon_2}$$
$$g_1 = \left(1 - \frac{\epsilon}{2E}\right)^2 + \tfrac{1}{4}\left(\frac{\epsilon}{E} - \frac{W^2}{s}\right)^2; \qquad g_2 = \left(\frac{\epsilon}{2E}\right)^2 - \frac{W^2}{2s}\left(1 + \frac{\epsilon}{2E} - \frac{W^2}{2s}\right). \tag{4.8}$$

(it is necessary to put $\boldsymbol{k}_{1\perp} = -\boldsymbol{k}_{2\perp}$ in $\mathrm{d}\sigma_{\gamma\gamma}/\mathrm{d}t$). In such a case one can define only $\mathrm{d}\sigma_{\gamma\gamma\to\pi\pi}/\mathrm{d}t$.

In the dominant range $k_{i\perp} \sim m_\pi$ a measurement accuracy for the pion moments of $\sim 2\%$ gives an error $\Delta k_{i\perp} \sim 3$ MeV/c. It means that the combinations which appear in (4.6), except $\mathrm{d}\sigma_{\gamma\gamma}/\mathrm{d}t$, can be measured in the range $k_\perp \gtrsim 10$–15 MeV/c only.

4.3. *Estimates of the measurable cross sections*

Discussing the feasibility of measurements for one or an other quantity, it is useful to have values for the related cross sections. Here highly rough estimates are sufficient and only that can be made when one has only very preliminary information on the two-photon amplitudes.

The cross sections for production of some hadron systems are plotted in figs. 22–23.

Let us give some estimations for $\sqrt{s} = 7$ GeV. In accordance with (4.12) for the investigation of the W^2 dependence of a $\sigma_{\gamma\gamma}$ at $W^2 = 5$ GeV^2 it is necessary to measure the cross sections which have the following order of magnitude (cf. (3.5–6)):

$$\Delta\sigma_{\mathrm{ee}\to\mathrm{eeh}} \approx \begin{cases} 10^{-34}\ \mathrm{cm}^2 & \text{for } \gamma\gamma \to \mathrm{h} \\ 10^{-35}\ \mathrm{cm}^2 & \text{for } \gamma\gamma \to \rho^0\rho^0. \end{cases} \tag{4.9}$$

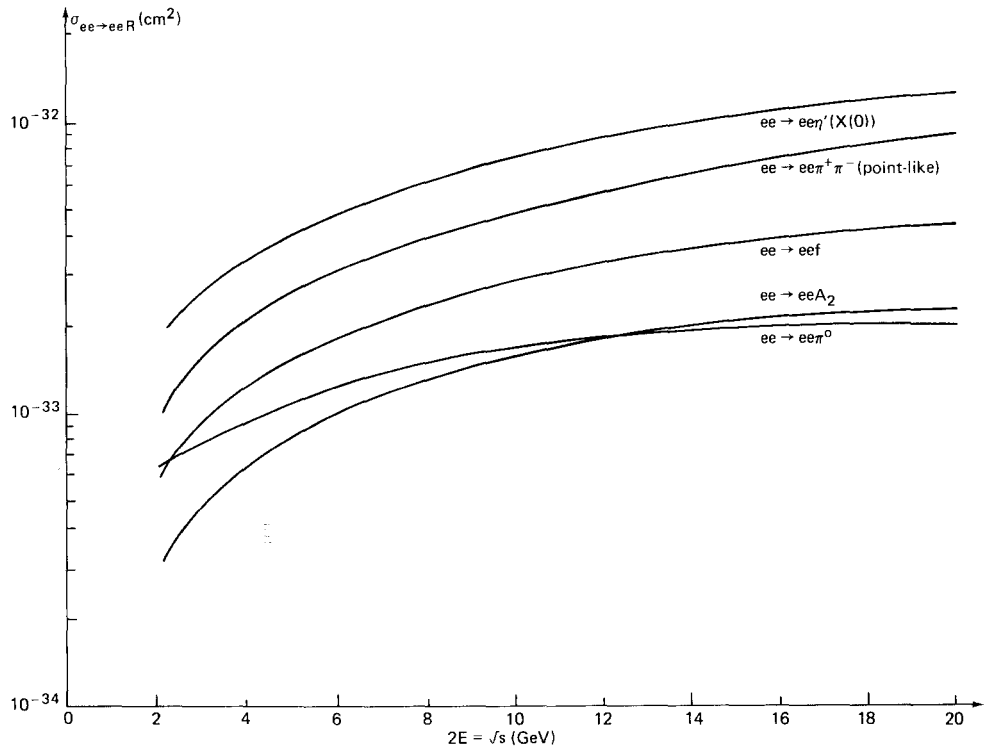

Fig. 22. Cross-sections for two-photon resonance production, $e^{\pm}e^{-} \to e^{\pm}e^{-}R$, calculated by means of eq. (4.13). Here the next values of two-photon widths $\Gamma^{\gamma\gamma}$ were used: a) for π^0-average world data [69]; b) for the X^0-product $B(X^0 \to \gamma\gamma)\Gamma_{max}$, where $B(X^0 \to \gamma\gamma)$ is the known branching ratio of $\gamma\gamma$ decay and Γ_{max} is the maximal instrumental value of the total width [69]; c) for other resonances $\Gamma^{\gamma\gamma} = \alpha^2\Gamma$, which is often the average value of different theoretical estimations. The $ee \to ee\pi^+\pi^-$ cross section is calculated by means of QED [4] (Born approximation).

Estimating the possibility of a measurement for the dependence of σ_{TT} on W^2 and q_i^2 one should keep in mind that each of the integrations over q_i^2 gives a large factor $\ln(m_\rho^2 s/m_e^2 W^2) \sim 15$. No such an integration takes place while measuring the cross section dependence on q_i^2 and the corresponding factor is replaced by $\Delta q_i^2/q_i^2$, i.e. in this case within the averaging interval $\Delta q_i^2/q_i^2 \sim \frac{1}{2}$, cross sections which are 30 times less, have to be measured (we do not take into account here the change of σ_{TT} while leaving the mass shell). Thus, to measure the dependence of the $\gamma\gamma \to h$ cross section on W^2 and q_i^2 one should measure cross sections which have the following order of magnitude:

$$\Delta\sigma_{ee\to eeh} \sim \begin{cases} 3 \times 10^{-36}\ \text{cm}^2; & |q_2^2| < m_\rho^2 \\ 10^{-37}\ \text{cm}^2; & \Delta q_2^2/q_2^2 = \frac{1}{2} \end{cases}; \quad \frac{\Delta W^2}{W^2} = \frac{1}{3}; \quad \frac{\Delta q_1^2}{q_1^2} = \frac{1}{2}; \quad W^2 \gtrsim 2\ \text{GeV}^2. \qquad (4.9b)$$

More detailed estimations can be obtained with the help of the equations discussed below. There the measurable cross section is expressed in terms of the $\gamma\gamma \to h$ cross sections which are the quantities of interest. For particular estimations it is necessary to use a definite assumption on these $\gamma\gamma \to h$ cross sections, e.g. one of those discussed in section 3; e.g., for the $\gamma\gamma \to \pi^+\pi^-$ transition near threshold ($W \sim 2m_\pi$) one can use the QED result and, for resonance production equation (3.24).

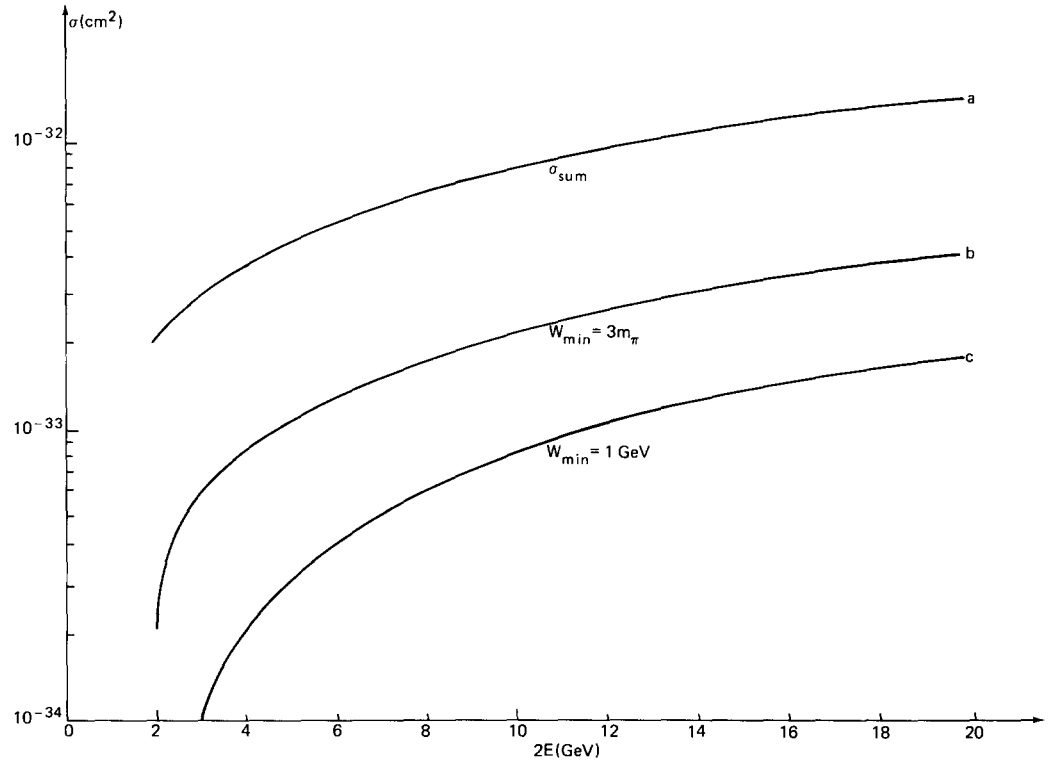

Fig. 23. The ee → eeh cross-sections. a) The total ee → eeh cross section, as a sum of contributions ee → ee$\pi^+\pi^-$, ee → eeS*, ee → eef, ee → eeA_2 and of curve b. b, c) The ee → eeh cross sections calculated for the $\sigma_{\gamma\gamma\to h} \approx \sigma_{\gamma p}\sigma_{\gamma p}/\sigma_{pp} \approx \alpha^2/3m_\pi^2$ and at $W^2_{min} = (3m_\pi)^2$ (b) or $W^2_{min} = 1$ GeV^2 (c).

1. *The set-up, in which the momenta of the scattered electrons are measured.*

A. Let us discuss firstly the question of finding the on mass shell cross section $\sigma_{\gamma\gamma}(W^2)$ and the role of experimental limitations in this case as well:

$$\theta_i \leqslant \theta_m < 1; \quad E_i \leqslant E_m; \quad (\omega^{exp}_{min} = E - E_m). \tag{4.10}$$

Under these conditions the measurable cross section has the form:*

*For obtaining this equation it is sufficient to use the equivalent photon expression (cf. (5.26)):

$$d\sigma = \sigma_{\gamma\gamma}(W^2)\frac{dW^2}{W^2}\int N(\omega_1)N\left(\omega_2 = \frac{W^2}{4\omega_1}\right)\frac{d\omega_1}{\omega_1}; \tag{4.11a}$$

$$N(\omega_i) = \frac{\alpha}{\pi}\left[\left(1 - \frac{\omega_i}{E} + \frac{\omega_i^2}{2E^2}\right)\ln\frac{q^2_{i\max}}{q^2_{i\min}} - \left(1 - \frac{\omega_i}{E}\right)\left(1 - \frac{q^2_{i\min}}{q^2_{i\max}}\right)\right].$$

Here

$$q^2_{i\min} = m_e^2\omega_i^2/E(E-\omega_i); \qquad q^2_{i\max} = \min\{m_\rho^2; E(E-\omega_i)\theta^2_m\}. \tag{4.11b}$$

The limits of integration over ω_1 in (4.11a) are determined either by the experimental limitations or – if no such limitations exist – by conditions $\omega_i < E$ and $q^2_{i\min} < q^2_{i\max}$, i.e.

$$\max\{\omega^{exp}_{1\min}; W^2/4\omega_{2\max}\} \leqslant \omega_1 \leqslant \min\{\omega^{exp}_{1\max}; W^2/4\omega_{2\min}; E\}. \tag{4.11c}$$

The expression obtained for the cross section $d\sigma/dW^2$ (a single integral) has the high accuracy $\eta \sim E^2\theta^2_m[m_\rho^2\ln(m_\rho^2 s/m_e^2W^2)]^{-1}$. Graphs for these cross sections for some particular values of the parameters W, θ_m, ω_{min} and s are given in refs. [16, 17, 5].

For estimations of experimental feasibilities less accuracy is sufficient. In particular, with logarithmic accuracy eq. (4.11) is reduced to (4.12).

$$\frac{d\sigma}{dW^2} = \left(\frac{\alpha}{\pi}\right)^2 \frac{\sigma_{\gamma\gamma}(W^2)}{W^2}\left[\left(\ln\frac{sE^2\theta_m^2}{W^2 m_e^2} - 1\right)^2 \varphi\left(\frac{s}{W^2}, \frac{W^2}{4\omega_{min}^2}\right) - \frac{1}{3}\left(\ln\frac{W^2}{4\omega_{min}^2}\right)^3\right],$$

$$\varphi(x, y) = \left(1 + \frac{1}{2x}\right)^2 \ln y - 2\sqrt{\frac{y}{x}}\left(1 + \frac{1}{2x}\right)\left(1 - \frac{1}{y}\right) + \frac{y}{2x}\left(1 - \frac{1}{y^2}\right). \tag{4.12}$$

The inaccuracy of this expression is limited to $\eta \sim [\ln(s^2\theta_m^2/W^2 m_e^2)]^{-1}$. (For $\sqrt{s} = 7$ GeV this inaccuracy becomes less than 0.1 already at $\theta_m \geqslant 1^0$.) This expression is correct for $E\theta_m < m_\rho$ and $W^2 < 4E\omega_{min}$. If $W^2 \geqslant 4E\omega_{min}$, then in (4.12)

$$\varphi(x, y) \to f(x) = \left(1 + \frac{1}{2x}\right)^2 \ln x - \frac{1}{2}\left(1 - \frac{1}{x}\right)\left(3 + \frac{1}{x}\right). \tag{4.12a}$$

If $E\theta_m > m_\rho$ then in (4.12)

$$E^2\theta_m^2 \to m_\rho^2. \tag{4.12b}$$

In particular, a resonance production cross section is obtained from (4.12) after substitution of $\sigma_{\gamma\gamma\to R}$ according to (3.24) [120]:

$$\sigma_{ee\to eeR} = (2J+1)\frac{8\alpha^2\Gamma^{\gamma\gamma}}{m_R^3}\left[\left(\ln\frac{sm_\rho^2}{m_R^2 m_e^2} - 1\right)^2 f\left(\frac{s}{m_R^2}\right) - \frac{1}{3}\left(\ln\frac{s}{m_R^2}\right)^2\right]. \tag{4.13}$$

Let us note that such an approximation is not valid for the ϵ-meson production since $\Gamma_\epsilon \sim m_\epsilon$.

Under the limitations (4.10) an effective hadron mass W cannot be less than $2\omega_{min}^{exp}$. If W only slightly exceeds $2\omega_{min}^{exp}$ or W is close to $\sqrt{s}$, the accessible phase-space volume is small and the limitation on the electron energy leads to small cross sections.

Equation (4.12) shows us that when leaving the threshold region $W \sim 2\omega_{min}^{exp}$ the main dependence on W has rhe form $d\sigma \propto [\sigma_{\gamma\gamma}(W^2)/W^2]\,dW^2$. If $\sigma_{\gamma\gamma}(W^2)$ decreases as W^2 increases the quantity $\Delta\sigma = \int_{W^2_{min}}^{W^2_{max}} (d\sigma_{ee\to eef}/dW^2)dW^2$ is determined by the value of the lower bound: $\Delta\sigma \sim \alpha^2\sigma_{\gamma\gamma}(W^2_{min})$. Such a W^2_{min} dependence takes place, e.g. for e^+e^- or $\mu^+\mu^-$ two-photon production, when $\Delta\sigma \sim \alpha^4/W^2_{min}$. If $\sigma_{\gamma\gamma}(W^2)$ changes weakly as W^2 increases then $\Delta\sigma \sim \alpha^2\sigma_{\gamma\gamma}^{char}\ln(W^2_{max}/W^2_{min})$. The same dependence on the region bounds should take place for hadron production as $\sigma_{\gamma\gamma\to h} \to$ const. when $W^2 \to \infty$. (Therefore, the often cited statement [167] that with increasing W^2_{min} the total observed ee → eeh cross section should fall as $1/W^2_{min}$ is incorrect.) In particular, fig. 23 shows that the cross sections calculated at different W^2_{min} are brought together as s increases. For example, at $\sqrt{s} = 20$ GeV the ratio $\Delta\sigma(W^2_{1\,min} = 0.16\ \text{GeV}^2)/\Delta\sigma(W^2_{2\,min} = 4\ \text{GeV}^2)$ is markedly smaller than the ratio $W^2_{2\,min}/W^2_{1\,min} = 25$. In particular, the asymptotical behaviour of the ee → eeh cross section which depends on W_{min} can be obtained after the substitution of the asymptotic value $\sigma_{\gamma\gamma} = \sigma_{\gamma p}\sigma_{\gamma p}/\sigma_{pp} \approx \alpha^2/3m_\pi^2$ into (4.12) [7]:

$$\sigma_{ee\to eeh} = \frac{\alpha^4}{18\pi^2 m_\pi^2}\ln\frac{sm_\rho^2}{m_e^2 W^2_{min}}\left(\ln\frac{s}{W^2_{min}}\right)^2 \ln\frac{sm_\rho^6}{m_e^6 W^2_{min}}. \tag{4.14}$$

B. *An estimation of feasibility of measuring* $\sigma_{\gamma\gamma}$ *depending on* W^2 *and* q_1^2 *at* $q_2^2 \approx 0$. Under the limitations (4.10) for the energies of both electrons and the emission angle of the second electron we have from (4.2):

$$d\sigma = \left(\frac{\alpha}{\pi}\right)^2 \frac{dq_1^2}{q_1^2} \frac{dW^2}{W^2} \left\{\varphi\left(\frac{s}{W^2}, \frac{W^2}{4\omega_{min}^2}\right)\sigma_{TT} + \tilde{\varphi}\left(\frac{s}{W^2}, \frac{W^2}{4\omega_{min}^2}\right)\sigma_{ST}\right\}\left[\ln\frac{E^2\theta_m^2}{W^2 m_e^2} - 1\right];$$

$$\tilde{\varphi}(x, y) = \left(1 + \frac{1}{x}\right)\ln y - \sqrt{\frac{y}{x}}\left(1 - \frac{1}{y}\right)\left(2 + \frac{1}{2x}\right) + \frac{y}{4x}\left(1 - \frac{1}{y^2}\right). \tag{4.15}$$

The accuracy of this expression is the same as that of (4.12).

C. The possibility of *measuring the $\gamma\gamma$-cross sections as a function of W, q_1^2 and q_2^2* can be estimated with the help of the distribution $d\sigma/dW^2 dq_1^2 dq_2^2$, obtained by Bonneau, Gourdin and Martin [170] for arbitrary values of q_i^2 and W^2.

In the important range for this purpose, $m_e^2 \ll |q_i^2| < W^2$, one can use (4.2) in which it is necessary to switch to new variables $d\varphi dq_1^2 dq_2^2 dW^2 d\omega_1$ and to perform the trivial integrations over φ and ω_1. In the other region of interest, $W^2 \ll |q_i^2| \ll s$, the measurable cross sections are very small. A corresponding estimate has been found by Kunzst [108]:

$$d\sigma = 12\frac{\alpha^2}{\pi^2}\frac{dq_1^2 dq_2^2 dW^2}{q_1^2 q_2^2} \cdot \frac{(q_1^2 + q_2^2)^2}{[(q_1^2 - q_2^2)^2 - 2W^2(q_1^2 + q_2^2)]^{3/2}}\left(\ln\frac{s}{2|q_1^2 + q_2^2|}\right)[\sigma_{TT} + \ldots]. \tag{4.16}$$

2. *The set-up in which the momenta of the produced hadrons only are measured.*

A. For *pair production* detail estimations can be obtained with the help of eq. (4.8). We shall give only a simple estimate for the cross section for production of relativistic particles emitted at large angles $\theta_i \sim \frac{1}{2}\pi$ with respect to the beam ($\pi - \theta_{min} \leqslant \theta_i \leqslant \theta_{min}$). It can be easily obtained from (5.47)

$$d\sigma_{ee \to eeA_1A_2} \approx \left(\frac{\alpha}{\pi}\right)^2 dW^2(\tfrac{1}{2}\pi - \theta_{min})^2 \left(\ln\frac{s}{m_e^2}\right)^2 d\sigma_{\gamma\gamma \to A_1A_2}(W^2, t = -\tfrac{1}{2}W^2)/dt. \tag{4.17}$$

In order to estimate the pion pair production cross section at not large W, the Born approximation for $d\sigma_{\gamma\gamma \to A_1A_2}/dt$ (E.6) can be used. It gives $\Delta\sigma \sim 5 \times 10^{-35}$ cm^2 at $W = 0.4$ GeV, $\sqrt{s} = 7$ GeV, $\theta_{min} = \frac{1}{4}\pi$ and $\Delta W^2/W^2 = 0.1$.

B. For *the $\gamma\gamma \to 3\pi$ transition* near threshold, the estimations of the measurable cross section are fullfilled in refs. [171]. (The background due to η decay is also discussed there.)

3. In the set-up, in which the momenta of the scattered electrons are measured, the separation from the background requires that one also record at least one hadron. To understand which restrictions are due to this requirement it is useful to know the character *of the hadron distribution in transverse momentum $k_{1\perp} \equiv p_\perp$*.

A. If the recorded electrons are scattered at small angle ($\gamma\gamma \to$ h transition on mass shell) the momenta of the photons and of the colliding electrons are practically collinear. Therefore the observed distribution in $p_\perp^2$ is the same as in the c.m.s. of the photons, i.e. it does not actually fall practically up to $p_\perp \sim 300$ MeV/c. Indeed, at $W \sim 1-2$ GeV, particle production should take place mainly via resonances R (with $m_R = W$). Since the resonance decay is quasi-isotropic in its rest frame, the distribution of the produced pions in $p_\perp^2$ does not fall up to $p_\perp \sim \frac{1}{4}W - \frac{1}{2}W$. At higher W diffractive photon excitation (i.e. processes of the type $\gamma\gamma \to \rho^0\rho^0$) should play an essential role. Since the decay of such produced vector mesons in their rest frame is quasi-isotropic the

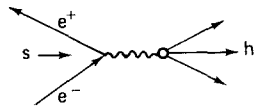

Fig. 24. The annihilation hadron production.

distribution in $p_\perp^2$ should not fall here also up to $p_\perp \sim \frac{1}{2}m_\rho$. (At this point the photon scattering processes can markedly distinguish itself from other hadron collisions in which the distribution in $p_\perp^2$ falls from $p_\perp^2 = 0$.)

B. Let only one final electron be recorded at not too small angle. In this case in order to get the distribution in $p_\perp^2$ one needs also to take into account the transverse movement of the whole $\gamma\gamma$-system with momentum $q_{1\perp} + q_{2\perp}$ (together with the above considered distribution over $p_\perp$ in the $\gamma\gamma$-system, which itself depends on q_i^2). A similar contribution is considered in ref. [153].

C. Let us note that in order to get the total distribution in $p_\perp^2$ for an inclusive set-up such as $e^\pm e^- \to \pi + ...$, it is necessary to take into account all contributions pointed out above together with that of bremsstrahlung production (fig. 27). The estimation [172] reached for such a set-up has only one of these contributions and is underestimated.

4.4. *The annihilation hadron production and its role in processes of higher order in* α

1. For not too high energies of the e^+e^- beams hadrons are practically produced only in the process with the least order in α i.e. annihilation (fig. 24). The energy dependence of this cross section is plotted in fig. 12. Some features of this process are discussed in sections 3.1 and 3.3.

Let us now compare briefly the annihilation channel of hadron production and the two-photon one. If the above estimations are valid for the two-photon channel, then for the present generation of accelerators with colliding $e^\pm e^-$ beams (see table 1) the cross sections for hadron production in the two-photon and in the annihilation channels differ less than in one order of magnitude.*

The angular distribution for hadrons produced in the e^+e^- annihilation is close to the isotropic one and their summary effective mass W equals $\sqrt{s}$. In contrast to this, for the two-photon production of hadrons the W is usually smaller than $\sqrt{s}$, and the beam direction is preferable in their angular distribution.

It is just that difference in the differential distribution that allows one to conclude that the two-photon contribution is relatively small (but noticeable) for the cross section, which has been measured in CEA-SPEAR experiments [67, 203] (namely, one record the event only where more than two particles are emitted with large angles, non-coplanar pair only are taken into account, etc.).

The actual role of the two-photon channel will be understood only in result of measurement including the recording of electrons or one in e^-e^- collisions.

*Up to 1973 one assumed that the $\sigma_{e^+e^- \to h}$ differs little from the $e^+e^- \to \mu^+\mu^-$ cross section for $s > 1$ GeV^2. On this basis one made the conclusion that the two-photon channel of the hadron production would dominate already at $\sqrt{s} \approx 4$–6 GeV. The recent CEA-SPEAR data [67, 203] have shown that the cross section of the annihilation production has a different behaviour. This fact has forced to withdraw our conclusion about the dominant role of the two-photon production in the mentioned energy range.

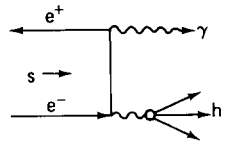

Fig. 25.

2. The same hadron system can be produced in some other processes with higher order in α (figs. 25–27). The cross sections of these processes are found theoretically, if the cross section for annihilation production at lower energies is known. Therefore, their study will not give new information on hadron production by photons. However, they must sometimes be taken into account in interpreting hadron production experiments.

The following estimations are valid for $\sqrt{s} \lesssim 10$ GeV if the σ_h will not increase essentially in this range.*

A. The process of fig. 25 is a radiative correction to the annihilation hadron production process. This process has been discussed in a number of papers (see, e.g. [172]). Its specific feature is an exact relation for the total momentum $|\boldsymbol{k}|$ and the effective mass W of the hadron system: $2|\boldsymbol{k}| = \sqrt{s}(1 - W^2/s)$. For this process

$$\frac{d\sigma_{e^+e^-\to\gamma h}}{dW^2} = \frac{\alpha}{\pi}\left(1 + \frac{W^4}{s^2}\right)\left(\ln\frac{s}{m_e^2} - 1\right)\frac{\sigma_{e^+e^-\to h}(W^2)}{s - W^2}. \tag{4.18}$$

This equation shows us what domains might give the relatively large contribution to the total cross section of hadron production: a) The domain $W \sim m_\rho$, where $\sigma_{e^+e^-\to h}$ is very large (e.g. $\sigma_{e^+e^-\to\gamma\rho} \approx 1$mb for $\sqrt{s} = 3$ GeV). The contribution from this domain decreases as s^{-1} when s increases. b) The domain $W^2 \sim s$, where $d\sigma_{e^+e^-\to\gamma h} \approx 1$ nb $dW^2/(s - W^2)$ for $\sqrt{s} \approx 3$–10 GeV.

Let us note that the singularity of eq. (4.18) at $W^2 \to s$ is the usual infrared divergence due to soft photon emission. This singularity disappears in the total cross section of hadron production after summing the contribution of the process in fig. 25 with the contributions of the other radiative corrections to the diagram in fig. 24 for the process $e^+e^- \to h$. (In this calculation one should write the $e^+e^- \to \gamma h$ cross section for $W^2 \approx s$ with higher accuracy than in (4.18).) The measurable radiative correction depends on the experimental set-up, but it is comparatively small (a few per cent).

B. The cross section of the process in fig. 26 is very small. The process in fig. 27 is discussed in section 4.6.

The next radiative derivatives of the above processes do not generate new effects, since electromagnetic interaction provide no mechanisms leading to the power growth of any cross sections with energies, and corrections of order $\alpha \ln E$ or even of order $\alpha \ln(E/m_e)\ln(E/m_\pi)$ are negligibly small.

*We shall make the most natural hypothesis that at $s \to \infty$ the σ_h falls down as s^{-1}. If such a behaviour will take place, the cross sections of the processes in figs. 25 and 26 fall down in a similar manner with a subsequent increase of s. In this case a relative contribution of all annihilation processes will quickly decrease.

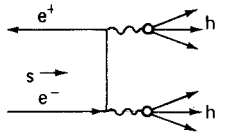

Fig. 26.

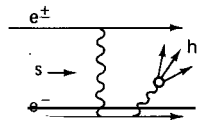

Fig. 27. The bremsstrahlung particle production.

4.5. $\gamma\gamma \to h$ *reaction study in the other regions. The* e^+e^- *beams*

Up to now we have only investigated in detail the most important case of two-photon production. It corresponds to the scheme of fig. 21, and to the region where $q^2_{1,2} < 0$. Such reactions can be studied both in e^+e^- and e^-e^- collisions.

However, one can, in principle, study the $\gamma\gamma \to$ h transition in other variation regions of q_i^2. The corresponding proposals [105, 174, 175] can in principle be realized in e^+e^- collisions only. Unfortunately, the cross sections for the relevant reactions are very small.

1. In papers [174, 175] it was pointed out that a study of the process of fig. 28 permit to extract information on the $\gamma\gamma \to$ h reaction in the region

$$s = q_1^2 > W^2; \qquad q_2^2 = 0. \tag{4.19}$$

The cross section for this process is not very small in that region where annihilation via vector meson production is observed, i.e. at $\sqrt{s} \approx m_V$ [174]. Here the cross section is expressed in terms of the widths for the radiative decays of the vector mesons. Conversaly just the same widths can be found while studying this process. Estimates for the related cross sections are given in [174]. In this process one can also study S-wave $\pi\pi$-scattering [175].

It is natural to expect that with energies extending beyond the resonant region, the behaviour of the cross section for the process of fig. 28 will be like that for one-photon annihilation. This process is either part of the one-photon annihilation processes or is described by associated radiation in annihilation hadron production. Therefore, at $s \to \infty$ one expects

$$\sigma_{28} \lesssim \frac{\alpha^3}{s} \ln s. \tag{4.20}$$

The diagrams of figs. 28 and 25 describe the same process $e^+e^- \to \gamma + h$. However, in a total cross section denoted by σ^{exp}, the contributions of these diagrams do not interfere, since the hadron systems which are respectively produced have different C-parity. At the same time, the cross section σ_{25} for the process of fig. 25 is completely calculated using the known annihilation produc-

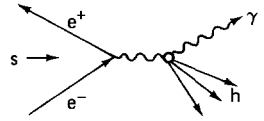

Fig. 28.

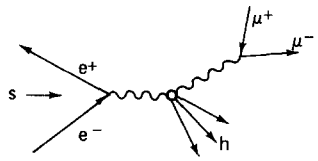

Fig. 29.

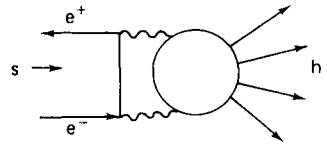

Fig. 30. The two-photon annihilation production.

tion cross section. Therefore, σ_{2s} can be simply subtracted from σ^{exp}, in order to obtain the interesting cross section for the process of fig. 28.

2. In the paper [105] it was suggested to use the process of fig. 29 for extracting information on the reaction $\gamma\gamma \to h$ in the region:

$$s = q_1^2 > W^2, q_2^2; \qquad q_2^2 > 0. \tag{4.21}$$

A study of this process at large values of q_i^2 and W^2 permits to test directly the predictions of the light cone bilocal operator algebra or the hypothesis of scale invariance (cf. section 3.3). One should note that

$$d\sigma_{24} \lesssim \frac{\alpha^4}{s} \ln s \frac{dq_2^2}{q_2^2} . \tag{4.22}$$

In ref. [105] the background problems for this reaction are also discussed.

3. At last, for studying the $\gamma\gamma \to h$ process or the properties of produced C-even hadron system one can, in principle, use experiments on two-photon annihilation into hadrons (fig. 30). In particular, the interference of the two-photon annihilation terms in the region of the f-meson leads to a marked (~10%) charge asymmetry in $\pi^+\pi^-$-production [176].

The observable cross section for the process of fig. 30 is expressed via amplitudes for the $\gamma\gamma \to h$ transition, which are integrated over a wide range of photon masses q_i^2 and transferred momenta compatible with a given value $W^2 = s = 4E^2$. Therefore, it is impossible to extract from here a direct information on the $\gamma\gamma \to h$ transition; special model assumptions are necessary for this*. On the other hand, the process of fig. 30 interferes strongly with that of fig. 26. The hadron systems produced in these processes have identical quantum numbers and even similar angular distributions. One may expect that the cross section for these processes is of order of $(\alpha^4/s)\ln^3 s$.

4.6. *The background problems in two-photon hadron production*

1. A physical process by means of which one can study the $\gamma\gamma \to h$ transition is the process $e^\pm e^- \to e^\pm e^- h$. It is, therefore, necessary to know, first of all, how to separate out in this process the interesting contribution of the two-photon mechanism of fig. 21 from the other ones which

*In this connection it should be noted also that the cross section of this reaction is not connected directly with the $\gamma\gamma$-elastic amplitude since here it is necessary also to take into account the cuts at $q_i^2 > 4m_\pi^2$ in the planes of the mass variables q_i^2.

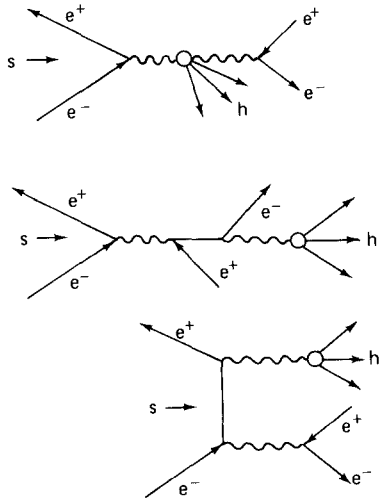

Fig. 31.

are represented in figs. 27 and 31. This becomes simpler due to the fact that, for this reaction, the two-photon mechanism is dominant. In fact, the relevant contribution to the cross section increases logarithmically with increasing energy. Annihilation diagram contributions and crossing-diagram contributions for this process (fig. 31) rapidly decreases with increasing s (as s^{-1}).

Bremsstrahlung production (fig. 27) contribution is the most important one: This process is discussed in detail in refs. [173].

Below we list, mainly, their results.

A. Due to the difference in C-parity for the produced hadron systems, the interference of the two-photon and bremsstrahlung mechanisms leads only to a hadron charge asymmetry. The contribution of this interference to the total cross section vanishes. As a result, the contribution of the two-photon mechanism to the ee → eeh cross section can be obtained subtracting from the experimental cross section the relatively small cross section for bremsstrahlung production. The latter is calculated using the known cross section for one-photon annihilation at smaller energies.

The contribution of the bremsstrahlung production to the cross section increases with increasing s. However, this contribution is markedly less than the two-photon one and its relative value decreases with increasing s. Moreover, the differential distributions for these channels are very different. Due to this difference, in particular, the bremsstrahlung contribution is negligibly small in the main domains for the two-photon production and for set-ups considered by us.

B. The cross section of the bremsstrahlung production for $W^2 \ll s$ has the simple form

$$d\sigma_{2\gamma} = \tfrac{2}{3}\left(\frac{\alpha}{\pi}\right)^2 \sigma_{e^+e^- \to h}(W^2)\,\frac{dW^2}{W^2}\,\ln\frac{W^2}{m_e^2}\,\ln\frac{s^2}{W^3 m_e}. \tag{4.23}$$

Comparing eqs. (4.23) and (5.28), one can see that this cross section does not top by 10% the two-photon one (at $W \neq m_\rho, m_\omega, m_\varphi$). For $W \approx m_\rho$ at present energies a bremsstrahlung contribution may be dominant. (This very W^2-domain gives the main contribution to the cross section of

the bremsstrahlung production; $\sigma_{ee\to ee\rho} \approx 0.6$ nb for $\sqrt{s} = 5$ GeV. A total contribution of the rest domain is very small.)

C. The main contribution to the cross section of the bremsstrahlung production corresponds, in contrast to the two-photon production, to the case when one of the electrons scatters almost backwards, but the other scatters forward at a small angle. Then both scattered electrons move along one of the beams, but hadrons move in the opposite direction. Their distribution in the total longitudinal momentum has a sharp peak for $k_z \sim \frac{1}{2}\sqrt{s}$, $d\sigma_{27} \propto dk_z/[\sqrt{s}+(W^2/\sqrt{s})-2\sqrt{(k_z^2+W^2)}]$. In particular, the large angle bremsstrahlung production is very suppressed.

D. The above conclusions about the relative value of the bremsstrahlung are conserved if, e.g. $m_e^2 < |q_1^2| < W^2$ and an integration over q_2^2 have been performed. If $m_e^2 \ll |q_1^2|$, $|q_2^2| < W^2$ the bremsstrahlung contribution is very suppressed. At the same time according to ref. [177] the bremsstrahlung contribution is dominant at $|q_i^2| \gg W^2$.

2. *Experimental set-ups.* In practice, and almost as a rule, all the particles cannot be recorded. Nevertheless, one can separate the two-photon channel of hadron production either detecting the ee → eeh reaction (set-up A), or separating directly the two-photon channel from the background due to all reactions with hadron production (set-up B).

A. If in measuring one or two scattered electrons are recorded, all the annihilation processes are separated automatically. To separate pure electromagnetic processes such as ee → eee$^+$e$^-$; ee → ee$\gamma\gamma$,... whose cross sections are very large (e.g. $(d\sigma_{ee\to ee\gamma\gamma}/dW^2) \sim \alpha^4/W^2m_e^2$) one should also record at least one produced hadron [7].

B. While studying two-photon production in a set-up when only the produced hadrons are recorded, the background is due to the annihilation channels. (In e$^-$e$^-$-beams this source of background is absent.) To separate out the two-photon channel in such a set-up at not too high energies some specific features of this channel can be used (e.g. the sharpness of the distribution in $k_\perp$, or – for pair production – in the noncoplanarity angle ψ, cf. section 4.1).

Let us note that in such an experimental set-up one should remind the processes in figs. 25 and 27. Their contributions may be excluded using such a fact that an essential part of the corresponding cross sections is connected with a large ($k_z \approx \frac{1}{2}\sqrt{s}$) longitudinal momentum of the whole hadron system.

5. Kinematics and differential distributions for two-photon particle production

We have considered above a wide range of physical problems connected with two-photon particle production. In this section we shall give a systematical derivation of the two mainly used formulas (1.8), (5.12), (5.40) and also some useful equations.

With this aim in mind, cross section for two-photon production (fig. 32) is written in such a form as *to extract explicitly the contribution of the (virtual)* $\gamma^*\gamma^* \to$ f *transition and those of the* $1 \to 1' + \gamma^*$ *and* $2 \to 2' + \gamma^*$ *vertices.* For the $\gamma^*\gamma^* \to$ f amplitudes we give a kinematic analysis using Lorentz and gauge invariance only. As a result we write the cross section as a sum of a rather small number of terms every one of which is simply the product of one $\gamma\gamma \to$ f invariant function and of the corresponding vertex contributions. Such a representation allows one to apply the obtained formulas to a wide number of two-photon processes, which differ from each other

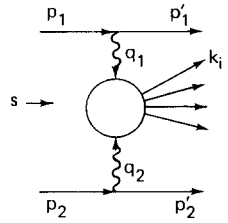

Fig. 32. The two-photon particle production. The colliding particles with momenta p_1 and p_2 change these momenta to p'_1 and p'_2 while interacting, and emit virtual photons with momenta $q_i = p_i - p'_i$, $(q_i^2 < 0)$. These colliding photons produce the finite particle system f, whose momentum is $k = \Sigma_j k_j = q_1 + q_2$ and effective mass is $W = \sqrt{k^2}$.

either by the kind of colliding particles used or by the nature of the produced system f. These expressions are convenient both for the extraction of information on the $\gamma\gamma \to$ f process and for the calculation of the cross section, when the $\gamma\gamma \to$ f amplitudes are known. Additionally, such a representation is the basis for obtaining various approximations and estimating their accuracy. One of these approximations is the equivalent photon approximation, which is obtained in section 5.3.

The cross section for two-photon production can be expressed in terms of the $M^{\mu\nu}$ amplitudes for the $\gamma\gamma \to$ f transition as follows (see notations in fig. 32 and in section 1.6):

$$d\sigma = \frac{(4\pi\alpha)^2}{q_1^2 q_2^2}\,\rho_1^{\mu\mu'}\rho_2^{\nu\nu'}M^{*\mu'\nu'}M^{\mu\nu}\,\frac{(2\pi)^4\delta(q_1+q_2-k)d\Gamma}{4\{(p_1p_2)^2-m_1^2m_2^2\}^{1/2}}\,\frac{d^3p'_1 d^3p'_2}{2E_1\,2E_2(2\pi)^6}. \tag{5.1}$$

Here $p_{1,2}$ are the momenta of the colliding particles, $q_i = p_i - p'_i$ are the momenta of the virtual photons, $k = \Sigma_i k_i = q_1 + q_2$ is the total momentum of the produced system f with mass $W = \sqrt{k^2}$ and the phase-space volume is $d\Gamma = \Pi_j d^3k_j/2\epsilon_j(2\pi)^3$. The matrix ρ_i corresponds to the vertex i. This matrix has the meaning of an (unnormalized) density matrix for the virtual photon, generated by the ith particle. For electron beams we have*

$$\rho_i^{\alpha\beta} = \frac{1}{2(-q_i^2)}\,\mathrm{Sp}[(\hat{p}_i + m_e)\gamma^\alpha(\hat{p}'_i + m_e)\gamma^\beta] = -\left(g^{\alpha\beta} - \frac{q_i^\alpha q_i^\beta}{q_i^2}\right) - \frac{(2p_i - q_i)^\alpha(2p_i - q_i)^\beta}{q_i^2}\,. \tag{5.2}$$

Let us note that this matrix is non-diagonal, i.e. *the virtual photons are polarized.*

Below we consider in detail two different sorts of distribution: a) one is over the momenta of scattered particles; b) the other is over the momenta of the particles of the produced system f.

As a rule, all the considerations in this section concern any processes with two-photon production. However, some definite formulas are written for the case of $e^\pm e^-$ collisions. For the description of two-photon production in collision with other particles it is sufficient to replace the expressions ρ_i (5.2) and the spectra (5.18), (5.23) which appear in these formulas by the corresponding ones given in appendix D.

*The factor $1/(-q_i^2)$ in ρ_i is introduced for convenience, since in virtue of current conservation at $q_i^2 \to 0$ one has $(2p_1 - q_1)^\mu(2p_1 - q_1)^{\mu'}M^{*\mu'\nu'}M^{\mu\nu} \propto q_1^2$.

5.1. *Kinematics of virtual γγ forward scattering* [163, 77, 7]

After integrating over the phase–space volume of the produced particles f, the result (5.1) will include the quantity

$$W^{\mu'\nu',\mu\nu} = \tfrac{1}{2}\int M^{*\mu'\nu'} M^{\mu\nu}(2\pi)^4\delta(q_1 + q_2 - k)\mathrm{d}\Gamma. \tag{5.3}$$

According to the optical theorem the quantity $W^{\mu'\nu',\mu\nu}$ is the absorptive part of the γγ-forward amplitude, connected with the cross section in the usual way. (The expression of this amplitude in terms of the electromagnetic currents is given in (3.16).)

In the expansion of $W^{\mu'\nu',\mu\nu}$ into the invariant functions one should take into account Lorentz invariance, T-invariance (symmetry in the substitution $\mu'\nu' \leftrightarrow \mu\nu$) and gauge invariance as well, i.e.

$$q_1^\mu W^{\mu'\nu',\mu\nu} = q_1^{\mu'} W^{\mu'\nu',\mu\nu} = q_2^\nu W^{\mu'\nu',\mu\nu} = q_2^{\nu'} W^{\mu'\nu',\mu\nu} = 0.$$

The tensors in which $W^{\mu'\nu',\mu\nu}$ is expanded can be constructed in terms of vectors q_1, q_2 and the tensor $g^{\alpha\beta}$. In order to take evidently into account the gauge invariance it is convenient to use their linear combinations:

$$Q_1 = \sqrt{\frac{-q_1^2}{X}}\left[q_2 - q_1\frac{(q_1q_2)}{q_1^2}\right]; \qquad Q_2 = \sqrt{\frac{-q_2^2}{X}}\left[q_1 - q_2\frac{(q_1q_2)}{q_2^2}\right]; \tag{5.4}$$

$$R^{\alpha\beta} = R^{\beta\alpha} = -g^{\alpha\beta} + X^{-1}[(q_1q_2)(q_1^\alpha q_2^\beta + q_1^\beta q_2^\alpha) - q_1^2 q_2^\alpha q_2^\beta - q_2^2 q_1^\alpha q_1^\beta]. \tag{5.5}$$

Here X/W^2 is the square of the photon three-momentum in the γγ-c.m.s.

$$X = (q_1q_2)^2 - q_1^2q_2^2 = \tfrac{1}{4}[W^4 - 2W^2(q_1^2 + q_2^2) + (q_1^2 - q_2^2)^2]. \tag{5.6}$$

The unit vectors Q_i are orthogonal to the vectors q_i and the symmetrical tensor $R^{\alpha\beta}$ is orthogonal both to q_1 and q_2, i.e. to Q_1 and Q_2:

$$q_1Q_1 = q_2Q_2 = 0; \qquad q_i^\alpha R^{\alpha\beta} = Q_i^\alpha R^{\alpha\beta} = 0; \qquad Q_1^2 = Q_2^2 = 1; \qquad R^{\alpha\beta}R^{\alpha\beta} = 2; \qquad R^{\alpha\beta}R^{\beta\gamma} = -R^{\alpha\gamma}.$$

We note, that $R^{\alpha\beta}$ is a metric tensor of a subspace which is orthogonal to q_1 and q_2. In the c.m.s. of the photons, only two components of $R^{\alpha\beta}$ are different from 0 ($R^{xx} = R^{yy} = +1$).

The choice of independent tensors in which the expansion is carried out, has a high degree of arbitrariness. We make this choice so that these tensors are orthogonal to each other, and the invariant functions have a simple physical interpretation:

$$\begin{aligned} W^{\mu'\nu',\mu\nu} &= R^{\mu\mu'}R^{\nu\nu'}W_{\mathrm{TT}} + R^{\mu\mu'}Q_2^\nu Q_2^{\nu'}W_{\mathrm{TS}} + Q_1^\mu Q_1^{\mu'}R^{\nu\nu'}W_{\mathrm{ST}} \\ &+ Q_1^\mu Q_1^{\mu'}Q_2^\nu Q_2^{\nu'}W_{\mathrm{SS}} + \tfrac{1}{2}[R^{\mu\nu}R^{\mu'\nu'} + R^{\mu\nu'}R^{\mu'\nu} - R^{\mu\mu'}R^{\nu\nu'}]W_{\mathrm{TT}}^\tau \\ &-[R^{\mu\nu}Q_1^{\mu'}Q_2^{\nu'} + R^{\mu\nu'}Q_1^{\mu'}Q_2^\nu + (\mu\nu \leftrightarrow \mu'\nu')]W_{\mathrm{TS}}^\tau \\ &+ [R^{\mu\nu}R^{\mu'\nu'} - R^{\mu\nu'}R^{\mu'\nu}]W_{\mathrm{TT}}^{\mathrm{a}} - [R^{\mu\nu}Q_1^{\mu'}Q_2^{\nu'} - R^{\mu\nu'}Q_1^{\mu'}Q_2^\nu + (\mu\nu \leftrightarrow \mu'\nu')]W_{\mathrm{TS}}^{\mathrm{a}}. \end{aligned} \tag{5.7}$$

The dimensionless invariant functions $W_{\mathbf{ab}}$ defined here depend only on the invariants $W^2 = (q_1 + q_2)^2$, q_1^2 and q_2^2. These invariant functions are simply connected with the γγ-helicity amplitudes in the γγ c.m.s. (the choice of phase is given in appendix C). The first four functions are

expressed through the cross sections σ_{ab} (a, b ≡ S for scalar photons, and a, b ≡ T for transverse photons). The amplitudes W^{τ}_{ab} correspond to transitions with spin-flip for each of the photons with total helicity conservation. The last two amplitudes are antisymmetric

$$
\begin{aligned}
&W_{TT} = 2\sqrt{X}\,\sigma_{TT} = \tfrac{1}{2}(W_{++,++} + W_{+-,+-});\\
&W_{TS} = 2\sqrt{X}\,\sigma_{TS} = W_{+0,+0}; \qquad W_{ST} = 2\sqrt{X}\,\sigma_{ST} = W_{0+,0+};\\
&W_{SS} = 2\sqrt{X}\,\sigma_{SS} = W_{00,00}; \qquad W^{\tau}_{TT} = 2\sqrt{X}\,\tau_{TT} = W_{++,--};\\
&W^{\tau}_{TS} = 2\sqrt{X}\,\tau_{TS} = \tfrac{1}{2}(W_{++,00} + W_{0+,-0});\\
&W^{a}_{TT} = 2\sqrt{X}\,\tau^{a}_{TT} = \tfrac{1}{2}(W_{++,++} - W_{+-,+-});\\
&W^{a}_{TS} = 2\sqrt{X}\,\tau^{a}_{TS} = \tfrac{1}{2}(W_{++,00} - W_{0+,-0});
\end{aligned}
\tag{5.8}
$$

$$
\sigma_{TS}(W^2, q_1^2, q_2^2) = \sigma_{ST}(W^2, q_2^2, q_1^2). \tag{5.9}
$$

For the process $\gamma\gamma \to e^+e^-$ (or $\gamma\gamma \to \mu^+\mu^-$) the corresponding amplitudes are given in appendix F.

The quantities σ_{TT} and τ_{TT} can also be expressed through the cross sections for the scattering of photons with parallel ($\sigma_{\parallel}$) and orthogonal ($\sigma_{\perp}$) linear polarization [170]:

$$
\sigma_{TT} = \tfrac{1}{2}(\sigma_{\parallel} + \sigma_{\perp}); \qquad \tau_{TT} = \sigma_{\parallel} - \sigma_{\perp}. \tag{5.10}
$$

Since the $W^{\mu'\nu',\mu\nu}$ tensor is regular at $q_i^2 \to 0$ and the vectors Q_i are singular at $q_i^2 \to 0$, near the mass shell (at $q_i^2 \to 0$) the cross sections of scalar photon scattering vanish. Here σ_{TT} and τ_{TT} are transformed into the corresponding quantities for real photoprocesses. In particular, at $q_i^2 = 0$, σ_{TT} coincides with the cross section $\sigma_{\gamma\gamma}$ of the $\gamma\gamma \to f$ transition for real non-polarized photons. As a result we have at $q_i^2 \to 0$

$$
\begin{aligned}
&\sigma_{TT}(W^2, q_1^2, q_2^2) \to \sigma_{\gamma\gamma}(W^2); \qquad \tau_{TT}(W^2, q_1^2, q_2^2) \to \tau_{\gamma\gamma}(W^2);\\
&\sigma_{TS} \propto q_2^2; \qquad \sigma_{ST} \propto q_1^2; \qquad \sigma_{SS} \propto q_1^2 q_2^2; \qquad \tau_{TS} \propto \sqrt{q_1^2 q_2^2}\,.
\end{aligned}
\tag{5.11}
$$

Let us note that, from the positiveness of the $\gamma\gamma$ cross-section at arbitrary photon polarization, some inequalities between the invariant functions (5.8), follow, e.g. $|\tau_{TT}| \leqslant 2\sigma_{TT}$; $2(\tau_{TS})^2 \leqslant 2\sigma_{SS}\sigma_{TT} + \sigma_{TS}\sigma_{ST}$ [170, 178].

The connection with helicity amplitudes in the t-channel and the Regge analysis for forward $\gamma\gamma$-amplitude are given in [77].

5.2. *Momentum distribution of the scattered particles*

The momentum distribution of the scattered particles p_1' and p_2' follows from (5.1) after integration over the phase space volume of the system f (see (5.3)). The differential cross section is then expressed in terms of cross sections σ_{ab} and of the amplitudes τ_{ab} for the $\gamma\gamma \to f$ transition (5.7–8). Substituting the expansion (5.7) into (5.1) and summing over μ, ν, μ', ν' we obtain the equation (1.8):

$$d\sigma = \frac{\alpha^2}{16\pi^4 q_1^2 q_2^2}\left[\frac{(q_1q_2)^2 - q_1^2q_2^2}{(p_1p_2)^2 - m_1^2m_2^2}\right]^{1/2} [4\rho_1^{++}\rho_2^{++}\sigma_{TT}$$
$$+ 2|\rho_1^{+-}\rho_2^{+-}|\tau_{TT}\cos 2\tilde{\varphi} + 2\rho_1^{++}\rho_2^{00}\sigma_{TS} + 2\rho_1^{00}\rho_2^{++}\sigma_{ST}$$
$$+ \rho_1^{00}\rho_2^{00}\sigma_{SS} - 8|\rho_1^{+0}\rho_2^{+0}|\tau_{TS}\cos\tilde{\varphi} + A\tau_{TT}^{a} + B\tau_{TS}^{a}] \frac{d^3p_1' d^3p_2'}{E_1E_2}. \quad (5.12)$$

Here $\tilde{\varphi}$ is the angle between the scattering planes of the colliding particles in the photon c.m.s. The quantities ρ_i^{ab} are the convolutions of the matrices $\rho_i^{\alpha\beta}$ with the coefficient of the expansion (5.7)*. All these quantities are expressed in terms of the measurable momenta p_i and p_i' only and to that extent are completely known. In particular, when using the expression for $\rho_i^{\alpha\beta}$ in (5.2), we obtain for $e^{\pm}e^{-}$ collisions:

$$2\rho_1^{++} = 2\rho_1^{--} = \rho_1^{\alpha\beta}R^{\alpha\beta} = X^{-1}(2p_1q_2 - q_1q_2)^2 + 1 + 4m_e^2/q_1^2;$$
$$\rho_1^{00} = \rho_1^{\alpha\beta}Q_1^{\alpha}Q_1^{\beta} = X^{-1}(2p_1q_2 - q_1q_2)^2 - 1;$$
$$8|\rho_1^{+0}\rho_2^{+0}|\cos\tilde{\varphi} = 4X^{-1}(2p_1q_2 - q_1q_2)(2p_2q_1 - q_1q_2)C[q_1^2q_2^2]^{-1/2}; \quad (5.13)$$
$$C = (2p_1 - q_1)^{\alpha}(2p_2 - q_2)^{\beta}R^{\alpha\beta} = -(2p_1 - q_1)(2p_2 - q_2) + X^{-1}(q_1q_2)(2p_1q_2 - q_1q_2)(2p_2q_1 - q_1q_2);$$
$$2|\rho_1^{+-}\rho_2^{+-}|\cos 2\tilde{\varphi} = C^2/q_1^2q_2^2 - 2(\rho_1^{++} - 1)(\rho_2^{++} - 1);$$
$$|\rho_2^{ab}| = |\rho_1^{ab}(1 \leftrightarrow 2)|; \quad |\rho_i^{+-}| = \rho_i^{++} - 1; \quad |\rho_i^{+0}| = \sqrt{(\rho_i^{00} + 1)|\rho_i^{+-}|}; \quad A = B = 0.$$

If the initial electrons are polarized, then in (5.2) the term $-2i(m_e/q_i^2)\epsilon^{\alpha\beta\gamma\delta}q_1^{\gamma}n_i^{\delta}$ is added. Now n_i is the electron polarization vector. With this used in (5.12) and (5.13) the coefficients A and B only (in front of the antisymmetric amplitudes) change

$$A = -\frac{16m_e^2}{\sqrt{q_1^2q_2^2}}(Q_1n_1)(Q_2n_2); \qquad B = \frac{16m_e^2}{\sqrt{q_1^2q_2^2}}n_1^{\alpha}R^{\alpha\beta}n_2^{\beta} \quad (5.13a)$$

(in the dominant region of phase space these coefficients are small).

Both quantities in (5.13) and the $\gamma\gamma$-system parameters are simply expressed in terms of the energies E_i and angles θ_i of the scattered electrons and of the angle φ between their scattering planes in the colliding electrons c.m.s.. This implies the relations (for $E_i \gg m_e$):

$$q_i^2 = -4EE_i\sin^2\tfrac{1}{2}\theta_i - q_{i\,min}^2; \qquad q_{i\,min}^2 = m_e^2\omega_i^2/EE_i; \qquad \omega_i = E - E_i; \quad (5.14)$$
$$W^2 = (q_1 + q_2)^2 = 4\omega_1\omega_2 - 2E_1E_2(1 - \cos\theta_1\cos\theta_2 - \sin\theta_1\sin\theta_2\cos\varphi);$$
$$2p_1q_2 = 4E\omega_2 - q_2^2; \qquad 2p_2q_1 = 4E\omega_1 - q_1^2.$$

The expressions (5.12–5.14) have been obtained in [2, 163, 7] and, later, by many other authors also [143, 164, 168, 170].

The momentum distribution of the electrons and of one or two of the produced particles is de-

*It is easy to test (cf. (B.3), (C.2), (C.9)), that the matrices ρ_i^{ab} are density matrices of virtual photons in the $\gamma\gamma$-helicity basis. The exact expressions for $\cos\tilde{\varphi}$ is given in (A.4).

scribed by more complex expressions than (5.12), (5.13). They contain 20 independent helicity amplitudes [143].

We note in conclusion that the quantities ω_i, E and $\cos\varphi$ are easily written in covariant form (cf. appendix A). The covariant expansion of the vectors q_i in terms of the vectors p_1 and p_2 and in the plane orthogonal to p_1 and p_2 is useful here $q_i = \alpha_i p_2 + \beta_i p_1 + q_{i\perp}$; $q_{i\perp}p_1 = q_{i\perp}p_2 = 0$. Then

$$\omega_i = q_i(p_1 + p_2)/\sqrt{s}; \qquad q_{i\perp}^2 < 0; \qquad \cos\varphi = -(q_{1\perp}q_{2\perp})/\sqrt{q_{1\perp}^2 q_{2\perp}^2}. \tag{5.15a}$$

(If, in the c.m.s. of the colliding particles one directs the Z-axis along a vector $p_1 = -p_2$, then $q_{i\perp} = (0, q_{i\perp}, 0) = (0, q_{ix}, q_{iy}, 0)$). In terms of these invariants, the phase space volume element of the scattered particles has the form

$$\frac{d^3p_1' d^3p_2'}{E_1E_2} = \frac{\pi s}{2[(p_1p_2)^2 - m_1^2m_2^2]} d(-q_1^2)d(-q_2^2)d\omega_1 d\omega_2 d\varphi. \tag{15.15b}$$

5.3. *Approximate formulas in the region of small scattering angles. Estimations for cross sections from below*

The formulas written in the previous section completely describe the momentum distribution of the scattered particles. It is of special interest to consider in detail the region of small electron scattering angles (i.e. and small "masses" of the photons) which gives the dominant contribution to the cross section. Here the expressions for the cross section and the kinematical relations are essentially simplified. In this region the contributions of the scalar photons can be neglected in virtue of (5.11), and in the quantities $2\sqrt{X}\,\sigma_{TT}$ and $2\sqrt{X}\,\tau_{TT}$, one can put $q_i^2 = 0$, i.e. one can replace them by $W^2\sigma_{\gamma\gamma}$ and $W^2\tau_{\gamma\gamma}$:*

$$d\sigma = \left(\frac{\alpha}{4\pi^2}\right)^2 \frac{W^2}{sq_1^2q_2^2}\left[4\rho_1^{++}\rho_2^{++}\sigma_{\gamma\gamma} + 2|\rho_1^{+-}\rho_1^{+-}|\tau_{\gamma\gamma}\cos 2\tilde{\varphi}\right]\frac{d^3p_1' d^3p_2'}{E_1E_2}. \tag{5.16}$$

If $|q_i^2| \ll W^2$, then the kinematic relationships (5.14) and the expressions for the density matrix elements (5.13) are simplified too. In particular, the angles between the electron scattering planes in the c.m.s. of the photons, $\tilde{\varphi}$, and in that of colliding electron, φ, coincide:

$$\begin{aligned}
&\tilde{\varphi} = \varphi; \qquad W^2 = 4\omega_1\omega_2 = 2\sqrt{X};\\
&-q_i^2 = \frac{q_{i\perp}^2}{1 - (\omega_i/E)} + q_{i\,\min}^2; \qquad q_{i\,\min}^2 = \frac{m_i^2\omega_i^2}{E(E-\omega_i)};\\
&\rho_i^{++} = \frac{2E(E-\omega_i)}{\omega_i^2}\left(1 - \left|\frac{q_{i\,\min}^2}{q_i^2}\right|\right) + 1.
\end{aligned} \tag{5.17}$$

If we now introduce suitable notations (with proper account of the phase-space volume transformation (5.15b))

*The region of validity of this approximation is discussed in detail below.

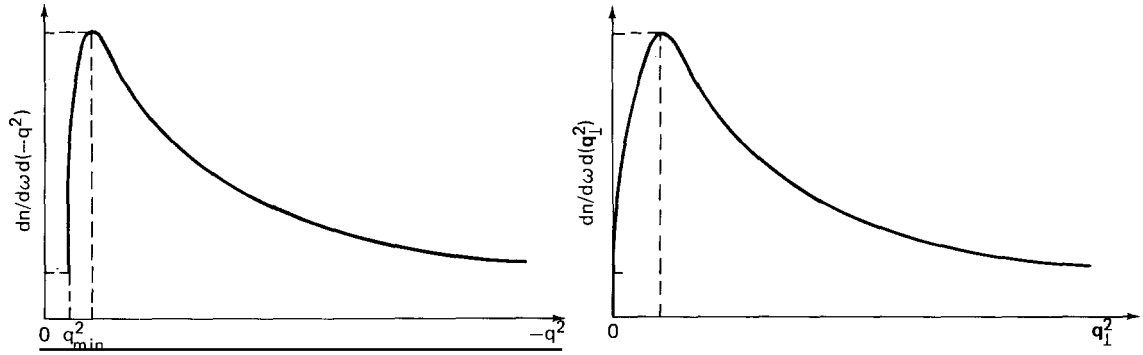

Fig. 33. The spectrum equivalent photons produced by electrons versus q^2 and versus $q_\perp^2$ (ω is fixed),
$dn = \frac{\alpha}{\pi}\frac{d(-q^2)}{|q^2|}\frac{d\omega}{\omega}\left[1 - \frac{\omega}{E} + \frac{\omega^2}{2E^2} + \frac{m^2\omega^2}{E^2q^2}\right]$.

$$dn_i = \frac{\alpha}{2\pi}\rho_i^{++}\frac{\omega_i d\omega_i d(-q_i^2)}{E^2|q_i^2|} = \frac{\alpha}{\pi}\cdot\frac{d\omega_i}{\omega_i}\cdot\frac{d(-q_i^2)}{|q_i^2|}\left[\left(1 - \frac{\omega_i}{E} + \frac{\omega_i^2}{2E^2}\right) - \left(1 - \frac{\omega_i}{E}\right)\left|\frac{q_{i\min}^2}{q_i^2}\right|\right]; \qquad (5.18)$$

$$\xi_i = \frac{|\rho^{+-}|}{\rho_i^{++}} = \frac{\rho_i^{++} - 1}{\rho_i^{++}},$$

then the differential cross section (5.16) is rewritten in the form

$$d\sigma = (\sigma_{\gamma\gamma} + \tfrac{1}{2}\xi_1\xi_2\tau_{\gamma\gamma}\cos 2\varphi)dn_1 dn_2 d\varphi/2\pi. \qquad (5.19)$$

The expressions (5.18–5.19) are the essence of *the equivalent photons approximation for the two-photon production,* which is written here in a Lorentz covariant form (cf. (5.15)). According to the terminology of this method dn_i is the number of equivalent photons, or the photon spectrum (the dependence of this spectrum on q_i^2 and $q_{i\perp}^2$ is given in fig. 33), and ξ_i are their polarizations.

Besides the cross section for non-polarized photon scattering $\sigma_{\gamma\gamma}$ the equation (5.19) *contains the interference term* $\tau_{\gamma\gamma}$. Its appearance is due to the polarization of the virtual photons. With azimuthal averaging this additional term disappears and we obtain

$$\langle d\sigma\rangle_\varphi = \sigma_{\gamma\gamma}dn_1 dn_2. \qquad (5.20)$$

The accuracy of the approximation (5.18–5.20). The sources of errors in the above approximation and their relative values are listed in table 4. Let us explain this table.

When writing the approximate expressions (5.17), quantities $\lesssim |q_i^2|/W^2$ were omitted and, hence, these expressions are correct for $|q_i^2| < W^2$. For $|q_i^2| > W^2$ the quantities ρ_i^{ab} decrease as $1/q_i^2$ when q_i^2 increases.

An other source of inaccuracy is due to our approximating (5.12) as (5.16), i.e. our neglecting contributions from scalar photons and the q^2-dependence in σ_{TT} and τ_{TT}. Since all ρ^{ab} are of the same order, the relative value of the neglected terms in above approximation, is defined only by quantities of the type σ_{ST}/σ_{TT} and $[\sigma_{TT}(q_1^2, q_2^2) - \sigma_{TT}(0, 0)]/\sigma_{TT}(0, 0)$.

Table 4
The sources of inaccuracy for the approximation (5.18–5.20). For $|q_i^2| > \Lambda_\gamma^2$ the quantities σ_{ab} and τ_{ab} decrease as a power with $-q_i^2$ increasing. For $|q_i^2| > W^2$ the quantities ρ_i^{ab} decrease as a power. For most processes under consideration the inequality $\Lambda_\gamma \lesssim W$ is valid.

Source of inaccuracy	Relative value of inaccuracy
Neglection of the scalar photon contributions	$\lesssim \|q_i^2\|/\Lambda_\gamma^2$ at $\|q_i^2\| < \Lambda_\gamma^2$
Neglection of the q_i^2-dependence in σ_{TT} and τ_{TT}	$\lesssim \|q_i^2\|/\Lambda_\gamma^2$ at $\|q_i^2\| < \Lambda_\gamma^2$
The approximate kinematical relations (5.17)	$\lesssim \|q_i^2\|/W^2$ at $\|q_i^2\| < W^2$

For the process $\gamma\gamma \to l^+l^-$ ($l \equiv e, \mu$) the quantities σ_{ab} and τ_{ab} are given in appendix E. These expressions show that the quantities σ_{TT} and τ_{TT} decrease with increasing q_i^2. Deviations of these quantities at $|q_i^2| \lesssim W^2$ from their mass shell values $\sigma_{\gamma\gamma}$ and $\tau_{\gamma\gamma}$ are of the order of q_i^2/W^2 at small $W \sim m_l$. Here the ratios σ_{ST}/σ_{TT}, σ_{TS}/σ_{TT}, σ_{SS}/σ_{TT} are of the same order. At $|q_i^2| \gg W^2$ the quantities σ_{ab} and τ_{ab} decrease with increasing $-q^2$ according to a power law. Thus, a value of the cross sections for scalar photon scattering and the variation of the cross sections σ_{TT} and τ_{TT} are determined by the same specific scale $\Lambda_\gamma \sim W$.*

For the $\gamma\gamma \to$ h transition there are presently no detailed experimental data. The study of the hadron form factors and of the cross sections for γ^*p scattering shows, that the specific scale for the variations of these quantities when q^2 varies, is of the order of m_ρ^2. It is then natural to expect that for the $\gamma\gamma \to$ h transitions the quantity $\Lambda_\gamma \sim m_\rho$, at least, at $W \gtrsim m_\rho$.

For the processes considered we have as a result,

$$\sigma_{ST}/\sigma_{TT}, \quad \sigma_{TS}/\sigma_{TT}, \quad \sigma_{SS}/\sigma_{TT}, \quad \tau_{TS}/\sigma_{TT} \lesssim |q_i^2|/\Lambda_\gamma^2; \tag{5.21}$$

$$\sigma_{TT}(W^2, q_1^2, q_2^2) = \sigma_{\gamma\gamma}(W^2)[1 + O(q_i^2/\Lambda_\gamma^2)];$$

$$\tau_{TT}(W^2, q_1^2, q_2^2) = \tau_{\gamma\gamma}(W^2)[1 + O(q_i^2/\Lambda_\gamma^2)].$$

$$\Lambda_\gamma \sim m_\rho \quad \text{for} \quad \gamma\gamma \to \text{h} \quad (\text{at } W \gtrsim m_\rho); \tag{5.22}$$

$$\Lambda_\gamma \sim W \quad \text{for} \quad \gamma\gamma \to l^+l^- \quad (\text{at } W \sim m_l).$$

To obtain a *distribution in photon frequencies*, i.e. over the scattered particle energies one should integrate (5.18) over $-q_i^2$ up to some $q_{i\max}^2$, that gives [16] **

$$dn_i = N(\omega_i)\, d\omega_i/\omega_i;$$

$$N(\omega_i) = \frac{\alpha}{\pi}\left[\left(1 - \frac{\omega_i}{E} + \frac{\omega_i^2}{2E^2}\right)\ln\frac{q_{i\max}^2}{q_{i\min}^2} - \left(1 - \frac{\omega_i}{E}\right)\left(1 - \frac{q_{i\min}^2}{q_{i\max}^2}\right)\right]. \tag{5.23a}$$

In the main logarithmic approximation one has:

$$dn_i = N(\omega_i)\frac{d\omega_i}{\omega_i} = \frac{\alpha}{\pi}\frac{d\omega_i}{\omega_i}\ln\frac{q_{i\max}^2}{q_{i\min}^2} = \frac{\alpha}{\pi}\frac{d\omega_i}{\omega_i}\ln\frac{E^2 q_{i\max}^2}{\omega_i^2 m_i^2}. \tag{5.23b}$$

*At $W \gg m_l$ the scales appear to be different. This case is considered in details in section 6.8.

**To avoid misunderstandings we note some inconsequence in notations: $q_{i\min}^2 = \min(-q_i^2)$; $q_{i\min}^2 \leqslant -q_i^2 \leqslant q_{i\max}^2$.

Note, that in this approximation the form of the spectrum does not depend on the type of particle producing the virtual photon.

The upper limit $q_{i\max}^2$ for the integration regions can be defined by the experimental conditions, e.g., the limitation in the emission angle of the electrons $\theta_i \leqslant \theta_m$. If $EE_i\theta_m^2 < \Lambda_\gamma^2$, then $q_{\max}^2 = EE_i\theta_m^2$. At $|q_i^2| \lesssim \Lambda_\gamma^2$ the main q^2-dependence in $d\sigma$ (5.12) is a logarithmic one: dq_i^2/q_i^2. After the integration over q_i^2 the terms taken into account are of the order $\int dq^2/q^2 \sim \ln(q_{\max}^2/q_{\min}^2)$ but the neglected terms are of the order (see table 4) $dq^2/\Lambda_\gamma^2 \sim q_{\max}^2/\Lambda_\gamma^2$. Therefore, the accuracy of the approximation is

$$\eta \sim \frac{q_{\max}^2}{\Lambda_\gamma^2 \ln(q_{\max}^2/q_{\min}^2)}. \tag{5.24a}$$

If the experimental conditions are such that, for example, $EE_i\theta_m^2 > \Lambda_\gamma^2$ or, if we are interested in the total cross section for the process, then the decrease of σ_{ab} and τ_{ab} at $|q_i^2| > \Lambda_\gamma^2$ and of ρ_i^{ab} at $|q_i^2| > W^2$ leads to an effective cut off of the integral on q_i^2 in (5.12) at $|q_i^2| > \Lambda_\gamma^2$. This allows to limit oneself to the integration of the approximate expressions (5.18–5.20) from $q_{i\min}^2$ to $q_{\max}^2 = \Lambda_\gamma^2$. The accuracy of the approximation here appears to be logarithmic:

$$\eta \sim [\ln(\Lambda_\gamma^2/q_{i\min}^2)]^{-1}. \tag{5.24b}$$

The above estimations of the accuracy show how to obtain simple and reliable *estimations for the cross section from below*. Such estimations are especially useful for the understanding of the feasibility of new experiments. The equation (5.24) shows that the contribution of the region $|q|^2 \leqslant q_{\max}^2 < \Lambda_\gamma^2$, rather accurately computed, gives a reliable estimation for the cross section. This is an estimation from below, since the rest of the region of the q^2-variable obviously gives a positive addition. If $q_{\max}^2$ decreases the calculated value of the cross section decreases but the estimation reliability increases. Such estimations are the more so important that, in known cases of two-photon particle production, the first corrections to the main logarithmic approximation are negative, and, at energies now accessible, they are of the same order as the main term (cf. appendix F).

For the process $pp \to ppe^+e^-$ such an estimation has been obtained in ref. [24] and for $ee \to ee\mu^+\mu^-$ in ref. [179]. For two-photon hadron production in colliding beams, similar estimations from below are given in section 4.3.

5.4. *Total four-momentum distribution for the produced system*

Momentum distributions for the scattered particles (5.12–5.16) are easily transformed into those over the total four-momenta of the produced system $k = q_1 + q_2$. The main contribution to the cross section is given by the region of small scattering angles, considered above.

Then we shall use the obtained approximate formulas for cross sections together with the simplified kinematical relations (5.16–5.20). The expressions obtained below describe actual distribution with a good accuracy. We stress that, without taking into account the q_i^2-dependence of σ_{ab}, a precise description is just impossible.

In the c.m.s. of the colliding particles we choose the z-axis along $\boldsymbol{p}_1 = -\boldsymbol{p}_2$. The energy of the produced system is simply the sum of the photon energies, $\omega_1 + \omega_2$; the transverse momentum $\boldsymbol{k}_\perp = \boldsymbol{q}_{1\perp} + \boldsymbol{q}_{2\perp}$, and the longitudinal momentum (in the same approximation as in (5.17)) is equal

to the photon frequency difference:

$$\epsilon = \omega_1 + \omega_2; \qquad k_z = \omega_1 - \omega_2; \qquad \omega_{1,2} = \tfrac{1}{2}(\epsilon \pm k_z). \tag{5.25}$$

Using these relations the $\omega_{1,2}$-distributions (5.20), (5.23) can be easily transformed into the ϵ *and* W^2 *(or* k_z *and* W^2*)-distributions as well as into the* ϵ *and* k_z *ones [34].*

Distribution in the effective mass of the produced system W follows from the integration of (5.20) and (5.23) over ω_1. Bounds for the latter are defined either by the experimental conditions, or – if there are no such limitations – by the conditions $\omega_i < E$ or $q^2_{i\,\min} < q^2_{i\,\max}$, i.e.

$$d\sigma = \sigma_{\gamma\gamma}(W^2)\,\frac{dW^2}{W^2}\int N(\omega_1)N\left(\omega_2 = \frac{W^2}{4\omega_1}\right)\frac{d\omega_1}{\omega_1}\,; \tag{5.26}$$

$$\max\left\{\omega^{\exp}_{1\,\min}\,; \frac{W^2}{4\omega_{2\,\max}}\right\} \leqslant \omega_1 \leqslant \min\left\{\omega^{\exp}_{1\,\max}\,; \frac{W^2}{4\omega^{\exp}_{2\,\min}}\,; E; E\,\frac{\sqrt{q^2_{1\,\max}}}{m_1}\right\}.$$

For electron beams one usually has $q^2_{i\,\max} > m_e^2$, and in the absence of experimental limitations, $\omega_{i\,\max} = E$. The order of the (5.26) inaccuracy is determined by the relation (5.24) (see, also, the discussion after (5.24)).

In order to illustrate this point we consider the main logarithmic approximation for e^+e^- pair production in the collision of charged particles [6]. In this case $q^2_{i\,\max} \sim m_e^2$, in the main region $\omega_i \ll E$. The spectrum has the form (5.23b) $N(\omega_i) = (2\alpha/\pi)\ln(E/\omega_i)$. Substituting this spectrum into (5.20) and integrating over ω_1 from $m_e m_2/E$ to $m_e E/m_1$, we obtain

$$\left(\frac{d\sigma}{dW^2}\right)_{Z_1Z_2 \to Z_1Z_2e^+e^-} = \frac{2\alpha^2(Z_1Z_2)^2\sigma_{\gamma\gamma\to e^+e^-}(W^2)}{3\pi^2W^2}\left(\ln\frac{p_1p_2}{m_1m_2}\right)^3. \tag{5.27}$$

Using the known expression (E.4) for $\sigma_{\gamma\gamma\to e^+e^-}$ in the integration over W^2, we get (1.2).

The other example is *hadron production in colliding electron beams.* In this case $q^2_{\max} \sim m_\rho^2$, and the quantity ω_i/E is not small. Besides, in the large energy range, one has $\ln(s/W^2) \ll \ln(m_\rho^2/m_e^2)$. Therefore, when calculating in the main logarithmic approximation one should find precisely the coefficient of the high power of $\ln(m_\rho^2/m_e^2)$ taking W^2/s as a not small value. With the accuracy $\eta \sim [\ln(sm_\rho^2/W^2m_e^2)]^{-1} < 0.1$ we have [7]:

$$\left(\frac{d\sigma}{dW^2}\right)_{e^\pm e^- \to e^\pm e^- h} = \left(\frac{\alpha}{\pi}\right)^2 \frac{\sigma_{\gamma\gamma\to h}}{W^2}\left[\left(\ln\frac{sm_\rho^2}{W^2m_e^2}\right)^2 f\left(\frac{s}{W^2}\right) - \tfrac{1}{3}\left(\ln\frac{s}{W^2}\right)^3\right]; \tag{5.28}$$

$$f(x) = \left(1 + \frac{1}{2x}\right)^2 \ln x - \tfrac{1}{2}\left(1 - \frac{1}{x}\right)\left(3 + \frac{1}{x}\right). \tag{5.29}$$

Of course, in the coefficient of $[\ln(s/W^2)]^3$ the contributions $\sim W^2/s$ are omitted since these terms can become of importance only at $W^2/s \ll 1$. This relation differs appreciably from the known result of Brodsky and others [3]: $d\sigma/dW^2 \sim (\alpha^2\sigma_{\gamma\gamma}/\pi^2W^2)\{\ln(s/m_e^2 - 1\}^2 f(s/W^2)$. The origin of these authors' error is discussed in section 6.

In two-photon processes the *distribution over the total transverse momentum* $\boldsymbol{k}_\perp = \boldsymbol{q}_{1\perp} + \boldsymbol{q}_{2\perp}$ is very specific. Let us consider as an example the distribution in $k_\perp^2$, ω_1, ω_2 [180]. To obtain it we rewrite the cross section (5.16–5.18) in terms of new variables, neglecting for simplicity the

terms $\sim (\omega_i/E)^2$:

$$d\sigma = \frac{\alpha^2}{\pi^4}\left(1-\frac{\omega_1}{E}\right)\left(1-\frac{\omega_2}{E}\right)\frac{d\omega_1 d\omega_2 d^2k_\perp}{\omega_1\omega_2} \times \int \frac{q_{1\perp}^2(k-q_1)_1^2(\sigma_{\gamma\gamma}+\frac{1}{2}\tau_{\gamma\gamma}\cos 2\varphi)d^2q_{1\perp}}{[q_{1\perp}^2+(m_1\omega_1/E)^2]^2[(k_\perp-q_{2\perp})^2+(m_2\omega_2/E)^2]^2}; \quad (5.30)$$

$$\cos\varphi = \frac{q_{1\perp}(k_\perp - q_{1\perp})}{|q_{1\perp}|\cdot|k_\perp - q_{1\perp}|}.$$

The appearance of $\tau_{\gamma\gamma}$ in (5.30) is due to the virtual photon polarization.

Let us first consider this distribution in the range $k_\perp^2 \gg (m_i\omega_i/E)^2$ (which gives the main contribution to the σ), limiting oneself by the main logarithmic approximation. For these values of $k_\perp$ the main contributions in the integral over $q_{1\perp}$ are given by the two symmetric sub-regions $(m_1\omega_1/E)^2 \ll q_{1\perp}^2 \ll k_\perp^2$ and $(m_2\omega_2/E)^2 \ll (k_\perp - q_{1\perp})^2 \ll k_\perp^2$. In the former one $k_\perp - q_{1\perp} \approx k_\perp$ and in the integrand (5.30) φ appears in $\cos 2\varphi$ only. Therefore, averaging over the directions of the vector $q_{1\perp}$ in this sub-region the term $\tau_{\gamma\gamma}$ disappears from the result. The integration over $q_{1\perp}^2$ gives here a large logarithm $\ln(E^2k_\perp^2/\omega_1^2m_1^2)$. Taking into account both the sub-regions, we obtain

$$d\sigma = \frac{2\alpha^2}{\pi^2}\left(1-\frac{\omega_1}{E}\right)\left(1-\frac{\omega_2}{E}\right)\frac{d\omega_1}{\omega_1}\frac{d\omega_2}{\omega_2}\frac{dk_\perp^2}{k_\perp^2}\sigma_{\gamma\gamma}\cdot\ln\frac{k_\perp^2(p_1p_2)}{W^2m_1m_2}. \quad (5.31)$$

A specific sharp distribution in the total transverse momentum $(dk_\perp^2/k_\perp^2)\ln k_\perp^2$ is due to the fact that a distribution over the "mass" q_i^2 of each photon has the form dq_i^2/q_i^2 with very small lower limit.

At small values of $k_\perp$ the coefficients of $\sigma_{\gamma\gamma}$ and $\tau_{\gamma\gamma}$ are of the same order. In particular, if $k_\perp = 0$, then $\cos 2\varphi = 1$, and

$$d\sigma \propto \alpha^2(\sigma_{\gamma\gamma}+\tfrac{1}{2}\tau_{\gamma\gamma})d\omega_1 d\omega_2 dk_\perp^2 . \quad (5.32)$$

5.5. *Production of pair. Momentum distribution of the particles produced in* $e^\pm e^-$ *collisions*

In this sub-section we shall consider the momentum distribution of the pair of produced particles A_1A_2 averaged over the spin orientation of particles A_1 and A_2. The result is written in terms of $\gamma\gamma \to A_1A_2$ amplitudes.* The formulas obtained describe also the multiple production in an inclusive set-up, then A_1 is one of the produced particles, and A_2 is a system combining all other produced particles.

Let us denote the momentum (energy) of a particle A_i by symbols $k_j(\epsilon_j)$. The total energy of the pair $\epsilon = \epsilon_1 + \epsilon_2$ and the longitudinal momentum $k_z = k_{1z} + k_{2z}$ are connected with the photon frequencies by the simple equation (5.25).

The distribution under consideration can be obtained from the equation (5.1) in the same manner as the approximate equations (5.19). With the quantity $T = \rho_1^{\mu\mu'}\rho_2^{\nu\nu'}M^{*\mu'\nu'}M^{\mu\nu}$ we may go from a summation over the vector indices $\mu\nu$, $\mu'\nu'$ to a summation over the helicities of virtual photons a, $b = \pm 1,0$, defined in the c.m.s. of the photons i.e. T is then represented as

*In appendix E the values of these amplitudes for e^+e^- or $\mu^+\mu^-$-pair production and for the $\gamma\gamma \to \pi^+\pi^-$ transition in the Born approximation (point-like pions) are written out.

$T = \rho_1^{a'a}\rho_2^{b'b}M^*_{a'b'}M_{ab}$. Just as before, the main contribution to the cross section for two-photon production is given by the region of small photon "masses". In this region the contributions of scalar photons (e.g. $M^*_{0+}M_{++}$), can be neglected in T. In all the remaining $\gamma\gamma \to A_1A_2$ helicity amplitudes, M_{ab}, one can neglect the q_i^2-dependence. That corresponds to the *equivalent photon approximation*. As a result,

$$T = 4\rho_1^{++}\rho_2^{++}\{\tfrac{1}{2}(|M_{++}|^2 + |M_{+-}|^2) - \xi_1 \mathrm{Re}(M^*_{-+}M_{++})\cos 2\tilde{\varphi}_1$$
$$-\xi_2 \mathrm{Re}(M^*_{+-}M_{++})\cos 2\tilde{\varphi}_2 + \tfrac{1}{2}\xi_1\xi_2[M^*_{-+}M_{+-}\cos 2(\tilde{\varphi}_1 + \tilde{\varphi}_2) + M^*_{++}M_{--}\cos 2(\tilde{\varphi}_1 - \tilde{\varphi}_2)]\}. \quad (5.33)$$

Here $\xi_i = |\rho_i^{+-}|/\rho_i^{++}$ is the i-photon polarization (5.18) and $\tilde{\varphi}_i$ is the angle between the scattering plane of the ith electron and that of A_1 production

$$\cos\tilde{\varphi}_i = -\frac{q_{i\perp}(k_{1\perp} - k_{2\perp})}{|q_{i\perp}||k_{1\perp} - k_{2\perp}|}\left[1 + O\left(\frac{|q_{i\perp}|}{|k_{i\perp}|}\right)\right]. \quad (5.34)$$

The quantities $M^*_{a'b'}M_{ab}$ depend on the invariants W^2, q_i^2 and $t = (q_1 - k_1)^2 = (q_2 - k_2)^2$ only. As we said above, we neglect the q_i^2 dependence assuming $q_i^2 = 0$ everywhere in M_{ab}. Then the dependence on the small variable $q_{i\perp}$ is still conserved, since

$$t = t_1^0 + 2q_{1\perp}k_{1\perp} + O(q_i^2) = t_2^0 + 2q_{2\perp}k_{2\perp} + O(q_i^2);$$
$$t_1^0 = m_{A_1}^2 - (\epsilon + k_z)(\epsilon_1 - k_{1z}), \qquad t_2^0 = m_{A_2}^2 - (\epsilon - k_z)(\epsilon_2 + k_{2z}) = t_1^0 + k_\perp(k_{1\perp} - k_{2\perp}) \quad (5.35)$$

(unlike t the quantities t_i^0 are expressed only through the measurable momenta). In accordance with the spirit of the approximation we put the quantities $q_{i\perp} = 0$, i.e. $t \approx t_1^0 \approx t_2^0$ in M_{ab}.

Let us compare (5.33) with (5.19). The first term in (5.33) refers to the scattering of non-polarized real photons and corresponds to $\sigma_{\gamma\gamma}$ while the latter refers to $\tau_{\gamma\gamma}$ in (5.19). In addition to them, equation (5.33) *contains the three new terms connected with the interference of amplitudes with various helicities.*

An integration over the phase–space volume of the scattered electrons is conveniently performed by means of the approximate relationship:

$$\delta(q_1 + q_2 - k)\frac{d^3p_1' d^3p_2'}{E_1E_2} = \frac{d^2q_{1\perp}}{2(E - \omega_1)(E - \omega_2)}. \quad (5.36)$$

As a result the cross section is expressed through the quantity T defined by (5.33), which is regular at $q_{i\perp} \to 0$, in such a form

$$d\sigma = \frac{\alpha^2}{s^2}\frac{T\, d^2q_{1\perp}}{[q_{1\perp}^2 + (m_e\omega_1/E)^2][(k_\perp - q_{1\perp})^2 + (m_e\omega_2/E)^2]}\cdot\frac{d^3k_1 d^3k_2}{2\epsilon_1 2\epsilon_2(2\pi)^6}. \quad (5.37)$$

Let us now find the distribution in $k_{1,2}$ in the *main logarithmic approximation* [180], which is often sufficient. The main contribution to the cross section is given by the region of not too small $k_\perp^2 \gg (m_e\omega_i/E)^2$; here the integral (5.37) is cut off at $q_{1\perp}^2 \sim k_\perp^2$. Therefore, the main logarithmic contribution is, as in (5.31), associated with the two subregions $(m_e\omega_1/E)^2 \ll q_{1\perp}^2 \ll k_\perp^2$ and $(m_e\omega_2/E)^2 \ll (k_\perp - q_{1\perp})^2 = q_{2\perp}^2 \ll k_\perp^2$. In the former one $q_{2\perp} \approx k_\perp$, and the angle $\tilde{\varphi}_1$ coincides with that of integration, while $\tilde{\varphi}_2$ coincides with the fixed angle χ between $k_\perp$ and $k_{1\perp} - k_{2\perp} \approx 2k_{1\perp}$.

Table 5
The sources of inaccuracy for the approximation (5.37). Here λ_q^2 and λ_t^2 are the specific scales of the M_{ab} dependence on q_i^2 and t respectively, $\lambda = \min(\lambda_q, \lambda_t)$.

Source of inaccuracy	Relative value of inaccuracy
Approximate kinematical relations (5.17), (5.25)	$\lesssim \lvert q_i^2\rvert/W^2$ at $\lvert q_i^2\rvert < W^2$
$\cos\tilde{\varphi}_i$ (5.34)	$\lesssim \lvert q_{i\perp}/k_{1\perp}\rvert$ at $\lvert q_{i\perp}\rvert < \lvert k_{1\perp}\rvert$
Neglection of the q_i^2-dependence in M_{ab} (5.33)	$\lesssim \lvert q_i^2\rvert/\lambda_q^2$ at $\lvert q_i^2\rvert < \lambda_q^2$
The approximation for $t = t_1^0 = t_2^0$ (5.35) in M_{ab}	$\lesssim \lvert q_{i\perp}k_{1\perp}/\lambda_t^2\rvert$
Neglection of the scalar photon contributions	$\lesssim \sqrt{-q_i^2}/\lambda_q$ at $\lvert q_i^2\rvert < \lambda_q^2$
Neglection of the interference with the bremsstrahlung production of fig. 27	$\lesssim \sqrt{-q_i^2}/W$ at $\lvert q_i^2\rvert < W^2$

Therefore, after integration over $q_{1\perp}$ in both subregions, we obtain, with the logarithmic accuracy

$$d\sigma = \frac{16\pi\alpha^2}{k_\perp^2 W^4}\left(1 - \frac{\omega_1}{E} + \frac{\omega_1^2}{2E^2}\right)\left(1 - \frac{\omega_2}{E} + \frac{\omega_2^2}{2E^2}\right)\times \tag{5.38}$$

$$\times \{\tfrac{1}{2}(|M_{++}|^2 + |M_{+-}|^2)(L_1 + L_2) - [\xi_1 L_2 \mathrm{Re}(M_{-+}^* M_{++}) + \xi_2 L_1 \mathrm{Re}(M_{+-}^* M_{++})]\cos 2\chi\}\frac{d^3k_1\, d^3k_2}{2\epsilon_1 2\epsilon_2 (2\pi)^6}.$$

In this approximation the expression for the polarization of the ith photon ξ_i is simplified as compared with (5.18), and

$$\xi_i = \frac{1-(\omega_i/E)}{1-(\omega_i/E)+(\omega_i^2/2E^2)}; \quad L_i = \ln\frac{k_\perp^2 E^2}{m_e^2\omega_i^2}; \quad \cos 2\chi = 2\frac{(k_\perp(k_{1\perp} - k_{2\perp}))^2}{k_\perp^2(k_{1\perp} - k_{2\perp})^2} - 1.$$

From eqs. (5.33)–(5.37) one can obtain the answer with *more accuracy than the logarithmic one*. To be convinced of this fact let us consider the sources of inaccuracies of approximation (5.33)–(5.37). They are listed in table 5. Table 5 shows that the main terms neglected are of the order $\sim q_{i\perp}/\lambda$ where λ is the least of the two scales λ_t and λ_q which are, generally, different. The expressions (E.5) show that this is the case for lepton pair production $\lambda^2 \sim m_l^2 + k_{1\perp}^2$. For the hadron production it is naturally to expect that $\lambda \gtrsim m_\pi$.

When integrating (5.37) over $q_{1\perp}$ the leading terms among those taken into account are of the order $\int d^2q_{1\perp}/q_1^2 q_2^2 \sim (1/k_\perp^2)\ln(k_\perp^2 E^2/m_e^2\omega_1\omega_2)$ (we remind that $q_i^2 = -[q_{i\perp}^2 + (m_e\omega_i/E)^2]/(1 - \omega_i/E)$ and that the terms neglected are of the order of $\int(q_{2\perp}/\lambda)d^2q_{1\perp}/q_1^2q_2^2 \sim (k_\perp/\lambda k_\perp^2)\ln(k_\perp^2E^2/m_e^2\omega_1^2)$. Therefore, the accuracy of the approximation after integration can be

$$\eta \sim |k_\perp|/\lambda. \tag{5.39}$$

It is just with such an accuracy that the differential cross section for the pion-pair production [18] and for the production of an arbitrary system of particles in [169], have been found. These results contain all the five combinations of the amplitudes M_{ab} in (5.33), and look very complex. In the main region $k_\perp^2 \gg (m_e\omega_i/E)^2$ the result [18, 169] can be written in the form

$d\sigma = [(16\pi\alpha)^2/k_\perp^2]\{f\cdot d\sigma_{\gamma\gamma\to A_1A_2}/dt + \ldots\}d\Gamma_{A_1A_2}$ with coefficients given by $f = C_1L_1 + C_2L_2 + C_3$, where the C_i are dimensionless quantities of the order of unity and independent of $k_\perp$. The quantities C_1 and C_2 are the same as in the logarithmic approximation (5.38). The greater accuracy of the approximations [18, 169] is due to nonlogarithmic terms of the C_3-type.

Beyond the equivalent-photon approximation. Already at relatively small $k_\perp$ the difference between (5.38) and formulas [18, 169] is an overshoot in accuracy. Really, the terms $(k_\perp/\lambda)L_i$ omitted in writing f at rather small $k_\perp$, are comparable with C_3. (So, at $s/W^2 \lesssim 100$ and at $k_\perp \sim 10$–20 MeV/c for the pion production $(k_\perp/m_\pi)L_i \sim 1 \sim C_3$.)

At the same time taking into account the main terms of the previously omitted ones is here rather simple. It permits one to increase the accuracy up to

$$\eta \sim \max\left\{\frac{|k_\perp|}{\lambda}\left(\ln\frac{k_\perp^2E^2}{m_e^2\omega_i^2}\right)^{-1};\quad \frac{k_\perp^2}{\lambda^2}\right\}.$$

(For the above parameters the relative error decreases from ~0.15 to ~ 0.02.) From table 5 we see that one has here to take into account corrections of the two types. Some of them (lines 2 and 4) are reduces to a translation of arguments in the results [18, 169]. The other corrections are new terms having amplitudes with one scalar photon (line 5) and those connected with interference between the two-photon diagram and the bremsstrahlung diagrams of fig. 27 (line 6). The corresponding calculation has been carried out in [166], both for scalar particle pair production, e.g. $\pi\pi$ or KK and for $\mu^+\mu^-$-pair production. The result has the form

$$d\sigma = d\sigma_{C=+} + d\sigma_{\text{interf}}$$

$$= \frac{16\pi\alpha^2}{k_\perp^2W^4}\left(1-\frac{\omega_1}{E}+\frac{\omega_1^2}{2E^2}\right)\left(1-\frac{\omega_2}{E}+\frac{\omega_2^2}{2E^2}\right)(\Phi_{C=+}+\Phi_{\text{interf}})\frac{d^3k_1d^3k_2}{2\epsilon_1 2\epsilon_2(2\pi)^6}. \tag{5.40}$$

A contribution of the C-even diagram of fig. 32 is

$$\begin{aligned}\Phi_{C=+} &= \tfrac{1}{2}(L_1-\xi_1)(|M_{++}|^2+|M_{+-}|^2)_{t=t_1^0} + \tfrac{1}{2}(L_2-\xi_2)(|M_{++}|^2+|M_{+-}|^2)_{t=t_2^0}\\ &-\xi_1(L_2-1-\xi_2)\mathrm{Re}(M_{-+}^*M_{++})_{t=t_2^0}\cos 2\chi_+ - \xi_2(L_1-1-\xi_1)\mathrm{Re}(M_{-+}^*M_{++})_{t=t_1^0}\cos 2\chi_-\\ &+\xi_1\xi_2M_{-+}^*M_{+-}\cos 4\chi + (L_1\xi_2^0-L_2\xi_1^0)|k_\perp|\mathrm{Re}\left(M_{-+}^*\frac{M_{0+}}{i\sqrt{-q_1^2}}+M_{--}^*\frac{M_{0+}}{i\sqrt{-q_1^2}}\right)\cos\chi. \end{aligned}\tag{5.41}$$

Here χ is the angle between the vectors $\boldsymbol{k}_\perp$ and $\boldsymbol{k}_\perp - \boldsymbol{k}_{2\perp}$ and

$$\cos 2\chi_\pm = \cos 2\chi - 4\frac{|\underline{k}_\perp|}{|\boldsymbol{k}_{1\perp}-\boldsymbol{k}_{2\perp}|}\frac{\epsilon_1-\epsilon_2\pm(k_{1z}-k_{2z})}{\epsilon_1+\epsilon_2\pm(k_{1z}+k_{2z})}\sin^2\chi\cos\chi;\qquad \xi_i^0 = \sqrt{2}\,\frac{1-(\omega_i/2E)}{1-(\omega_i/E)+(\omega_i^2/2E^2)}.$$

For the quantities with logarithmic terms L_i, the value of the argument t (t_1^0 or t_2^0) is given. For the rest of them the difference between t_1^0 or t_2^0 is unessential. (We remind that at $q_i^2 \to 0$ the quantity $M_{0\pm}/\sqrt{-q_1^2}$ is finite.)

The quantity Φ_{interf} is the contribution from the interference of the two-photon and of the bremsstrahlung production. This quantity describes the charged asymmetry in A_1A_2 emission. For pions (F_π is the pion form factor)

$$\Phi_{\text{interf}} = -\pi\alpha k_\perp(k_{1\perp} - k_{2\perp})\left[\frac{\xi_2 \mathrm{Re}(F_\pi^* M_{++}) - \mathrm{Re}(F_\pi^* M_{+-})}{\omega_1(E-\omega_2)} L_1 \mp \frac{\xi_1 \mathrm{Re}(F_\pi^* M_{++}) - \mathrm{Re}(F_\pi^* M_{+-})}{\omega_2(E-\omega_1)} L_2\right] \quad (5.42)$$

For the $\mu^+\mu^-$ pair production (the particle mass is μ)

$$\Phi_{\text{interf}} = 4\pi^2\alpha^2 \frac{k_1(k_{1\perp} - k_{2\perp})}{k_{1\perp}^2 + \mu^2}\left[\frac{4\xi_2\mu^2 + 2W^2 - 4k_{1\perp}^2}{\omega_1(E-\omega_2)} \mp \frac{4\xi_1\mu^2 + 2W^2 - 4k_{1\perp}^2}{\omega_2(E-\omega_1)} L_2\right]. \quad (5.43)$$

The "minus" sign corresponds to positron–electron and the "plus" sign to electron–electron collision.

The generalization of the results (5.40–5.43) to the production of an arbitrary system of hadrons is reduced to a small increase in the number of independent combinations of helicity amplitudes.

5.6. *Particle pair production. Some specific features*

The formulas of the previous sub-section fully describe the differential distribution in the particle momenta of the produced pair in the region which gives the main contribution to the cross section. We shall discuss now some specific features of this distribution.

From eq. (5.38) it is seen that the angular distribution of the produced particle posses an azimuthal asymmetry (the terms proportional to cos 2χ). The appearance of this asymmetry is the natural result of the fact that the virtual photons are polarized.

In particular, if both particles A_1 and A_2 are emitted at large angles $\theta_1, \theta_2 \sim 1$, then $\omega_1 \approx \omega_2$. If additionally the energies ϵ_i of these particles are low in comparison with E, then the terms $\omega_i^2/2E^2$ can be neglected, i.e. one can put $\xi_1 = \xi_2 = 1$. The result (5.38) is simplified accordingly

$$\mathrm{d}\sigma = \frac{2\alpha^2}{\pi^4 k_\perp^2}\left(1 - \frac{\epsilon}{E}\right)\frac{\mathrm{d}\sigma_{\gamma\gamma}}{\mathrm{d}t}(1 - \rho^{(2)}\cos 2\chi)\ln\frac{k_\perp^2 s}{m_e^2 W^2}\frac{\mathrm{d}^3k_1\mathrm{d}^3k_2}{\epsilon_1\epsilon_2}; \quad (5.44)$$

$$\frac{\mathrm{d}\sigma_{\gamma\gamma}}{\mathrm{d}t} = \frac{|M_{++}|^2 + |M_{+-}|^2}{32\pi W^4}; \qquad \rho^{(2)}\frac{\mathrm{d}\sigma_{\gamma\gamma}}{\mathrm{d}t} = \frac{\mathrm{Re}[(M_{+-}^* + M_{+-}^*)M_{++}]}{32\pi W^4}. \quad (5.45)$$

Here $\mathrm{d}\sigma_{\gamma\gamma}/\mathrm{d}t$ is the $\gamma\gamma \to A_1A_2$ differential cross section for real nonpolarized photons, and $\rho^{(2)}\mathrm{d}\sigma_{\gamma\gamma}/\mathrm{d}t$ corresponds to the interference of the amplitudes with the difference of the total helicities of the photons equal to 2.

In the leading approximation, the distribution of the produced particles is a charge symmetric one. The charge asymmetry which is due to the interference between the two-photon production and the bremsstrahlung production (5.42), is small.

Some particular distributions are also quite specific. They can be obtained by integrating (5.38), (5.44) over unessential parameters. The distribution as a function of the first particle momentum $|k_1|$ as well as that of the angles θ_1 and θ_2 of both particles of a pair and of the angle of non-coplanarity ψ (between $k_{1\perp}$ and $-k_{2\perp}$) is obtained after integration of (5.38) over $|k_2|$. Since in the main region $k_{1\perp}^2 \gg k_\perp^2$, one has then to put $k_{1\perp} = -k_{2\perp}$ everywhere, except in the rapidly changing factors $1/k_\perp^2$ and cos 2χ, for which we have

$$\cos 2\chi = \frac{x^2 - 4\sin^2(\psi/2)}{x^2 + 4\sin^2(\psi/2)}; \qquad k_\perp^2 = k_{1\perp}^2[x^2 + 4\sin^2(\psi/2)]; \quad x = \frac{|k_{1\perp}| - |k_{2\perp}|}{|k_{1\perp}|}.$$

It follows that

$$\int \frac{d|k_2|}{k_\perp^2} = \frac{\pi}{2|k_1|\sin\theta_1 \sin\theta_2 |\sin(\psi/2)|}; \qquad \int \frac{d|k_2|}{k_\perp^2}\cos 2\chi = 0. \tag{5.45a}$$

Thus, the distribution over $|k_1|$, θ_1, θ_2, ψ or some of these parameters is expressed only by the differential cross section for the nonpolarized photons $d\sigma_{\gamma\gamma}/dt$ [180, 34] in the leading approximation. Substituting the latter relation into (5.38), we have at $m_e^2/s \ll \psi^2 \ll 1$ [165, 181]

$$d\sigma = \frac{2\alpha^2}{\pi^2}\left[\left(1-\frac{\epsilon}{2E}\right)^2 + \tfrac{1}{4}\left(\frac{\epsilon}{E}-\frac{W^2}{s}\right)^2\right]\frac{d\sigma_{\gamma\gamma}}{dt}\left(\ln\frac{sk_{1\perp}^2\sin^2(\psi/2)}{m_e^2 W^2}\right) \tag{5.46}$$

$$\times \frac{|k_1|^3\sin^2\theta_1}{\epsilon_1\epsilon_2\sin^2\theta_2|\sin(\psi/2)|}\, d|k_1|d\theta_1 d\theta_2 d\psi.$$

Note, that the distribution in ψ is sharp: $(d\psi/\psi)\ln\psi$.

Also, the distribution in $|k_1|$, θ_1, θ_2 has the form

$$d\sigma = \frac{2\alpha^2}{\pi^2}\left[\left(1-\frac{\epsilon}{2E}\right)^2 + \tfrac{1}{4}\left(\frac{\epsilon}{E}-\frac{W^2}{s}\right)^2\right]\frac{d\sigma_{\gamma\gamma}}{dt}\left(\ln\frac{s}{m_e^2}\right)^2 \frac{|k_1|^3\sin^2\theta_1}{\epsilon_1\epsilon_2\sin^2\theta_2}\, d|k_1|d\theta_1 d\theta_2. \tag{5.47}$$

For lepton pair production such a result has been obtained by Landau and Lifshitz [6]. They carried out calculations in the laboratory system $p_2 = 0$ using the variables $\epsilon_{iL} = k_i p_2/m_2$ and $k_{1\perp}$. For transformation to the c.m.s. it is sufficient to make a trivial substitution:

$$\frac{d\epsilon_{1L}\, d\epsilon_{2L}\, d^2k_{1\perp}}{\epsilon_{1L}\epsilon_{2L}} \to 2\pi \frac{|k_1|^3\sin^2\theta_1}{\epsilon_1\epsilon_2\sin^2\theta_2}\, d|k_1|d\theta_1 d\theta_2;$$

$$W^2 \approx (m_e^2 + k_{1\perp}^2)(\epsilon_{1L}+\epsilon_{2L})^2/\epsilon_{1L}\epsilon_{2L} \to 4\omega_1\omega_2.$$

The further integration over ϵ_{iL} and $k_{1\perp}$ is also contained in [6] (see also [182]).

5.7. *Photoproduction in the Bethe-Heitler-Primakoff scheme and possibility of observation of the* $\gamma\gamma \to$ h *transition*

Photoproduction on nuclei (fig. 34) is also a widely known mechanism for the two-photon production of particles. For e^+e^- pair production such a mechanism has been discussed for the first time by Bethe and Heitler [183]. This process was observed many times, in particular, for testing QED (see review [184]). Primakoff [160] suggested to use it to measure the π^0 lifetime. Both the width of the η^0 and the most accurate value of the π^0 lifetime have been obtained by this method.

The cross section of this process, integrated over the phase space volume of the produced system, has a form similar to (5.12)

$$d\sigma = \frac{\alpha}{4\pi^2|q_2^2|}\,\frac{q_1q_2}{q_1P}\left[2\rho_2^{++}\sigma_{TT} + \rho_2^{00}\sigma_{TS} + |\rho_2^{+-}|\left(2\,\frac{|e\widetilde{P}|^2}{|\widetilde{P}^2|}-1\right)\tau_{TT}\right]\frac{d^3P'}{E'};$$

$$\widetilde{P}^\mu = R^{\mu\nu}P^\nu \approx 2q_{2\perp}^\mu q_1 P/W^2; \qquad \rho_2^{++} \approx |\rho_2^{+-}|. \tag{5.48}$$

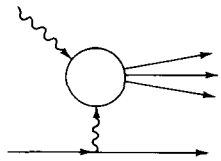

Fig. 34. The Bethe–Heitler–Primakoff effect – photoproduction off the Coulomb field of nucleus. The nucleus momentum is P (P'), mass is m_p and $q_2 = P - P'$.

Here e is the polarization vector of a real photon, ρ_2^{ab} is the density matrix of the virtual photon, emitted by the nucleus (see appendix D), and the quantities σ_{TT}, σ_{TS} and τ_{TT} have in their arguments $q_1^2 = 0$. For nonpolarized light the term containing τ_{TT} vanishes in (5.48). The total transverse momentum of the produced system of particles is $\boldsymbol{k}_\perp = \boldsymbol{q}_{2\perp} = -\boldsymbol{P}'_\perp$.

In the region giving the main contribution to the cross section $|q_2^2|$ is small. Therefore, with a good accuracy one can neglect σ_{TS} and take σ_{TT} and τ_{TT} on mass shell. In the production on a nucleus with charge Ze and form factor F one gets for non-polarized photons

$$d\sigma = \frac{Z^2\alpha}{\pi} F^2(q_2^2)\sigma_{\gamma\gamma}(W^2)\frac{dW^2}{W^2}\frac{q_{2\perp}^2}{q_2^4}dq_2^2. \tag{5.49}$$

In the laboratory frame $\boldsymbol{P} = 0$ (ω_1 is the frequency of the ingoing photon, θ is the nucleus recoil angle)

$$q_1 P = \omega_1 m_p; \quad W^2 = 2\omega_1 P_z; \quad -q_{2\perp}^2 = \boldsymbol{P}'^2; \quad q_{2\perp}^2/q_2^2 \approx \sin^2\theta; \quad q_{2\,\min}^2 = (W^2/2\omega_1)^2.$$

The scale Λ_γ^2 of the cut off of the integral over q_2^2 due to σ_{TT} can be considerably greater than the scale Λ_F^2 of a variation of the nucleus form factor. If the form factor is known up to a value $-q_2^2$ markedly exceeding the value Λ_F^2, then after integrating (5.49) over q_2^2 we obtain a result with high accuracy [180]

$$\eta \sim (\Lambda_F/\Lambda_\gamma)^2[\ln(4\omega_1^2\Lambda_F^2/W^4)]^{-1}. \tag{5.50}$$

In principle, this mechanism can be used in order to obtain information on the $\gamma\gamma \to h$ transition [160, 163, 185, 186]. But here a difficulty arises due to the separation of the contribution of this particular channel from that of usual photoproduction off nucleus. The possibility of extracting the Primakoff-effect contribution from this background is connected with small values $k_\perp$ in the two-photon production (cf. the specific $\boldsymbol{k}_\perp = \boldsymbol{q}_{2\perp}$-distribution in fig. 33). The observation of such a dependence near the maximum requires either a measurement of the nucleus recoil momentum or a very exact measurement of the momenta of all the produced particles. Because of the small value of $k_\perp$ (i.e. also the virtual photon mass q_2^2) the $\gamma\gamma \to h$ cross section can be studied here but on mass shell only. (For photoproduction on nuclei with $Z \gg 1$ the small value of the effective values of q_2^2 is also connected with the cut off due to the nucleus form factor.)

Let us give a characteristic value. The cross section for the two-photon ϵ-meson production on xenon at $\omega_1 \sim 20$ to 40 GeV is of the order of 10μb.

The above discussion can be extended to *electroproduction off nuclei* with a small modification only.

6. The equivalent photon approximation (EPA)

The idea of the equivalent photon approximation belongs to Fermi [187], who paid attention to the fact, that the field of a fast charged particle is similar to an electromagnetic radiation. This radiation may be interpreted as a flux of photons distributed with some density $n(\omega)$ on a frequency spectrum. Therefore, the electromagnetic interaction of this particle, e.g. with a nucleus is reduced to the interaction of such photons with the nucleus. This thought has been used and developed for the calculation of the cross section of interaction of relativistic charged particles in the papers of Williams and Weizsäcker [15]. In these early papers a semi-classical approach was used for obtaining the equivalent photon spectrum $n(\omega)$. M. and G. Nordheims et al. [188] have used the old perturbation theory for that purpose. In the papers of Dalitz and Yennie, Curtis, D. and P. Kesslers [189] the same results were obtained by means of Feynman diagrams. However, the equivalent photon spectra obtained in these papers may be used for solving only a small range of problems. The most consistent derivation of EPA, with discussion of various situations, is given in the paper of Pomeranchuk and Shmushkevitch [185]. In the paper of Gribov et al. [190] some calculations necessary for the derivation of EPA are performed in a simple and consistently covariant form*. Unfortunately, all these papers do not contain a discussion of the applicability range of EPA and of its accuracy.

This defect takes place also in the EPA description available in text-books, at least those known to us [182].

In the last years, EPA was widely used to obtain various cross sections for two-photon particle production. When solving this problem in a number of papers the spectra from refs. [189] beyond their applicability range of simply erroneous spectra were used. On the other hand, a number of incorrect or inaccurate statements pertaining to the essence and the advantages of EPA were given**.

For this reason we considered it to be useful to derive in details EPA in this section and to discuss important errors and inaccuracies encounted in its use.

6.1. *The essence of EPA*

From the present point of view EPA (Weizsäcker-Williams' method) is in essence only a simple and convenience method for the approximate calculation of Feynman diagrams for the collision of fast charged particles.

As an example we shall consider inelastic electron scattering off proton in the lowest order in α.

*The most detailed history of EPA and its derivation is contained in Kessler's report [191].

**As an example, we point out a funny incident which happened with a formula for the cross section for e^+e^- or $\mu^+\mu^-$ pair production in collision of fast charged particles. The correct asymptotic behaviour of the cross section for this process (1.2) was obtained by Landau and Lifshitz in 1934 [6]. At the same time this result was confirmed in papers by Williams [15], Bhabha [19] and Racah [12] and it has been included in the text-books (Williams obtained his result by means of EPA). Nevertheless, just recently two papers [5, 192] were published, in which incorrect formulas for the same cross section were obtained by different methods and in a review [50] quite a wrong statement was even proclaimed, namely that the results of both these papers coincide with the recent (correct) calculations [193]. This incorrect result was repeated in review [14] also.

These errors are given proper attention in refs. [34, 170] (in details see sub-section 6.7). Nevertheless, recently one more paper [194] has appeared which concludes that this discrepancy is due to the fact that the authors with the correct result [6, 170] "integrate over all electron scattering angles, rather than just over the region of validity of the equivalent photon approximation", i.e. that the applicability range of EPA gives quite another value for the asymptotics of this process compared to both the correct formula [6] and the incorrect one [5]

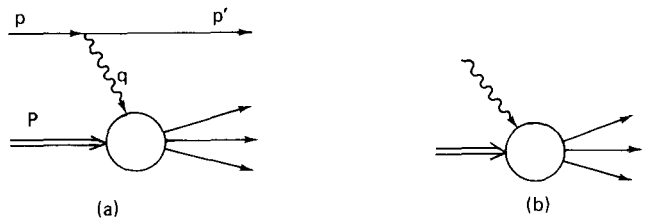

Fig. 35. Electroproduction and photo-absorption.

The connection of this process with photo-absorption on proton is evident from fig. 35. However in this photo-absorption amplitude *the photon is off mass shell and no longer transversely polarized.* The equivalent photon approximation consists in ignoring both these deviations from real photo-absorption. As a result, the cross section for inelastic electron scattering off proton is expressed in terms of the cross section $\sigma_\gamma(\omega)$ for the absorption of real photons with frequency ω:

$$d\sigma_{ep} = \sigma_\gamma(\omega)dn. \tag{6.1}$$

The quantity dn in this equation is called the equivalent photon number or spectrum. The dependence of the spectrum dn on the photon frequency ω and its mass squared q^2 is unambiguously defined by the form of the $e \to e'\gamma^*$ vertex.

A consistent analysis of the terms neglected in going from the accurate expression of the diagram of fig. 35a to the approximate relation (6.1) permits in a natural manner to estimate the applicability range of EPA and its accuracy. This can be performed in a general form for every reaction. In this case the details of the result depend essentially on the characteristic behaviour met when moving off mass shell for photoprocess amplitudes.

In most of the physically interesting cases such a parameter Λ_γ (a dynamical cut off) exists such that, at $|q^2| < \Lambda_\gamma^2$, the photo-absorption cross sections differ only slightly from their values on the mass shell and quickly decrease at $|q^2| > \Lambda_\gamma^2$. This particular feature permits one to use EPA for the description of the cross sections at $|q^2| < \Lambda_\gamma^2$. (Let us note, that sometimes a cut off on q^2 may be also due to the form factor at the $1 \to 1'\gamma$ vertex, e.g., for Coulomb proton scattering on nucleus.)

On the other hand, the $|q^2| < \Lambda_\gamma^2$ domain gives the main contribution to the total cross section, since the contribution of small q^2 is enhanced logarithmically.

Therefore, the integral over the $(-q^2 < \Lambda_\gamma^2)$ domain, with an approximate expression of type (6.1) as an integrand, describes correctly the frequency distribution and the total cross section*. The accuracy of the approximation obtained here can be either logarithmic or higher, if there are other cut off factors.

Thus, for the practical use of EPA one should elucidate in each case, whether there is a dynamical cut-off (the Λ_γ-parameter), and estimate it. An essential advantage of EPA consists in the fact that, when using it, it is sufficient to know the photo-absorption cross section on the mass shell only. Details of its off mass shell behavior are not essential.

*The integration of the approximate expression (6.1) over the entire kinematically allowed q^2-change region leads, as a rule, to erroneous expressions, since in this mode of operation the $(|q^2| > \Lambda_\gamma^2)$-domain is able to give a large fictitious contribution.

Note, that the virtual photons are polarized. This stipulates an azimuthal asymmetry for some distributions. (An example is offered by the distribution over the scattered particle momenta in the two-photon production.)

We shall give the derivation of EPA in terms of the well known example of inelastic ep scattering. Let us note, that in all approximate formulas given below a small value for the ω/E ratio is not assumed. The only requirement is put on the ultra-relativistic nature of a scattered electron ($E - \omega \gg m_e$) and is commonly made.

6.2. *Connection with the photo-absorption cross sections*

In this sub-section a derivation of eq. (6.8) expressing the cross section for electroproduction (fig. 35a) in terms of the cross section for virtual photo-absorption (fig. 35b) [195] is given.

Denoting the virtual photo-absorption amplitude by M^μ, averaging over the initial spin states, and summing over the final ones, we obtain

$$d\sigma_{ep} = \frac{4\pi\alpha}{(-q^2)} M^{*\nu} M^\mu \rho^{\mu\nu} \frac{(2\pi)^4 \delta(p + P - p' - k) d\Gamma}{4\sqrt{(pP)^2 - p^2 P^2}} \frac{d^3 p'}{2E'(2\pi)^3}. \tag{6.2a}$$

Here Γ is a phase space volume of the produced particle system (with total momentum k), and

$$\rho^{\mu\nu} = \frac{1}{2(-q^2)} \mathrm{Sp}[(\hat{p} + m_e)\gamma^\mu(\hat{p}' + m_e)\gamma^\nu] = -\left(g^{\mu\nu} - \frac{q^\mu q^\nu}{q^2}\right) - \frac{(2p-q)^\mu (2p-q)^\nu}{q^2}. \tag{6.2b}$$

The $\rho^{\mu\nu}$ quantity is the (non-normalized) density matrix of the virtual photon produced by an electron. Let us note that the $\rho^{\mu\nu}$ is non-diagonal, i.e. the virtual photons *are polarized.* The expression (6.2) is written in such a form as to introduce naturally the terminology which is suitable for EPA. Namely, instead of speaking about the ep collision (fig. 35a) one may speak about the collision of a virtual photon with the proton (fig. 35b). Then the number of photons with a given polarization in a given element $d^3p' = d^3q$ of the phase space volume is proportional to the quantity $\rho^{\mu\nu} d^3q/q^2$.

After integration over the phase space volume Γ of the produced system of particles, the following quantity will be included in the result (6.2):

$$W^{\mu\nu} = \tfrac{1}{2} \int M^{*\nu} M^\mu (2\pi)^4 \delta(q + P - k) d\Gamma. \tag{6.3}$$

In accordance with the optical theorem, $W^{\mu\nu}$ is the absorptive part of the γp-forward amplitude, connected with the cross section in the usual way. The tensors according to which $W^{\mu\nu}$ is expanded, can be constructed only of the q, P vectors and $g^{\mu\nu}$ tensor. In order to take into account explicitly gauge invariance $q^\mu W^{\mu\nu} = q^\nu W^{\mu\nu} = 0$, it is convenient to use the following linear combinations:

$$Q = \sqrt{\frac{-q^2}{(qP)^2 - q^2 P^2}} \left[P - q \frac{(qP)}{q^2}\right]; \qquad qQ = 0, \qquad Q^2 = 1;$$

$$R^{\mu\nu} = R^{\nu\mu} = -g^{\mu\nu} + [(qP)(q^\mu P^\nu + q^\nu P^\mu) - q^2 P^\mu P^\nu - P^2 q^\mu q^\nu]/[(qP)^2 - q^2 P^2]; \tag{6.4}$$

$$q^\mu R^{\mu\nu} = Q^\mu R^{\mu\nu} = 0.$$

Having expanded $W^{\mu\nu}$ in these tensors, we obtain

$$W^{\mu\nu} = R^{\mu\nu}W_T(q^2, qP) + Q^\mu Q^\nu W_S(q^2, qP). \tag{6.5}$$

The dimensionless invariant functions W_T and W_S are simply connected with the cross section for transverse or scalar photon absorption σ_T and σ_S respectively*:

$$W_T = 2\sqrt{(qP)^2 - q^2P^2}\ \sigma_T; \qquad W_S = 2\sqrt{(qP)^2 - q^2P^2}\ \sigma_S. \tag{6.6}$$

Substituting (6.5), (6.6) into (6.2), we obtain

$$d\sigma = \frac{\alpha}{4\pi^2|q^2|}\left[\frac{(qP)^2 - q^2P^2}{(pP)^2 - p^2P^2}\right]^{1/2}(2\rho^{++}\sigma_T + \rho^{00}\sigma_S)\frac{d^3p'}{E'}. \tag{6.8}$$

Here the coefficients ρ^{ab} are the elements of the density matrix (6.2b) in the γp-helicity basis:

$$2\rho^{++} = \rho^{\mu\nu}R^{\mu\nu} = \frac{(2pP - qP)^2}{(qP)^2 - q^2P^2} + 1 + \frac{4m_e^2}{q^2};$$

$$\rho^{00} = \rho^{\mu\nu}Q^\mu Q^\nu = 2\rho^{++} - \frac{4m^2}{q^2} - 2. \tag{6.9}$$

It is further convenient to use the covariant variables

$$\omega = \frac{qP}{m_p}; \qquad E = \frac{pP}{m_p}; \qquad \frac{d^3p'}{E'} = \frac{d\omega\, d(-q^2)d\varphi}{2\sqrt{E^2 - m_e^2}} \to \pi\frac{d\omega\, d(-q^2)}{\sqrt{E^2 - m_e^2}}. \tag{6.10}$$

In the lab-system ($\boldsymbol{P} = 0$) the invariant E coincides with the electron energy, and ω coincides with the photon energy; φ is the azimuthal angle for the scattered electron. (Integration over φ is performed trivially in our case.)

At $E - \omega \gg m_e$, the photon mass q^2 varies in the range:

$$q^2_{min} = \frac{m_e^2\omega^2}{E(E-\omega)}\left[1 + O\left(\frac{m_e^2}{(E-\omega)^2}\right)\right] \leqslant -q^2 \leqslant 4E(E-\omega). \tag{6.11}$$

6.3. q^2-dependence of the quantities ρ^{ab} and σ_a

A. The $W^{\mu\nu}$ tensor (6.3) is, obviously, regular at $q^2 = 0$. At the same time and in accordance with (6.4) the $Q^\mu Q^\nu$ factor in (6.5) increases as $(q^2)^{-1}$ at $q^2 \to 0$. Therefore,

*Such a connection becomes obvious if one takes proper account of simple equations for the photon polarizations vectors $e(a)$ in the γp c.m.s. (cf. (B.3), (B.4))

$$e(0) = iQ; \qquad e^{*\mu}(+1)e^\nu(+1) + e^{*\mu}(-1)e^\nu(-1) = R^{\mu\nu}. \tag{6.7}$$

The W_T and W_S functions are connected with the commonly used W_1 and W_2 functions (3.11) by means of simple relations

$$8\pi^2\alpha m_p W_1 = W_T; \qquad 8\pi^2\alpha m_p W_2 = \frac{|q^2|m_p^2}{(qP)^2 - q^2P^2}(W_T + W_S).$$

Let us note that our normalization of σ_a differs from the one introduced by Hand [195]: $W_a = (2qP + q^2)\sigma_{a(Hand)}$; a = T, S.

$$W_S \propto \sigma_S \sim q^2; \qquad \text{at } q^2 \to 0. \tag{6.12}$$

At $q^2 \to 0$ the quantity σ_T approaches the cross section σ_γ for real non-polarized photon absorption.

For the construction of EPA this purely kinematical information is insufficient. It is necessary to have a dynamical information on a character of the q^2 dependence of σ_a.

In our particular case – inelastic ep scattering – experiment shows that as $-q^2$ increases σ_T decreases as $(-q^2)^{-a}$ with $a \geqslant 1$ and that the characteristic scale of this change *is of the order of* m_ρ^2. (In particular, at $|q^2| < m_\rho^2$ one has $[\sigma_T - \sigma_\gamma]/\sigma_\gamma \lesssim |q^2|/m_\rho^2$.) The quantity σ_S increases firstly (6.12), but it does not exceed σ_T in order of magnitude and, at large values of $|q^2|$, it falls down as σ_T also.

In numerous cases which are of practical importance the q^2 dependence of σ_T and σ_S is of the same nature. For example, the Bethe–Heitler process $e\gamma \to ee^+e^-$ (fig. 36) may be treated as inelastic electron scattering off the photon target. Therefore, this process cross section is expressed in terms of virtual $\gamma^*\gamma \to e^+e^-$ cross sections (E.3). In this case $\sigma_T \equiv \sigma_{TT}$ decreases with the increase of q^2 and first $\sigma_S \equiv \sigma_{ST}$ increases from zero and then decreases. According to (E.3) a specific scale for the above changes is of the order of W^2.

Therefore, one may state that, for both these examples,

$$W_S = 2\sqrt{(qP)^2 - q^2P^2}\ \sigma_S \lesssim \frac{|q^2|}{\Lambda_\gamma^2}(qP)\sigma_\gamma, \tag{6.13}$$

$$W_T = 2\sqrt{(qP)^2 - q^2P^2}\ \sigma_T(\omega, q^2) = 2(qP)\sigma_\gamma(\omega)\,[1 + O(q^2/\Lambda_\gamma^2)] \quad \text{at } |q^2| < \Lambda_\gamma^2$$

and when $|q^2| > \Lambda_\gamma^2$, σ_T and σ_S vanish as a power when $|q^2|$ increases. One also has

$$\Lambda_\gamma \sim m_\rho \qquad \text{for the electroproduction off proton,}$$

$$\Lambda_\gamma \sim W \qquad \text{for the Bethe–Heitler process.} \tag{6.13a}$$

If the conditions (6.13) are not fulfilled, a special consideration is necessary. One such example is analysed in section 6.8. Below, everywhere except in section 6.8 we consider the cases in which conditions (6.13) are fulfilled.

B. In our case the q^2 dependence of ρ^{++} and ρ^{00} (6.9) is entirely known. Both these quantities are almost of the same order. In addition

$$2\rho^{++} = (2E - \omega)^2/\omega^2 + 1 + 4m_e^2/q^2 \qquad \text{at} \qquad |q^2| \ll \omega^2 \tag{6.14}$$

and for $|q^2| > \omega^2$ the quantities ρ^{++} and ρ^{00} decrease quickly with increasing $|q^2|$. At $q^2_{\min} < -q^2 < \omega^2$ the quantity ρ^{++} does not practically depend on q^2.

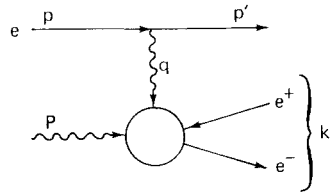

Fig. 36. The Bethe–Heitler process, $e\gamma \to ee^+e^-$ treated as inelastic electron scattering on photon target, $P^2 = 0$, $q = p - p'$, $W^2 = (q+P)^2$.

C. As a result, the q^2-dependence of the cross section $d\sigma_{ep}$ (6.8) has the following properties. In a wide range of not very large q^2, $q^2_{min} < -q^2 \ll \omega^2, \Lambda^2_\gamma$, its dependence is logarithmic: $d\sigma \propto dq^2/q^2$. With further increase of q^2 the cross section $d\sigma$ decreases quickly. The beginning of this decrease is determined either by the dynamical cut off at $|q^2| \sim \Lambda^2_\gamma$ (6.13) or by the kinematical one, at $|q^2| \sim \omega^2$ (6.14).

D. The virtual photons can also be produced by *other particles, e.g. by pion or proton.* In appendix D the corresponding expressions for ρ^{++} and ρ^{00} are given.

If one first does not take into account the q^2-dependence of form factors, then, as before, for $|q^2| < \omega^2$ the quantity ρ^{++} does not practically depend on q^2, and for $|q^2| > \omega^2$, ρ^{++} decreases quickly as $|q|^2$ increases and $\rho^{00} \approx \rho^{++}$. The q^2-dependence of the form factors leads to an extra decrease of ρ^{++}. For pion e.g. ρ^{++} and ρ^{00} are proportional to $|F_\pi(q^2)|^2$ (F_π is the pion form factor). As $|q^2|$ increases this form factor decreases and we denote by Λ the specific scale of this decrease. Consequently, the quantities ρ^{++} and ρ^{00} decrease quickly for

$$|q^2| > \min(\omega^2, \Lambda^2), \tag{6.15}$$

at $|q^2| \ll \min(\omega^2, \Lambda^2)$ the quantity ρ^{++} does not practically depend on q^2.

6.4. *EPA. The ω, q^2-distributions*

The small q^2 domain gives the main contribution to the cross section of processes under consideration. In this domain our expression for the cross section (6.8) can be essentially simplified. When switching to the approximate formulas of EPA two simplifications are performed. First the scalar photon contribution σ_S is neglected, second $\sqrt{(qP)^2 - q^2P^2}\,\sigma_T(\omega, q^2)$ is substituted by its on-shell value $(qP)\sigma_\gamma(\omega)$. As a result the photon frequency and "mass" distribution has the form

$$d\sigma_{ep} = \sigma_\gamma(\omega)\, dn(\omega, q^2), \tag{6.16a}$$

$$dn = \frac{\alpha}{2\pi E^2}\,\rho^{++}\omega d\omega\,\frac{d(-q^2)}{|q^2|} = \frac{\alpha}{4\pi E^2}\left[\frac{(2E-\omega)^2}{\omega^2 - q^2} + 1 + \frac{4m^2}{q^2}\right]\frac{\omega d\omega d(-q^2)}{|q^2|}. \tag{6.16b}$$

The dn-quantity is an equivalent photon number.

Let us emphasize that the whole formulation of EPA should also include statements on the domain, where these equations are a good approximation to the exact result (6.8). This requires a special consideration in each case.

Since in the case under consideration $2\rho^{++}$ and ρ^{00} are of the same order, the approximation (6.16) is correct in the domain

$$|q^2| < \Lambda^2_\gamma. \tag{6.16c}$$

Here $\sigma_S \ll \sigma_T$ and the q^2 dependence in $\sqrt{(qP)^2 - q^2P^2}\,\sigma_T$ can be neglected. Due to (6.13) the accuracy of such an approximation is

$$\eta \sim |q^2|/\Lambda^2_\gamma. \tag{6.16d}$$

In numerous cases of physical interest the only range of importance is that of not very small frequencies $\omega \gtrsim \Lambda_\gamma$. Here the terms of the order of q^2/ω^2 should be rejected as the overshoot of accuracy, and the expressions for the spectrum can be simplified (cf. (6.11))

$$dn = \frac{\alpha}{\pi}\frac{d\omega}{\omega}\frac{d(-q^2)}{|q^2|}\left[1 - \frac{\omega}{E} + \frac{\omega^2}{2E^2} - \left(1 - \frac{\omega}{E}\right)\left|\frac{q^2_{min}}{q^2}\right|\right]. \tag{6.16e}$$

6.5. *EPA. The ω-distribution*

Let us show that the distribution in the photon frequency can be obtained by a simple integration of (6.16) over the region of small q^2 (i.e. over the validity region for (6.16)) and find out the limits of this region together with the accuracy of the approximations.

After integrating (6.16) over the region $q^2_{min} \leqslant -q^2 \leqslant q^2_{max}$ the cross section can be written in the form

$$d\sigma = \sigma_\gamma(\omega)\, dn(\omega); \tag{6.17a}$$

$$dn(\omega) = \int_{q^2_{min}}^{q^2_{max}} dn(\omega, q^2) = N(\omega)\, d\omega/\omega;$$

$$N(\omega) = \frac{\alpha}{\pi}\left[\left(1 - \frac{\omega}{E} + \frac{\omega^2}{2E^2}\right)\ln\frac{q^2_{max}}{q^2_{min}} - \left(1 - \frac{\omega}{2E}\right)^2 \ln\frac{\omega^2 + q^2_{max}}{\omega^2 + q^2_{min}} - \frac{m_e^2\omega^2}{E^2 q^2_{min}}\left(1 - \frac{q^2_{min}}{q^2_{max}}\right)\right]. \tag{6.17b}$$

For the description of the ω-distribution, one should choose a lower limit of the q^2-integration region which is equal to the kinematic limit (6.11), i.e. $q^2_{min} = m_e^2\omega^2/E(E - \omega)$.

The upper limit q^2_{max} is usually less than the kinematic limit $4E(E - \omega)$ (6.11). The value of q^2_{max} differs from problem to problem and is defined either by cut off parameters (6.13–6.15) or by the experimental limitations.

Let us go to the description of some important particular cases.

A. *The high-frequency part of the ω-distribution ($\omega \gtrsim \Lambda_\gamma$) in the absence of experimental limitations.* For $\omega \gtrsim \Lambda_\gamma$ the dynamical cut off is the actual one and one should take $q^2_{max} = \Lambda^2_\gamma$. Indeed, for $|q^2| < \Lambda^2_\gamma$, the main q^2-dependence of $d\sigma_{ep}$ (6.8) is logarithmic (dq^2/q^2). After integration over $-q^2 < \Lambda^2_\gamma$ the terms taken into account in the approximation (6.16) are of the order of $\int dq^2/q^2 \sim \ln(\Lambda^2_\gamma/q^2_{min})$.

The contribution to the integral of the neglected terms in this region is of the order of $\int dq^2/\Lambda^2_\gamma \sim 1$. Since for $|q^2| > \Lambda^2_\gamma$ both σ_T and σ_S decrease quickly, the integral contribution of this domain to the entire ω-distribution is also of the order of unity. Therefore, EPA (6.17) with $q^2_{max} = \Lambda^2_\gamma$ describes the high-energy part of the ω-distribution with an accuracy

$$\eta \sim [\ln(\Lambda^2_\gamma/q^2_{min})]^{-1}; \qquad (\omega \gtrsim \Lambda_\gamma; q^2_{max} = \Lambda^2_\gamma). \tag{6.18a}$$

With this accuracy the expression for spectrum (6.17b) can be simplified:

$$dn(\omega) = \frac{\alpha}{\pi}\left[\left(1 - \frac{\omega}{E} + \frac{\omega^2}{2E^2}\right)\ln\frac{\Lambda^2_\gamma E(E - \omega)}{m_e^2\omega^2} - \left(1 - \frac{\omega}{E}\right)\right]\frac{d\omega}{\omega}. \tag{6.18b}$$

B. For *the low-frequency part of the ω-distribution* ($\omega < \Lambda_\gamma$) instead of the dynamical cut-off (at $|q^2| \sim \Lambda_\gamma^2$) the kinematic cut-off at $|q^2| \sim \omega^2$ (due to denominator $\omega^2 - q^2$ in the main term of (6.9)) is the actual one. Operating just in the same manner as above we must take $q^2_{max} = \omega^2$ and neglect the q^2-dependence in ρ^{++} (except for the term $4m_e^2/q^2$ (6.14)). As a result, the low-frequency part of the ω-dependence is described by EPA (6.17) with $q^2_{max} = \omega^2$. The accuracy of this approximation is

$$\eta \sim [\ln(\omega^2/q^2_{min})]^{-1} \sim 1/\ln(E^2/m_e^2). \tag{6.19a}$$

The simplified spectrum $dn(\omega)$ has the form

$$dn = \frac{\alpha}{\pi}\frac{d\omega}{\omega}\left(1 - \frac{\omega}{E} + \frac{\omega^2}{2E^2}\right)\ln\frac{E(E-\omega)}{m_e^2}. \tag{6.19b}$$

However, since the ρ^{++} quantity is entirely known, the approximation accuracy can be markedly improved if one widens the integration up to $q^2_{max} = \Lambda_\gamma^2$. The estimation of the accuracy of the resulting approximation is similar to the one performed when obtaining (6.18a). (Now, however the neglected terms are of the order $(\omega^2/\Lambda_\gamma^2)\ln(\Lambda_\gamma^2/\omega^2)$.) As a result, EPA with the spectrum (6.17b) for $q^2_{max} = \Lambda_\gamma^2$ describes the low-frequency part of the ω-dependence with an accuracy

$$\eta \sim \frac{\omega^2}{\Lambda_\gamma^2}\frac{\ln(\Lambda_\gamma^2/\omega^2)}{\ln(\omega^2/q^2_{min})} \approx \frac{\omega^2}{\Lambda_\gamma^2}\frac{\ln(\Lambda_\gamma^2/\omega^2)}{\ln(E^2/m_e^2)}; \qquad (\omega < \Lambda_\gamma;\ q^2_{max} = \Lambda_\gamma^2). \tag{6.19c}$$

Within this accuracy limitation the result does not change, if the integration is additionally widened to the domain $|q^2| > \Lambda_\gamma^2$ taking q^2_{max} equal, e.g. to the kinematic limit $4E(E-\omega)$ (6.11). Then one obtains [188, 5] the known expression for the spectrum:

$$dn = \frac{\alpha}{\pi}\left[2\left(1 - \frac{\omega}{E} + \frac{\omega^2}{2E^2}\right)\ln\frac{2E(E-\omega)}{m_e(2E-\omega)} + \frac{\omega^2}{2E^2}\ln\frac{2E-\omega}{\omega} - 1 + \frac{\omega}{E}\right]\frac{d\omega}{\omega}. \tag{6.19d}$$

(Using this expression out of its range of validity has been the source of numerous errors, cf. section 6.7.)

Let us note, that the spectrum (6.17b) with $q^2_{max} = \Lambda_\gamma^2$ may be used for the description of the whole ω-distribution with an accuracy not worse than logarithmic.

C. Let us now consider *the effect of the experimental limitations* on the spectrum. As an example we shall analyse the ω-distribution for such experimental conditions, when only the events with electrons scattered at small angle $\theta < \theta_m \ll 1$ are observed. Here $|q^2| \leqslant E(E-\omega)\theta_m^2$. If this value is larger than Λ_γ^2 it is obvious, that the previous estimations are valid. However, if this experimental limitation is more restrictive than the dynamical or kinematic cut offs, i.e. $E(E-\omega)\theta_m^2 < \omega^2, \Lambda_\gamma^2$, then (6.17) with $q^2_{max} = E(E-\omega)\theta_m^2$ describes the frequency distribution with a higher accuracy

$$\eta \sim \frac{q^2_{max}}{\Lambda_\gamma^2}\left[\ln\frac{q^2_{max}}{q^2_{min}}\right]^{-1}; \qquad q^2_{max} = E(E-\omega)\theta_m^2 < \omega^2, \Lambda_\gamma^2. \tag{6.20}$$

Just in the same manner, one can also describe the low-frequency spectrum edge $\omega^2 < E(E-\omega)\theta_m^2 < \Lambda_\gamma^2$ (with the accuracy (6.19a)).

D. If the virtual photons are not produced by electron, as in the above examples, but, e.g.

by pion or proton, then an extra cut off at $|q^2| = \Lambda^2$ arises due to the form factors (cf. (6.15)). The only case, when this cut-off is the actual one, i.e. $\Lambda < \omega, \Lambda_\gamma$, requires here a special discussion. If the form factors are well known up to $|q^2| \sim \Lambda_\gamma^2$ (or up to those values $|q^2| < \Lambda_\gamma^2$, at which they become negligibly small), then the ω-distribution can be described by EPA (6.17a) with $q^2_{\max} = \Lambda_\gamma^2$. In this case the accuracy $\eta \sim (\Lambda/\Lambda_\gamma)^2[\ln(\Lambda^2/q^2_{\min})]^{-1}$. The respective expression for the spectrum, produced by proton is given in appendix D. Simpler expression can be obtained in the logarithmic approximation, where a specific form for the form factor q^2-dependence is inessential. Here one should put $q^2_{\max} = \Lambda^2$ (in this case $\eta \sim [\ln(\Lambda^2/q^2_{\min})]^{-1}$).

6.6. *EPA. The momentum distribution of secondaries*

The momentum distribution of secondaries involves a new important feature – it is here necessary to take into account the polarization of the virtual photon. The photon polarization is unessential, if the integration over the momenta of the secondaries is performed (and, therefore, any specific direction is preferred). For this reason the diagonal elements of the density matrix ρ^{ab} only are present in (6.8), and the cross section for absorption of non-polarized light σ_γ only appears in the result (6.16), (6.17).

For definiteness let us consider the distribution over the momentum k_1 of one of the secondaries. This momentum determines a specific direction, and terms which describe an azimuthal asymmetry arise in the cross section. They are proportional to the non-diagonal elements of the photon density matrix ρ^{+-}, ρ^{+0}.

As above, taking into account the contributions of the transverse photons only, and neglecting the q^2-dependence, we come to the equation of EPA with just the same spectrum, $dn(\omega, q^2)$, as in (6.16):

$$d\sigma_{ep} = \left[\frac{d\sigma_\gamma}{d^3k_1} + \tfrac{1}{2}\,\xi\cos 2\varphi\,\frac{d(\sigma_\parallel - \sigma_\perp)}{d^3k_1}\right] d^3k_1\, dn(\omega, q^2)\,\frac{d\varphi}{2\pi}. \tag{6.21a}$$

Here φ is the (azimuthal) angle between the planes of electron scattering and k_1 production in the γp c.m.s. (i.e. between the planes (p, p') and (k_1, q)), and ξ is the photon polarization:

$$\xi = \frac{|\rho^{+-}|}{\rho^{++}} = 1 - \frac{1}{\rho^{++}}; \qquad \cos\varphi \approx \frac{p'_\perp k_{1\perp}}{|p'_\perp| \cdot |k_{1\perp}|}. \tag{6.22}$$

Finally, $\sigma_\parallel$ and $\sigma_\perp$ are the absorption cross sections for a transversely polarized photon either in the (k_1, q) plane $(\sigma_\parallel)$ or orthogonal to it $(\sigma_\perp)$ $(d\sigma_\gamma = \frac{1}{2}d(\sigma_\parallel + \sigma_\perp))$. In the helicity representation the quantity $d(\sigma_\parallel - \sigma_\perp)$ is due to the interference of the γp amplitudes for right-handed and left-handed polarized photons $(d(\sigma_\parallel - \sigma_\perp) \propto -2M^*_+M_-)$.

When writing the approximate expression (6.21a) the largest among the neglected terms of the type $M^*_0M_+$ are due to the interference of scattering amplitudes for scalar and transverse photons. By analogy with (6.12), these terms decrease as $\sqrt{-q^2}$ as $q^2 \to 0$. Generally speaking the $\tilde{\Lambda}_\gamma^2$ scale of the q^2-dependence of the differential cross sections differs also from Λ_γ^2. As a result, the EPA accuracy (6.21a) is

$$\eta \sim \sqrt{|q^2|}/\tilde{\Lambda}_\gamma. \tag{6.21b}$$

This accuracy is markedly worse than that found for the total cross section (6.16d). After azimuthal integration (over φ) the term connected with an interference of scalar and transverse photons disappears. Then corrections to (6.21) proportional to $\sqrt{-q^2}$ are lost and an accuracy of the type (6.16) $\eta \sim q^2/\Lambda_\gamma^2$ is restored.

6.7. *Features of EPA in the two-photon case. Some widely spread errors and inaccuracies*

Many problems on the two-photon production are solved by means of EPA. Using this approximation has permitted to obtain (in sections 4 and 5) a number of useful distributions in a comparatively simple form*. The derivation of EPA given in section 5 was performed using the same procedure as done above in sections 6.2–6.6. In this sub-section we shall only show some features specific to the two-photon case in comparison with the one-photon one.

1. The exact relationship (6.8) expressed $d\sigma_{ep}$ in terms of the photoabsorption cross sections σ_T and σ_S. It was the starting point while constructing EPA in the one-photon case. For $|q^2| < \Lambda_\gamma^2$ we neglected the contribution from scalar photons and substituted σ_T by its on-shell value σ_γ, rewriting the cross section in the form

$$d\sigma_{ep} \propto \rho^{++}\sigma_\gamma \frac{d^3p'}{E'} \propto \sigma_\gamma\, dn(\omega, q^2). \tag{6.22a}$$

This relation is, in fact, the essence of EPA in the one-photon case.

In the two-photon case we have transformed the exact relation (5.12) in the same manner to the form (5.16) for $|q_i^2| < \Lambda_\gamma^2$:

$$d\sigma_{ee} \propto \rho_1^{++}\rho_2^{++}(\sigma_{\gamma\gamma} + \tfrac{1}{2}\xi_1\xi_2\tau_{\gamma\gamma}\cos 2\tilde{\varphi})\, d^3p_1'\, d^3p_2'/E_1'E_2'. \tag{6.22b}$$

(Let us remind that Λ_γ^2 is a characteristic scale for the q^2-dependence of the $\gamma\gamma$ scattering cross sections and ξ_i stands for the ith photon polarization.)

One would think that the equation (6.22b) is directly transformed into the simple EPA-relation (5.19):

$$d\sigma_{ee} = [\sigma_{\gamma\gamma} + \tfrac{1}{2}\xi_1\xi_2\tau_{\gamma\gamma}\cos 2\varphi]\, dn(\omega_1, q_1^2)dn(\omega_2, q_2^2)d\varphi/2\pi \tag{6.23a}$$

(φ is the angle between the scattering planes of the electrons).

However, the real situation is not such a simple one. It is essential that the quantity ρ_1^{++} (5.13) in (6.22b) depends not only on the momentum of the "own" photon q_1, but also on the momentum of the "strange" photon q_2. Therefore, equation (6.22b) does not directly reduce to (6.23a). However, such a reduction turns out to be possible when $|q_i^2| \ll W^2$. Indeed, the quantity $\rho_1^{++} - 2m^2/q_1^2$ (5.13) depends only on $(q_1q_2)/(p_1p_2)$ and $q_1^2q_2^2/W^4$. It is easy to show that at $|q_i^2| < W^2$ with an accuracy not worse than q_i^2/W^2 the quantity $(q_1q_2)/(p_1q_2) = (q_1p_2)/(p_1p_2)$. Therefore, in this region the q_2-dependence of ρ_1^{++} is inessential.

*Let us list some results obtained by means of EPA. In section 5 we obtained the next distributions: for the total four-momentum of the produced system (section 5.4), over the momenta of the secondaries (5.38, 5.45, 5.47) and over the noncoplanarity angle ψ in a particle pair production (5.46). A number of estimations of observable quantities for various experimental set-ups are obtained in section 4.3. By means of EPA also the estimations from below for the $pp \to ppe^+e^-$ [24] and $ee \to ee\mu^+\mu^-$ [179] processes were obtained.

As a rule, the condition $|q_i^2| \ll W^2$ is not an extra limitation, since the *dynamical cut off* ($|q_i^2| \sim \Lambda_\gamma^2$) appears earlier, i.e. $\Lambda_\gamma \lesssim W$. However, even if the dynamical cut-off is absent, i.e. $\Lambda_\gamma > W$, the description by means of (6.23a) turns out to be usually valid due to *the kinematical cut-off at* $|q_i^2| \sim W^2$ (the quick decrease of the quantities ρ_i^{++} at $|q_i^2| > W^2$). Thus, the region for EPA validity is determined by the conditions

$$|q_i^2| < W^2, \qquad |q_i^2| < \Lambda_\gamma^2. \tag{6.23b}$$

It is necessary to emphasize that the kinematical cut-off met in the two-photon case is essentially different from that met in the one-photon case (6.14), where the similar cut-off appears at $|q_i^2| \sim \omega^2$. Moreover, unlike what occurs in the one-photon case, the restriction $|q_i^2| < W^2$ is necessary in the two-photon case to write EPA in the factorizable form (6.23a).

2. Let us describe the *relation between spectra in the one-photon and two-photon cases.* The quantity ρ^{++} (6.9) in (6.22a) depends on the momenta of the electron p, the photon q and the proton (target) P. For the quantities ρ^{ab} going to the two-photon case (6.22b) implies only a substitution in the target (proton → photon). In particular, ρ_1^{++} (5.13) can be obtained through (6.9) by means of the substitution $p \to p_1$, $q \to q_1$, $P \to q_2$. As it was said above for $|q_1^2| < W^2$ the q_2-dependence of ρ_1^{++} is substituted by its p_2-dependence. Therefore, it is natural, that the spectra (5.18) obtained here have the same form as the spectrum (6.16a) obtained in the one-photon case when it was obtained under the restriction $|q^2| < \omega^2$.

3. In order to describe distributions integrated over q_i^2 it is sufficient to integrate (6.23) over the domain (6.23b). The contribution of the region, where $|q_i^2| > W^2$ or $|q_i^2| > \Lambda_\gamma^2$, is negligibly small because of the decreasing value of σ_{ab} for $|q_i^2| > \Lambda_\gamma^2$ (the dynamical cut-off) and of ρ_i^{++} for $|q_i^2| > W^2$ (the kinematical cut-off). As a result, the spectra (5.23) are obtained. The leading approximation for them can be written in the form

$$\mathrm{d}n(\omega_i) = \frac{\alpha}{\pi} \frac{\mathrm{d}\omega_i}{\omega_i} \left(1 - \frac{\omega_i}{E} + \frac{\omega_i^2}{2E^2}\right) \ln \frac{E^2 q_{i\,\max}^2}{\omega_i^2 m_e^2}. \tag{6.24}$$

Here $q_{\max}^2$ either coincides with Λ_γ^2 or W^2 (if $\Lambda_\gamma > W$), or $q_{\max}^2$ is determined by the experimental limitations.

4. In a number of papers, the description of the two-photon production is done with spectra which are very different from (5.23). They can not be obtained from exact formulas for the two-photon production. As a rule, the genesis of these errors may be connected with the incorrect choice of cut-off. This is simply demonstrated in the leading approximation, where all spectra have the same form as (6.24) but the values of $q_{i\,\max}^2$ differ from exact ones. The kinematical and dynamical cuts-off Λ_{kin}^2 and Λ_{dyn}^2, which are actually used by various authors are listed in table 6.

a) There is a widely spread mistake which consists in using for a two-photon case the same spectrum (6.19d) as the one obtained in the one-photon case, with no dynamical cut-off taken into account (cf. [119, 3, 5, 14]). This corresponds to a kinematical cut-off at $|q_i^2| \sim \omega_i^2$. At present energies using this spectrum do not lead to large numerical errors in calculations of the two-photon hadron production since here $\omega_i \sim W \sim \Lambda_\gamma$. For example, the exact expression for

Table 6
The upper limits of integration over $|q_i^2|$ which are used actually while obtaining the spectra.

References	a) [119, 3, 5, 14]	b) [170]	c) [194]	d) [192]	correct
kinematical cut-off Λ^2_{kin}	ω_i^2	W^2	ω_i^2	–	W^2
dynamical cut-off Λ^2_{dyn}	–	–	Λ^2_γ	–	Λ^2_γ

the cross section

$$d\sigma_{ee\to eeh}/dW^2 \propto \left(\ln\frac{sq^2_{max}}{W^2m_e^2} - 1\right)^2 f\left(\frac{s}{W^2}\right) - \frac{1}{3}\left(\ln\frac{s}{W^2}\right)^3$$

(4.12) is replaced by $(\ln(s/m_e^2) - 1)^2 f(s/W^2)$ when calculating by means of (6.19d). At $q^2_{max} \sim W^2$ and $\ln(s/W^2) \ll \ln(s/m_e^2)$ the numerical difference between these two expressions is small. However, such a replacement leads to the wrong functional s-dependence, e.g., the high energy value of $d\sigma/dW^2$ or the total cross section for the processes $ee \to eee^+e^-$, $ee \to ee\mu^+\mu^-$ – etc., which one calculated by means of the spectrum (6.19d), are $\frac{3}{2}$ times larger than the correct (1.2)*. Another illustration is the graphs of the $ee \to ee\pi^0$, $ee \to ee\eta$ cross sections which are given in [50, 14]. In these graphs the difference between the exact results and that obtained by means of the spectrum (6.19d) increases with the E growth. (Let us remind that the EPA accuracy is improved when the E increases.) An erroneous distribution in the limiting value for the angle $\theta_m(\theta_i < \theta_m)$ of the electron recording [115, 14] is also due to the use of a wrong kinematical cut off. (The correct distribution is given in section 4.3.)

b) The significance of a correct kinematical cut-off has been emphasized in ref. [170]. The relations given in [170] are directly applicable to lepton pair production with $W \sim m_l$, when $\Lambda_\gamma \sim W$. However, using these formulas for the description of hadron production (e.g. $ee \to eeh$), where $\Lambda_\gamma < W$, will lead to a noticeable error in the asymptotic of the total cross-section.

c) The kinematical cut off at $|q^2| \sim \omega_i^2$ occurs in ref. [194] as a result of an inaccurate use of the requirement of Lorentz-invariance of the spectrum. The resulting conclusion [194] made on the inapplicability of EPA for the description of $d\sigma/dW^2$ and total cross sections is also wrong.

d) The spectrum used in ref. [192] corresponds to the integration of the expression for dq^2/q^2 over the whole kinematically allowed domain (6.11) (one-photon case). Let us note that in ref. [192] a wrong result is observed too with using own version of the Cheng and Wu technique.

5. The distribution (6.23) has an azimuthal asymmetry (the term $\xi_1\xi_2\tau_{\gamma\gamma}\cos 2\varphi$), which is due to the virtual photon polarization. Thus, in the two-photon case, the observable cross-section is not expressed in term of the non-polarized photon scattering cross section $\sigma_{\gamma\gamma}$ only. This property is also present in the distribution for the total transverse momentum $k_\perp$ of the produced system (5.32).

Recently, attention on this fact was drawn by Cheng and Wu [18]. They interpreted it as an indication of EPA inapplicability in the two-photon case. From our point of view the question is only concerned with inapplicability of the EPA formulation when proper account of the virtual

*Exact results for the e^+e^- and $\mu^+\mu^-$-production cross sections are collected in appendix F. They coincide asymptotically with the result of EPA (1.2).

photon polarization is not taken in solving such problems. Such a restrictive interpretation of EPA is not due to essence of approximation scheme. Let us emphasize, that the virtual photon polarization in the one-photon case also results an essential effect on the momentum distribution of the produced particle momenta (6.21). A similar EPA modification has already been given in refs. [185, 195]. In particular, as is shown in section 5.5, results of Cheng and Wu [18] can indeed be obtained by means of EPA.

6. In conclusion, let us pay attention to one more specific possibility of using the EPA technique. For two-photon production EPA corresponds to a picture, according to which virtual photons almost move along the collision axis. Therefore, e.g. in the case of an A_1A_2 pair production considered in the c.m.s. of the colliding particles $p_1 + p_2 = 0$, the momenta of A_1 and A_2 and the momentum $p_1 = -p_2$ are coplanar. It may seem from here that EPA does not permit to obtain the distribution in agle ψ which measures the deviation from coplanarity. However, this opinion (see e.g. [50, 14]) is wrong.

Actually, the use of spectra taking proper account of the q_i^2 dependence (5.18) corresponds to taking the photon transverse motion in the range $q_{i\perp}^2 < \Lambda_\gamma^2$, ($q_{i\perp}^2 \approx -q_i^2(1 - \omega_i/E)$) in EPA. With due regard of this dependence, EPA allows to obtain the distribution $d\sigma/d\psi$ (5.46) for particle pair production as well as for distributions in the total transverse momentum $k_\perp$ (5.31) (at $k_\perp^2 < \Lambda_\gamma^2$) and other similar distributions.

6.8. *An example of EPA inapplicability. The two-photon production of massive lepton pairs*

The possibility of using EPA for particular processes was linked to a specific form for the q^2-dependence of the virtual photoprocess cross section (6.13) (cf. (5.21)). We, however, know a few cases, where this dependence is of different form and, as a result, EPA is not applicable. These cases are bremsstrahlung particle production (fig. 27) [173b], $\nu\bar{\nu}$-pair production in ee collision (fig. 37) [196], and the two-photon production of a lepton pair with large effective mass* [180].

Let us consider the last case. Using the exact $\gamma\gamma \to l^+l^-$ (here $l \equiv e, \mu$) cross-sections (E.1) it is easy to obtain, that for $W^2 \gg m_l^2$ an essential (power) decrease of σ_{TT} occurs only for $|q_i^2| \gtrsim W^2$. For $|q_i^2| < W^2$, the quantities σ_{TS}, σ_{ST}, σ_{SS} are negligibly small in comparison with σ_{TT}, but in σ_{TT}, the q^2-dependence is essential in the large domain $W^2m_l^2 < q_1^2q_2^2 < W^4$ (here however σ_{TT} decreases only logarithmically):

$$\sigma_{TT} = \sigma_{\gamma\gamma}\left\{1 - \frac{\ln(1+a) + a(1+a)^{-1}}{\ln(W^2/m_l^2) - 1} + O\left(\frac{q^2}{W^2}\right)\right\};$$

$$a = (m_l^2 - q_1^2)(m_l^2 - q_2^2)(m_lW)^{-2}; \qquad \sigma_{\gamma\gamma} = \frac{4\pi\alpha^2}{W^2}\left(\ln\frac{W^2}{m_l^2} - 1\right); \tag{6.25}$$

$$\sigma_{TS}, \sigma_{ST}, \sigma_{SS} \lesssim (|q_i^2|/W^2)\sigma_{\gamma\gamma}; \qquad \tau_{TT} \lesssim (q_1^2q_2^2/W^4)\sigma_{\gamma\gamma}.$$

At the same time, the contribution from the domain $W^2m_l^2 < q_1^2q_2^2 < W^4$ is not small. Therefore, for $\ln(W^2/m_l^2) \gtrsim \ln(p_1p_2/m_1m_2)$ one should use the more complicated formula (σ_{TT} from (6.25))

*The total cross section for lepton production is exactly calculated by EPA since the main contribution in that case comes from the domain $W \sim m_l$, where the inequalities (5.21) are correct.

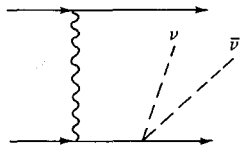

Fig. 37.

$$d\sigma = \left(\frac{\alpha}{2\pi}\right)^2 \frac{\omega_1\omega_2}{E^4} d\omega_1 d\omega_2 \int \frac{dq_1^2\, dq_2^2}{q_1^2 q_2^2} \rho_1^{++}\rho_2^{++}\sigma_{TT}(W^2, q_1^2, q_2^2) \tag{6.26}$$

instead of (5.26).

The situation is simplified for massive lepton pair production in hadron collisions for $m_l W \gg m_\rho^2$. In this case the integrals are actually cut off at $|q_i^2| \sim \frac{1}{4}m_\rho^2$ because of form factors, and $|\sigma_{TT}(W^2, q_1^2, q_2^2) - \sigma_{TT}(W^2, 0, 0)| \lesssim (m_\rho^2/4Wm_l)\sigma_{\gamma\gamma}$. For that reason, EPA (5.26) turns out to be correct. In this case the cross section $d\sigma/dW^2$ is expressed through a single new scaling function $J(s/W^2)$ [34] (see table 7)

$$d\sigma_{pp\to pp\mu^+\mu^-}/dW^2 = (2\alpha/\pi)^2 J(s/W^2)\, \sigma_{\gamma\gamma\to\mu^+\mu^-}(W^2)/W^2. \tag{6.27a}$$

When calculating the function J in terms of the spectrum (D.7) (taking form factors into account), the inaccuracy of the approximation (6.27a) is

$$\eta \sim \left(\frac{m_\rho^2}{4Wm_\mu}\right)^2 \left(\ln\frac{s}{W^2}\right)^{-1}. \tag{6.27b}$$

The W^2-dependence of the contribution (6.27a) is plotted in fig. 8 for $s = 2500\ \text{GeV}^2$. Other contributions to the cross section of the observable process $pp \to \mu^+\mu^- + \ldots$ are discussed at the end of sub-section 2.1.

Table 7

s/W^2	20	25	31	51	70	100	280	625	2500	10^4
$J(s/W^2)$	0.2	0.29	0.42	0.88	1.3	2	5.3	10	24.6	49

Appendices

A. Some kinematical relations

Let us consider the collision of two particles with momenta q and p. We introduce a metric tensor $R^{\mu\nu}(q, p)$ in a subspace orthogonal to the four-vectors q and p (cf. (5.3))

$$R^{\mu\nu}(q, p) = -g^{\mu\nu} + \frac{(qp)(q^\mu p^\nu + q^\nu p^\mu) - q^2 p^\mu p^\nu - p^2 q^\mu q^\mu}{(qp)^2 - q^2 p^2}. \tag{A.1}$$

For any arbitrary vector r, one can define a component orthogonal to q and p: $r_\perp^\mu = -R^{\mu\nu}(q, p)r^\nu$.

The scalar product of the corresponding orthogonal parts $r_\perp$ and $f_\perp$ of two arbitrary vectors r and f can then be written in the form:

$$(r_\perp f_\perp)\big|_{q,p} = -r^\mu R^{\mu\nu}(q, p) f^\nu = (r_\perp f)\big|_{q,p} = (r f_\perp)\big|_{q,p}; \quad r_\perp^\mu\big|_{q,p} = -R^{\mu\nu}(q, p) r^\nu. \tag{A.2}$$

In this review we wrote a number of relations for two-photon production, writing the momentum k_j of any produced particle in terms of its components in the c.m.s. of the colliding particles p_1 and p_2 (they are the energy ϵ_j, longitudinal momentum k_{jz} and the transverse momentum $k_{j\perp}$). Such relations are easy to transform to any frame, using the covariant form of these quantities (at $p_1^2 = p_2^2$)

$$\epsilon_j = \frac{k_j(p_1 \pm p_2)}{\sqrt{(p_1 + p_2)^2}}; \qquad k_{jz} = -\frac{k_j(p_1 - p_2)}{\sqrt{-(p_1 - p_2)^2}}; \qquad k_{j\perp}^\mu = -R^{\mu\nu}(p_1, p_2) k_j^\nu. \tag{A.3}$$

Finally, an angle $\tilde{\varphi}$ between the electron scattering planes in the photons c.m.s. is defined by the relations:

$$\cos\tilde{\varphi} = -\frac{\tilde{p}_{1\perp}\tilde{p}_{2\perp}}{\sqrt{\tilde{p}_{1\perp}^2 \tilde{p}_{2\perp}^2}}; \qquad \tilde{p}_{i\perp}^\mu = -R^{\mu\nu}(q_1, q_2) p_i^\nu \tag{A.4}$$

B. Some covariant relations for the polarization vectors of a virtual photon

Let us consider the collision of a space-like photon with momentum q ($q^2 < 0$) with any other particle (with momentum P). We shall denote the polarization vector of this photon by $e^\mu(a)$ in the c.m.s. ($a = 0$ refers to scalar (S) polarization and $a = \pm 1$ refers to the transverse (T) one). Obviously,

$$\begin{aligned} &q e(a) = 0; \qquad e^{*\mu}(a) e^\mu(b) = (-1)^a \delta_{ab}; \\ &\textstyle\sum_a (-1)^a e^{*\mu}(a) e^\nu(a) = g^{\mu\nu} - q^\mu q^\nu / q^2. \end{aligned} \tag{B.1}$$

Moreover, with the usual choice of transverse polarization vectors we have

$$e^*(\pm 1) = -e(\mp 1). \tag{B.2}$$

It is clear, that the transverse polarization vectors $e(\mp 1)$ in c.m.s. are orthogonal to $\boldsymbol{q} = -\boldsymbol{P}$ and have only space-like components. This means, that they form a basis for a subspace orthogonal to the four-vectors q and P, i.e. (cf. (A.1))

$$e^{*\mu}(+1)\, e^\nu(+1) + e^{*\mu}(-1)\, e^\nu(-1) = R^{\mu\nu}(q, P). \tag{B.3}$$

Similarly, the vector $e(0)$ is orthogonal to q and $e(\pm 1)$. Furthermore, an other unit vector $Q \propto P - q(qP)/q^2$ has similar properties. Therefore, these two vectors should be proportional to each other. In accordance with the normalization condition one may take

$$e(0) = iQ = i \sqrt{\frac{-q^2}{(qP)^2 - q^2 P^2}} \left[P - q\frac{(qP)}{q^2}\right]. \tag{B.4}$$

In this manner one can obtain

$$e^{*\mu}(\pm 1)\, e^{\nu}(\pm 1) = \tfrac{1}{2}\left[R^{\mu\nu}(q, P) \pm \mathrm{i}\frac{\epsilon^{\mu\nu\alpha\beta} q^{\alpha} P^{\beta}}{\sqrt{(qP)^2 - q^2 P^2}}\right]. \tag{B.5}$$

Let us note that the above relations for $e(a)$ are correct when one takes the polarization vectors in the c.m.s. in the form

$$e(\pm 1) = \mp\frac{1}{\sqrt{2}}(0, 1, \pm \mathrm{i}, 0); \qquad e(0) = \mathrm{i}Q = \frac{\mathrm{i}}{\sqrt{-q^2}}(|\boldsymbol{q}|, 0, 0, \omega). \tag{B.6}$$

C. Helicity amplitudes for forward $\gamma\gamma$-scattering

The $\gamma\gamma \to$ f helicity amplitudes M_{ab} are defined by the relation

$$M_{ab} = M^{\mu\nu} e_1^{\mu}(a) e_2^{\nu}(b). \tag{C.1}$$

Here the usual choice of polarization vectors $e_i(a)$ is assumed (cf. App. B, Q_i-vectors are defined in (5.4))

$$e_2(\pm 1) = e_1(\mp 1); \qquad e_i^{*}(\pm 1) = -e_i(\mp 1); \qquad e_1(0) = \mathrm{i}Q_1; \qquad e_2(0) = -\mathrm{i}Q_2. \tag{C.2}$$

In accordance with this the helicity amplitudes for the absorptive part of the $\gamma\gamma$-forward amplitude $W^{\mu'\nu',\mu\nu}$ which is connected with $M^{\mu\nu}$ by the relation (5.3) are defined by the relation:

$$W_{a'b',ab} = e_1^{*\mu'}(a')\, e_2^{*\nu'}(b')\, W^{\mu'\nu',\mu\nu} e_1^{\mu}(a)\, e_2^{\nu}(b). \tag{C.3}$$

Due to P- and T-invariance

$$W_{a'b',ab} = W_{-a'-b',-a-b} = W_{ab,a'b'}. \tag{C.4}$$

It follows from total helicity conservation for forward scattering and P- and T-invariance (C.4), that forward $\gamma\gamma$-scattering is described in terms of eight independent helicity amplitudes. We choose their simple linear combinations (5.8) as invariant amplitudes.

The polarization vector forms a complete orthonormal system (B.1). Therefore, it follows from (C.3), that

$$W^{\mu'\nu',\mu\nu} = \sum_{aba'b'} (-1)^{a+b+a'+b'} e_1^{\mu'}(a')\, e_2^{\nu'}(b')\, W_{a'b',ab} e_1^{*\mu}(a)\, e_2^{*\nu}(b). \tag{C.5}$$

Using (C.4) one can easily write the expansion coefficients $W^{\mu'\nu',\mu\nu}$ (C.5) in terms of the invariant amplitudes. They are sums of a small number of products of polarization 4-vectors. As a result we obtain the covariant expansion (5.7).

For instance, the coefficient determined for $W_{+0,+0} \equiv W_{\mathrm{TS}}$ is

$$R_{\mathrm{TS}}^{\mu'\nu',\mu\nu} = [e_1^{\mu'}(+1)\, e_1^{*\mu}(+1) + e_1^{\mu'}(-1)\, e_1^{*\mu}(-1)]\, e_2^{\nu'}(0) e_2^{*\nu}(0). \tag{C.6}$$

This may be written taking into account (B.3) and (C.2) in covariant form

$$R_{\mathrm{TS}}^{\mu'\nu',\mu\nu} = R^{\mu\mu'} Q_2^{\nu} Q_2^{\nu'}. \tag{C.7}$$

Similarly, the coefficient determined for $W_{++,00} \equiv W_{\mathrm{TS}}^{\tau} + W_{\mathrm{TS}}^{\mathrm{a}}$ is

$$[e_1^{\mu'}(+1)\, e_2^{\nu'}(+1) + e_1^{\mu'}(-1)\, e_2^{\nu'}(-1)]\, e_1^{*\mu}(0)\, e_2^{*\nu}(0) + (\mu\nu \leftrightarrow \mu'\nu').$$

By means of the equalities (C.2) we obtain

$$-[e_1^{\mu'}(+1)\, e_1^{*\nu'}(+1) + e_1^{\mu'}(-1)\, e_1^{*\nu'}(-1)]\, e_1^{*\mu}(0)\, e_2^{*\nu}(0) + (\mu\nu \leftrightarrow \mu'\nu') = -[R^{\mu'\nu'} Q_1^{\mu} Q_2^{\nu} + R^{\mu\nu} Q_1^{\mu'} Q_2^{\nu'}]. \tag{C.8}$$

The density-matrix elements (5.2) are defined in the helicity basis by the relation

$$\rho_i^{ab} = (-1)^{a+b} e_i^{\alpha}(a) \rho_i^{\alpha\beta} e_i^{*\beta}(b). \tag{C.9}$$

D. The photon density-matrix and spectra for various particles

Keeping in mind the processes, in which photons may be emitted by various particles, we shall give a generalized density-matrix of a virtual photon (5.2) in the case, when the initial and final particles are not polarized (a structure of this matrix is determined by gauge invariance conditions):

$$\rho_i^{\alpha\beta} = -\left(g^{\alpha\beta} - \frac{q_i^{\alpha} q_i^{\beta}}{q_i^2}\right) C_i(q_i^2) - \frac{(2p_i - q_i)^{\alpha}(2p_i - q_i)^{\beta}}{q_i^2} D_i(q_i^2). \tag{D.1}$$

The quantities C_i and D_i are given in table 8 for various particles.

Going from the representation (D.1) to the helicity basis can be done by means of (B.1–4), (C.2), (C.9). For example, for the two-photon process

$$\rho_i^{++} = \tfrac{1}{2} \rho_i^{\mu\nu} R^{\mu\nu} = C_i + 2D_i \frac{\tilde{p}_{i\perp}^2}{q_i^2}; \qquad \tilde{p}_{i\perp}^{\mu} = -R^{\mu\nu}(q_1, q_2) p_i^{\nu}; \tag{D.2}$$

$$\rho_i^{00} = -C_i - 4 \frac{D_i}{q_i^2} (p_i Q_i)^2 .$$

In the full form this density-matrix is (a', $a = 1, 0, -1$)

$$\rho_1^{a'a} = \begin{pmatrix} \rho_1^{++} & -\mathrm{i}|\rho_1^{+0}|\mathrm{e}^{\mathrm{i}\tilde{\varphi}_1}; & -|\rho_1^{+-}|\mathrm{e}^{2\mathrm{i}\tilde{\varphi}_1} \\ \mathrm{i}|\rho_1^{+0}|\mathrm{e}^{-\mathrm{i}\tilde{\varphi}_1}; & \rho_1^{00}; & -\mathrm{i}|\rho_1^{+0}|\mathrm{e}^{\mathrm{i}\tilde{\varphi}_1} \\ -|\rho_1^{+-}|\mathrm{e}^{-2\mathrm{i}\varphi} & \mathrm{i}|\rho_1^{+0}|\mathrm{e}^{-\mathrm{i}\tilde{\varphi}_1}; & \rho_1^{++} \end{pmatrix}; \tag{D.3}$$

$$|\rho_i^{+-}| = \rho_i^{++} - C_i; \qquad |\rho_i^{+0}| = \sqrt{|\rho_i^{+-}|(\rho_i^{00} + C_i)};$$

and $\tilde{\varphi}_i$ is the azimuthal angle of the vector p_i in the photon c.m.s.

In the same approximation as used for (5.18), the equivalent photon spectra have the form

$$\begin{aligned} \mathrm{d}n_i &= \frac{\alpha}{\pi} \frac{\mathrm{d}\omega_i}{\omega_i} \frac{\mathrm{d}(-q_i^2)}{|q_i^2|} \left[\left(1 - \frac{\omega_i}{E}\right) D_i + \frac{\omega_i^2}{2E^2} C_i - \left(1 - \frac{\omega_i}{E}\right) \left|\frac{q_{i\min}^2}{q_i^2}\right| D_i\right] \\ &= \frac{\alpha}{\pi} \frac{\mathrm{d}\omega_i}{\omega_i} \frac{\mathrm{d}(-q_i^2)}{|q_i^2|} \left[\left|\frac{q_{i\perp}^2}{q_i^2}\right| D_i + \frac{\omega_i^2}{2E^2} C_i\right]. \end{aligned} \tag{D.4}$$

In the dominant region $\omega_i \ll E$ the coefficient in front of C_i is small, and this term may often be

Table 8
Here G_E, G_M and F_π are the form factor of proton and pion. For the transition of hadron into jet (mass M), W_1 and W_2 are the usual structural functions of deep inelastic ep-scattering (3.11). For the nuclei with charge Ze the form factor $D(0) = Z^2$, $C(0) \sim 1$.

particle	C	D
pointlike spinless	0	1
lepton $l \equiv e, \mu$	1	1
π	0	F_π^2
p	$G_M^2(q^2)$	$\frac{4m_p^2 G_E^2 - q^2 G_M^2}{4m_p^2 - q^2}$
hadron → jet	$-\frac{2m}{q^2}\int W_1(M_1^2 q^2)\mathrm{d}M^2$	$\frac{1}{2m}\int W_2(M^2, q^2)\mathrm{d}M^2$
nuclei with charge Ze	$\sim \mu^2 F_M^2(q^2)$	$Z^2 F^2(q^2)$

neglected. This corresponds to neglecting a magnetic moment (spin). In this case the photon polarization is $\xi_i = 1$.

The spectrum $N(\omega_i)$ is obtained after integrating (D.4) over $-q_i^2$. In a number of cases $N(\omega_i)$ is easily calculated. So, for leptons ($C_i = D_i = 1$) $N(\omega_i)$ is calculated in (5.18).

For pointlike spinless particles $C_i = 0$, $D_i = 1$ and

$$\mathrm{d}n_i = N(\omega_i)\frac{\mathrm{d}\omega_i}{\omega_i}; \qquad N(\omega_i) = \frac{\alpha}{\pi}\left(1 - \frac{\omega_i}{E}\right)\left[\ln\frac{q_{i\max}^2}{q_{i\min}^2} - 1 + \frac{q_{i\min}^2}{q_{i\max}^2}\right]. \tag{D.5}$$

If one can neglect the q^2 dependence of the form factors, then (D.5) is also correct for pions and kaons. However, for protons $D(0) = 1$, $C(0) = G_M^2(0) = \mu_p^2 \approx 7.78$,

$$N(\omega_i) = \frac{\alpha}{\pi}\left[\left(1 - \frac{\omega_i}{E} + \mu_p^2\frac{\omega_i^2}{2E^2}\right)\ln\frac{q_{i\max}^2}{q_{i\min}^2} - \left(1 - \frac{\omega_i}{E}\right)\left(1 - \frac{q_{i\min}^2}{q_{i\max}^2}\right)\right]. \tag{D.6}$$

Finally we shall give the equivalent photon spectrum produced by proton taking into account the q^2-dependence of the form factors. In the usual dipole approximation for form factors we have $G_E = G_M/\mu_p = (1 - q^2/q_0^2)^{-2}$; $q_0^2 \approx 0.71\ \mathrm{GeV}^2$,

$$\mathrm{d}n(\omega_i) = \frac{\alpha}{\pi}\frac{\mathrm{d}\omega_i}{\omega_i}\left(1 - \frac{\omega_i}{E}\right)\left[\varphi_i\left(\frac{q_{i\max}^2}{q_0^2}\right) - \varphi_i\left(\frac{q_{i\min}^2}{q_0^2}\right)\right]; \tag{D.7}$$

$$\varphi_i(x) = (1+ay_i)\left[-\ln(1+x^{-1}) + \sum_{k=1}^{3}\frac{1}{k(1+x)^k}\right] - \frac{(1-b)y_i}{4x(1+x)^3} + c(1+\tfrac{1}{4}y_i)\left[\ln\frac{1+x-b}{1+x} + \sum_{k=1}^{3}\frac{b^k}{k(1+x)^k}\right];$$

$$y_i = \frac{\omega_i^2}{E(E-\omega_i)}, \quad a = \tfrac{1}{4}(1+\mu_p^2) + \frac{4m_p^2}{q_0^2} \approx 7.16; \quad b = 1 - \frac{4m_p^2}{q_0^2} \approx -3.96; \quad c = \frac{\mu_p^2 - 1}{b^4} \approx 0.028.$$

In conclusion, let us give the expressions for the spectrum of equivalent photons produced by an atom. For $q^2_{\min} \lesssim m_e^2\alpha^2 Z^{2/3}$ screening by atomic electrons becomes here essential. Then, according to [182]

$$dn = \frac{2Z^2\alpha}{\pi}\frac{d\omega}{\omega}\ln\frac{183}{Z^{1/3}}. \tag{D.8}$$

E. The $\gamma\gamma \to e^+e^-(\mu^+\mu^-)$ cross sections and the Born approximation for $\gamma\gamma \to \pi^+\pi^-$

Using the calculations [197] for $\gamma\gamma \to e^+e^-(\mu^+\mu^-)$ and taking into account the projection operators defined in (5.7) we obtain ($m \equiv m_{e,\mu}$)

$$\sigma_{TT} = \frac{\pi\alpha^2}{W^2x}\left\{(q_1q_2)L\left[2 + \frac{2m^2}{x} - \left(\frac{2m^2}{q_1q_2}\right)^2 + \frac{q_1^2+q_2^2}{x} + \frac{q_1^2q_2^2W^2}{2x(q_1q_2)^2} + \tfrac{3}{4}\left(\frac{q_1^2q_2^2}{x(q_1q_2)}\right)^2\right]\right.$$
$$\left. -\Delta t\left[1 + \frac{m^2}{x} + \frac{q_1^2+q_2^2}{x} + \frac{q_1^2q_2^2}{T} + \tfrac{3}{4}\frac{q_1^2q_2^2}{x^2}\right]\right\};$$

$$\sigma_{TS} = -\frac{\pi\alpha^2q_2^2}{W^2x^2}\left\{\Delta t\left[1 + \frac{q_1^2}{T}\left(6m^2 + q_1^2 + \tfrac{3}{2}\frac{q_1^2q_2^2}{x}\right)\right]\right.$$
$$\left. -\frac{L}{q_1q_2}\left[4m^2x + q_1^2(W^2+2m^2) + q_1^2\left(q_1^2 + q_2^2 + \tfrac{3}{2}\frac{q_1^2q_2^2}{x}\right)\right]\right\};$$

$$\sigma_{ST} = \sigma_{TS}(q_1^2 \leftrightarrow q_2^2);$$

$$\sigma_{SS} = \frac{\pi\alpha^2q_1^2q_2^2}{W^2x^3}\left\{\frac{L}{q_1q_2}(2W^2x + 3q_1^2q_2^2) - \Delta t\left(2 + \frac{q_1^2q_2^2}{T}\right)\right\}; \tag{E.1}$$

$$\tau_{TT} = -\frac{\pi\alpha^2}{4W^2x}\left\{\frac{2\Delta t}{x}\left[2m^2 + \frac{(q_1^2-q_2^2)^2}{W^2} + \tfrac{3}{2}\frac{q_1^2q_2^2}{x}\right]\right.$$
$$\left. +\frac{L}{q_1q_2}\left[16m^4 - 16m^2(q_1^2+q_2^2) - 4q_1^2q_2^2\left(2 + \frac{2m^2}{x} + \frac{q_1^2+q_2^2}{x} + \tfrac{3}{4}\frac{q_1^2q_2^2}{x^2}\right)\right]\right\};$$

$$\tau_{TS} = -\frac{\pi\alpha^2\sqrt{q_1^2q_2^2}}{W^2x^2}\left\{L\left(2m^2 + q_1^2 + q_2^2 + \tfrac{3}{2}\frac{q_1^2q_2^2}{x}\right) + \Delta t\left(2 - \tfrac{3}{2}\frac{q_1q_2}{x}\right)\right\};$$

$$\tau_{TT}^a = -\frac{\pi\alpha^2(q_1q_2)}{W^2x}\left\{2L\left(\frac{q_1q_2}{x} - 1\right) - \frac{\Delta t}{q_1q_2}\left(\frac{2q_1q_2}{x} - 1 - \frac{q_1^2q_2^2}{T}\right)\right\};$$

$$\tau_{TS}^a = \frac{\pi\alpha^2}{W^2x^2}(q_1^2q_2^2)^{3/2}(q_1q_2)^{-1}\left[L + \frac{(q_1q_2)\Delta t}{T}\right].$$

Here

$$W^2x = (q_1q_2)^2 - q_1^2q_2^2, \qquad \Delta t \equiv t_{\max} - t_{\min} = \sqrt{4x(W^2-4m^2)},$$

$$T = (m^2 - t_{max})(m^2 - t_{min}) = 4xm^2 + q_1^2 q_2^2,$$

$$L = \ln \frac{m^2 - t_{min}}{m^2 - t_{max}} = \ln \frac{(q_1 q_2 + \frac{1}{2}\Delta t)^2}{4xm^2 + q_1^2 q_2^2} \,. \tag{E.2}$$

In the case where one photon is real (e.g. $q_2^2 = 0$) it follows from (E.1) that

$$\sigma_{TT} = \frac{\pi\alpha^2}{(q_1 q_2)^3} \left\{ L[2(q_1 q_2)^2 + 2m^2 W^2 - 4m^4 + q_1^2 W^2] - \frac{\Delta t}{q_1 q_2} [(q_1 q_2)^2 + m^2 W^2 + q_1^2 W^2] \right\} ; \tag{E.3}$$

$$\sigma_{ST} = -\frac{\pi\alpha^2 q_1^2}{(q_1 q_2)^4} [W^2 \Delta t - 4m^2 (q_1 q_2) L] ;$$

$$\tau_{TT} = -\frac{\pi\alpha^2}{2(q_1 q_2)^4} [\Delta t(2m^2 W^2 + q_1^4) + 8m^2 (q_1 q_2)(m^2 - q_1^2) L] ;$$

$$\tau_{TT}^a = -\frac{\pi\alpha^2}{(q_1 q_2)^2} \left\{ 2[W^2 - (q_1 q_2)] L - \Delta t \left(\frac{2W^2}{q_1 q_2} - 1 \right) \right\} ;$$

here

$$\Delta t = (W^2 - q_1^2) \sqrt{1 - \frac{4m^2}{W^2}} ; \qquad L = 2\ln \left(\frac{W}{2m} + \sqrt{\frac{W^2}{4m^2} - 1} \right) ; \quad 2q_1 q_2 = W^2 - q_1^2 .$$

Finally, if both photons are real $q_1^2 = q_2^2 = 0$, only three non-zero quantities remain, namely

$$\sigma_{TT} = \frac{4\pi\alpha^2}{W^2} \left[\left(1 + \frac{4m^2}{W^2} - \frac{8m^4}{W^4} \right) L - \left(\frac{1}{W^2} + \frac{4m^2}{W^4} \right) \Delta t \right] \equiv \sigma_{\gamma\gamma}; \tag{E.4}$$

$$\tau_{TT} = -\frac{16\pi\alpha^2 m^2}{W^6} (\Delta t + 2m^2 L) \equiv \tau_{\gamma\gamma}; \qquad \tau_{TT}^a = -\frac{4\pi\alpha^2}{W^4} (W^2 L - 3\Delta t);$$

$$\Delta t = W^2 \sqrt{1 - \frac{4m^2}{W^2}} ; \qquad L = 2\ln \left(\frac{W}{2m} + \sqrt{\frac{W^2}{4m^2} - 1} \right).$$

We now give the expressions for the amplitudes in (5.38–48) written in terms of W^2 and $r^2 = (tu - m^4)/W^2$ in two important cases (see for example [166]).*

The lepton pair production ($m \equiv m_{e,\mu}$)

$$\tfrac{1}{2}(|M_{++}|^2 + |M_{+-}|^2) = 16\pi W^4 \frac{d\sigma_{\gamma\gamma}}{dt} = (4\pi\alpha)^2 \frac{2m^2(W^2 - 2m^2) + 2r^2(W^2 - 2r^2)}{(m^2 + r^2)^2} ;$$

*The quantity r^2 is the squared transverse momentum of the pion in the photons c.m.s. Its approximative expression in terms of measurable values has the form:

$$r^2 = \frac{tu - m^4}{W^2} = k_{1\perp}^2 - 2k_\perp k_{1\perp} \cdot \begin{cases} (\epsilon_1 - k_{1z})/(\epsilon - k_z) \text{ at } t = t_1^0 \\ (\epsilon_1 + k_{1z})/(\epsilon + k_z) \text{ at } t = t_2^0 \end{cases} ; \quad r^2 \mp k_{1\perp}^2 \text{ at } t \approx t_1^0 \approx t_2^0.$$

$$\mathrm{Re}(M^*_{-+}M_{++}) = -(4\pi\alpha)^2\,\frac{8m^2r^2}{(m^2+r^2)^2}\,; \qquad M^*_{-+}M_{+-} = -(4\pi\alpha)^2\,\frac{8r^4}{(m^2+r^2)^2}\,; \tag{E.5}$$

$$\mathrm{Re}\left(M^*_{-+}\,\frac{M_{0+}}{i\sqrt{-q_1^2}} + M^*_{--}\,\frac{M_{0-}}{i\sqrt{-q_1^2}}\right) = (4\pi\alpha)^2\,\frac{4\sqrt{2}\,r(t-u)(m^2-r^2)}{W^2(m^2+r^2)^2}\,.$$

The corresponding expression for *pion pair production in Born approximation* (pointlike pions) can be useful

$$M_{++} = M_{--} = \frac{8\pi\alpha m^2}{m^2+r^2}\,; \qquad M_{+-} = M_{-+} = \frac{8\pi\alpha r^2}{m^2+r^2}\,; \qquad \frac{M_{0+}}{i\sqrt{-q_1^2}} = -\frac{M_{0-}}{i\sqrt{-q_1^2}} = -\frac{4\sqrt{2}\pi\alpha r(t-u)}{W^2(m^2+r^2)}\,. \tag{E.6}$$

The total $\gamma\gamma \to \pi^+\pi^-$ cross section on the mass shell (in Born approximation) equals:

$$\sigma_{\gamma\gamma\to\pi^+\pi^-} = \frac{2\pi\alpha^2}{W^2}\left[\sqrt{1-\frac{4m^2}{W^2}}\left(1+\frac{4m^2}{W^2}\right) - \frac{4m^2}{W^2}\left(2-\frac{4m^2}{W^2}\right)\ln\left(\frac{W}{2m} + \sqrt{\frac{W^2}{4m^2}-1}\right)\right]. \tag{E.7}$$

F. The total cross section for the lepton pair electromagnetic production in the collision of charged particles

The cross section for e^+e^- pair production in the collision of fast charged particles (with a power accuracy) has the form

$$\sigma_{Z_1Z_2\to Z_1Z_2e^+e^-} = \frac{28(Z_1Z_2\alpha^2)^2}{27\pi m_e^2}\,(l^3 - Al^2 + Bl + C) + O(1/p_1p_2); \qquad l = \ln\frac{2(p_1p_2)}{m_1m_2}\,. \tag{F.1}$$

The coefficient A is the same for all the processes considered below

$$A = 178/28 \approx 6.36. \tag{F.2}$$

The coefficients B and C depend essentially on the nature of the collided particles.

Racah [12] has calculated the cross section for e^+e^- pair production in the collision of two heavy particles with charges Z_1e and Z_2e:

$$B = \tfrac{1}{28}(7\pi^2 + 370) \approx 15.7;$$

$$C = -\tfrac{1}{28}[348 + \tfrac{13}{2}\pi^2 - 21\zeta(3)] \approx -13.8; \qquad \zeta(3) \approx 1.202. \tag{F.3}$$

(The coefficients A and B have been calculated recently in [193, 198]. They turn out to coincide with (F.2–3).)

The cross sections for the processes $ep \to epe^+e^-$ and $ee \to eee^+e^-$ are calculated in refs. [193, 179] neglecting the contributions due to an interference between produced and scattered electrons*.

$$B \approx 2.6; \qquad C \approx 40 \quad \text{for} \quad ep \to epe^+e^-$$

$$B \approx -11; \qquad C \approx 100 \quad \text{for} \quad ee \to eee^+e^-. \tag{F.4}$$

*According to [199] these contributions change B and C weakly.

The cross section for the $\mu^+\mu^-$ pair production in ee or e^+e^- collisions has been calculated by Baier and Fadin [4, 193], Kuraev and Lipatov [179] (see also [205]):

$$\sigma_{e^\pm e^- \to e^\pm e^- \mu^+ \mu^-} = \frac{28\alpha^4}{27\pi m_\mu^2}(l^3 - Al^2 + Bl + C), \tag{F.5}$$

$$A = \tfrac{178}{28} \approx 6.36; \qquad B = -\tfrac{1}{28}[42l_\mu^2 + 196.4l_\mu + \tfrac{7}{75} + 21\pi^2 + 152] \approx -258,$$

$$C = \tfrac{1}{28}[14l_\mu^3 + 184.8l_\mu^2 + (1109 + \tfrac{31}{150} - 7\pi^2)l_\mu + (36 + \tfrac{7}{15})\pi^2 + \tfrac{51403}{18} - 189\zeta(3) - \tfrac{12748}{125}] \approx 1850;$$

$$l_\mu = \ln\frac{m_\mu^2}{m_e^2} \approx 10.7.$$

Let us note, for $\sqrt{s} < 1$ GeV the cross section (F.5) would be negative. This means that it is necessary also to take into account here the terms of order of s^{-1}. Therefore, at energies now achievable the estimation from below turns out to be more useful (see the end of sub-section 5.3). The significance of terms of the order of s^{-1} is discussed in detail in ref. [205].

Notes added in proof

1. (To sub-section 3.3). Recently A. Bodek et al. (SLAC-PUB-1442 (1974), submitted to Phys. Rev. Lett.) reported on "Observed deviations from scaling of the proton electromagnetic structure functions". This means that a short distance interaction is markedly complicated than it seems in the simplest variants of the parton model and with usual assumptions on the light cone current commutators. This conclusion is confirmed also by preliminary data on the annihilation $e^+e^- \to h$ [203].

2. (To sub-section 3.1). A possible role of both radiative corrections and two-photon production of hadrons in the SPEAR-type experiments is discussed in the paper of Ginzburg, Meledin and Serbo (Phys. Lett. in print). The corresponding corrections to the observed cross section are not too large but taking account of them can help in resolving the "energy crisis" which is now discussed by a number of authors (see e.g. Ellis's talk given at the London conference (1974)).

3. (To sub-section 3.1). G. Barbiellini et al. (Frascati preprint LNF-74/10(P) (1974)) reported on observation of single event for the $e^+e^- \to e^+e^-X^0(\eta')$ process. The value of $\Gamma_{\eta' \to \gamma\gamma} = 11^{+8}_{-6}$ keV or alternatively an upper limit $\Gamma_{\eta' \to \gamma\gamma} \leqslant 33$ keV with 95% confidence level is obtained.

4. (To sub-section 6.7). Recently Grammer and Kinoshita (preprint CLNS-201 (1974)) have compared the results of the exact calculation and those obtained by the two approximate methods called by them DEPA and WW. The first method (DEPA) corresponds to using a spectrum (6.19d), the second one (WW) is a simplified variant of DEPA; it is just WW used in refs. [119, 3, 5, 14].

It has appeared that for the reaction ee → ee $\mu^+\mu^-$ in transition from WW to DEPA an accuracy of approximation improves markedly (the error $\lesssim$ 10–15%). A description by DEPA turns out to be unsatisfactory only at very high energies ($\sqrt{s} > 100$ GeV). The causes of such discrepancy from the exact results are the same as for WW (cf. sub-section 6.7).

A similar comparison was also carried out for the reactions ee → eeX, where X = π^0, η, $\pi^+\pi^-$ – with neglecting the strong interactions of hadrons. It was concluded also that DEPA is here also a good approximation for now obtainable energies.

This last statement seems to us quite baseless, even if, first of all, accurate calculation is impossible here because the off mass shell behaviour of hadronic amplitudes (depending on photon

masses) is unknown. With the information available on these amplitudes the cross section of the given processes can be found only with logarithmic accuracy which is not high at present energies. This very accuracy is given by an equivalent photon approximation (EPA) discussed in section 6. At the same time the EPA provides a high (power) accuracy (cf. (4.11), (6.20)) for determining the cross sections with the corresponding (experimental) limitations on the electron scattering angles. Such an accuracy cannot be obtained by means of WW or DEPA.

References

[1] N. Arteaga-Romero, A. Jaccarini and P. Kessler, Compt. Rend. 269B (1969) 153, 1129;
A. Jaccarini et al., Lett. Nuovo Cim. 4 (1970) 933.
[2] V.E. Balakin, V.M. Budnev and I.F. Ginzburg, Zh. Eksp. Teor. Fiz. Pis'ma 11 (1970) 559 (JETP Lett. 11 (1970) 388).
[3] S.J. Brodsky, T. Kinoshita and H. Terazawa, Phys. Rev. Lett. 25 (1970) 972.
[4] V.N. Baier and V.S. Fadin, Lett. Nuovo Cim. 1 (1971) 481.
[5] S.J. Brodsky, T. Kinoshita and H. Terazawa, Phys. Rev. D4 (1971) 1532.
[6] L.D. Landau and E.M. Lifshitz, Sov. Phys. 6 (1934) 244.
[7] V.M. Budnev and I.F. Ginzburg, Phys. Lett. 37B (1971) 320.
[8a] Proc. VIII Int. Conf. on High Energy Acc., CERN, Geneva (1971).
[8b] G.I. Budker et al., Proc. III Sov. Symp. on Acc. of Charg. Particl. Moskow, Nauka, vol. 1 (1973) 318;
G.I. Budker et al., Proc. VIII Int. Conf. on Acc. of Charg. Particles, Erevan, vol. 2 (1970) 37.
[9] V.E. Balakin et al., Phys. Lett. 34B (1971) 663;
V.E. Balakin et al., Yad. Fiz. 16 (1972) 729.
[10] C. Bacci et al., Lett. Nuovo Cim. 3 (1972) 709.
[11] G. Barbiellini et al., Phys. Rev. Lett. 32 (1974) 385.
[12] G. Racah, Nuovo Cim. 14 (1937) 93.
[13] V.N. Baier et al., Phys. Lett. 49B (1974) 385.
[14] H. Terazawa, Rev. Mod. Phys. 45 (1973) 615.
[15] E.J. Williams, Kgl. Danske Vidensk. Selskab. Mat.-Fiz. Medd. 13 (1935) N4;
K.F. von Weizsäcker, Z. Physik 88 (1934) 612.
[16] N. Arteaga-Romero et al., Phys. Rev. D3 (1971) 1569, 2927;
J. Parisi and P. Kessler, Phys. Rev. D5 (1972) 2229. 2237.
[17] A.K. Slivkov and Sh.M. Shvarzman, Yad. Fiz. 16 (1972) 802.
[18] H. Cheng and T.T. Wu, Nucl. Phys. B32 (1971) 461; Phys. Lett. 36B (1971) 241.
[19] H.J. Bhabha, Proc. Roy. Soc. A 152 (1935) 559.
[20] V.G. Gorshkov, Usp. Fiz. Nauk 110 (1973) 45.
[21] S.R. Kelner, Yad. Fiz. 5 (1967) 1092;
S.R. Kelner and Yu.D. Kotov, Yad. Fiz. 7 (1968) 360.
[22] G. Khristiansen et al., Yad. Fiz. 15 (1972) 966.
[23] B.V. Geshkenbein and M.V. Terentjev, Phys. Lett. 37B (1971) 497; Yad. Fiz. 14 (1971) 1227.
[24] V.M. Budnev, I.F. Ginzburg, G.V. Meledin and V.G. Serbo, Phys. Lett. 39B (1972) 526; Nucl. Phys. 63B (1973) 519.
[25] M. Allen, G. Abrams et al., preprint SLAC-146 LBL-750 (1972).
[26] H. Alvensleben et al., Phys. Rev. Lett. 30 (1973) 328.
[27] P.J. Biggs et al., Phys. Rev. Lett. 27 (1971) 1157.
[28] V.F. Boldyshev and Yu.P. Peresunko, Yad. Fiz. 14 (1971) 1027; 19 (1974) 144.
[29] E.A. Vinokurov and E.A. Kuraev, Eksp. Teor. Fiz. 63 (1972) 1142.
[30] J.H. Christenson et al., Phys. Rev. Lett. 25 (1970) 1523.
[31] V.A. Matveev, R.M. Muradyan and A.N. Tavkhelidze, Particles and Nucleus, vol. 2 (1971) part 1.
[32] V.M. Budnev, I.F. Ginzburg, G.V. Meledin and V.G. Serbo, Zh. Eksp. Teor. Fiz. Pis'ma 12 (1970) 349 (JETP Lett. 12 (1970) 238).
[33] K. Fujikawa, Nuovo Cim. 12A (1972) 117.
[34] V.M. Budnev, I.F. Ginzburg, G.V. Meledin and V.G. Serbo, Particles and Nucleus, vol. 4 (1973) 239.
[35] M.S. Chen et al., Phys. Rev. D7 (1973) 3485.
[36] H. Cheng and T.T. Wu, Phys. Rev. D1 (1970) 3414.

[37] L.N. Lipatov and G.V. Frolov, Yad. Fiz. 13 (1971) 588 (Sov. J. Nucl. Phys. 13 (1971) 333).
[38] V.G. Serbo, Eksp. Teor. Fiz. Pis'ma 12 (1970) 50, 452 (JETP Lett. 12 (1970) 39).
[39] R.W. Brown et al., Phys. Rev. Lett. 28 (1972) 123.
[40] R.W. Brown et al., preprint BNL 18023 (1973).
[41] G.V. Meledin, V.G. Serbo and A.K. Slivkov, Zh. Eksp. Teor. Fiz. Pis'ma 13 (1971) 98 (JETP Lett. 13 (1971) 68).
[42] V.S. Fadin and V.A. Khoze, Zh. Eksp. Teor. Fiz. Pis'ma 17 (1973) 438.
[43] V.I. Strazhev and L.M. Tomilchik, Particles and Nucleus, vol. 4 (1973) 187.
[44] N. Cabibbo and E. Ferrari, Nuovo Cim. 23 (1962) 1147.
[45] M. Ruderman and D. Zwanziger, Phys. Rev. Lett. 22 (1969) 146.
[46] J.L. Newmeyer and J.S. Trefil, Nuovo Cim. 8A (1972) 703.
[47] M. Perl, preprint SLAC-1062 (1972).
[48] S.S. Gerstein, L.G. Landsberg and V.N. Folomeshkin, Yad. Fiz. 15 (1972) 345.
[49a] O.P. Sushkov, V.V. Flambaum and I.B. Khriplovich, Yad. Fiz., in print.
[49b] N.L. Ter-Isaakyan and V.A. Khoze, Zh. Eksp. Teor. Fiz. 62 (1972) 42.
[50] S.J. Brodsky, Proc. Int. Symp. on Electron and Photon Inter., Cornell, Ithaca (1971).
[51] J. Lefrancois, Proc. Int. Symp. on Electron and Photon Inter., Cornell, Ithaca (1971);
V.A. Sidorov, Proc. Int. Symp. on Electron and Photon Inter., Cornell, Ithaca (1971).
[52a] G. Barbarino et al., Lett. Nuovo Cim. 3 (1972) 689.
[52b] F. Ceradini et al., Phys. Lett. 43B (1973) 341.
[53] A. Bramon and M. Greco, Lett. Nuovo Cim. 3 (1972) 693.
[54] H.H. Bingham et al., Phys. Lett. 41B (1972) 635;
M. Davier et al., preprint SLAC-1205 (1973).
[55] V.L. Auslander et al., Yad. Fiz. 9 (1969) 114.
[56] D. Benaksas et al., Phys. Lett. 39B (1972) 289.
[57] V.E. Balakin et al., Phys. Lett. 41B (1972) 205.
[58] G. Barbiellini et al., Lett. Nuovo Cim. 6 (1973) 557.
[59] M. Bernardini et al., Phys. Lett. 46B (1973) 261.
[60] G.J. Gounaris and J.J. Sakurai, Phys. Rev. Lett. 21 (1968) 244.
[61] M. Castellano et al., Nuovo Cim. 14A (1973) 1.
[62] G. Cosme et al., Phys. Lett. 40B (1972) 685.
[63] L.M. Kurdadze et al., Phys. Lett. 42B (1972) 515.
[64] C. Bacci et al., Phys. Lett. 38B (1972) 551;
C. Bacci et al., Phys. Lett. 44B (1973) 533.
[65] F. Ceradini et al., Phys. Lett. 42B (1972) 501;
F. Ceradini et al., Phys. Lett. 47B (1974) 80.
[66] B. Bartoli et al., Phys. Rev. D6 (1972) 2374.
[67] A. Litke et al., Phys. Rev. Lett. 30 (1973) 1189;
G. Tarnopolsky et al., Phys. Rev. Lett. 32 (1974) 432.
[68] H. Strauch, Proc. Int. Symp. on Electron and Photon Inter., Bonn (1973);
M. Bernardini et al., Proc. Int. Symp. on Electron and Photon Inter., Cornell, Ithaca (1971).
[69] Particle data group, Review of Particle Properties, Rev. Mod. Phys. 45, No. 2 (1973).
[70] J.D. Bjorken, preprint SLAC-PUB 1318 (1973).
[71] R.P. Feynman, Phys. Rev. Lett. 23 (1969) 1415.
[72] V.N. Gribov and I.Ya. Pomeranchuk, Phys. Rev. Lett. 8 (1962) 343.
[73] K.A. Ispiryan and S.G. Matinyan, Zh. Eksp. Teor. Fiz. Pis'ma 7 (1968) 232.
[74] V.M. Budnev, I.F. Ginzburg and V.G. Serbo, Lett. Nuovo Cim. 7 (1973) 13.
[75] R.L. Anderson et al., Phys. Rev. Lett. 30 (1973) 149.
[76] G.M. Radutsky, Yad. Fiz. 8 (1968) 115;
B. Schrempp-Otto et al., Phys. Lett. 36B (1971) 463;
A. Bramon and M. Greco, Nuovo Cim. Lett. 2 (1971) 522.
[77] V.M. Budnev , V.L. Chernyak and I.F. Ginzburg, Nucl. Phys. B34 (1971) 470.
[78] E.D. Bloom et al., Phys. Rev. Lett. 23 (1969) 930;
M. Breidenbuch, Phys. Rev. Lett. 23 (1969) 935.
[79] K. Berkelman, Proc. XVI Int. Conf. on High Energy Phys., Batavia (1972).
[80] S.D. Drell, D.J. Levy and T.M. Yan, Phys. Rev. 187 (1969) 2159; D1 (1970) 1617.
[81] P.V. Landshoff and J.C. Polkinghorne, Phys. Reports 5 (1972) 1.
[82] J.D. Bjorken and E.A. Paschos, Phys. Rev. 185 (1969) 1975.

[83] H.A. Kastrup, Ann. Phys. 7 (1962) 383;
J. Wess, Nuovo Cim. 18 (1960) 1086.
[84] K. Wilson, Phys. Rev. 179 (1969) 1499.
[85] A.M. Polyakov, Zh. Eksp. Teor. Fiz. 59 (1970) 542; 60 (1971) 1572.
[86] R. Brandt, Phys. Rev. Lett. 23 (1969) 1260;
B.L. Ioffe, JETP Lett. 9 (1969) 97;
R. Jackiw, R. Van Royen and G. West, Phys. Rev. D2 (1970) 2473;
H. Leutwyler and J. Stern, Nucl. Phys. B20 (1970) 77.
[87] G. Altarelli and H. Rubinstein, Phys. Rev. 187 (1969) 2111.
[88] K. Wilson, Phys. Rev. D3 (1971) 1818.
[89] A.V. Efremov and I.F. Ginzburg, Fortschr. der Phys. B22, No. 9 (1974).
[90] J.D. Bjorken, Phys. Rev. 179 (1969) 1547.
[91] R. Brandt and G. Preparata, Nucl. Phys. B27 (1971) 541;
Y. Frishman, Phys. Rev. Lett. 25 (1970) 966.
[92] N.N. Bogolubov, V.S. Vladimirov and A.N. Tavkhelidze, TMF 12 (1972) 3, 305.
[93] A.V. Efremov and I.F. Ginzburg, Phys. Lett. 36B (1971) 371.
[94] J.D. Bjorken, Phys. Rev. 148 (1966) 1467.
[95] N. Cabibbo, G. Parisi and M. Testa, Lett. Nuovo Cim. 4 (1970) 35.
[96] V.N. Gribov, B.L. Ioffe and I.Ya. Pomeranchuk, Yad. Fiz. 6 (1967) 587.
[97] D.J. Gross and F. Wilczek, Phys. Rev. Lett. 30 (1973) 1343;
H.D. Politzer, Phys. Rev. Lett. 30 (1973) 1346.
[98] N.S. Craigie, A.B. Kraemmer and K.D. Rothe, preprint DESY 73/11 (1973).
[99] J.D. Bjorken and S.J. Brodsky, Phys. Rev. D1 (1970) 1416.
[100] E.V. Shuryak, Phys. Lett. 34B (1971) 509.
[101] V.N. Gribov and L.N. Lipatov, Phys. Lett. 37B (1971) 78; Yad. Fiz. 15 (1972) 781, 1218.
[102] R. Gatto, P. Menotti and I. Vendramin, Ann. Phys. N.Y. 79 (1973) 1.
[103] V.L. Chernyak, Yad. Fiz. 16 (1972) 778.
[104] H. Fritzsch and M. Gell-Mann, preprint CALT 68-297.
[105] D.J. Gross and S.B. Treiman, Phys. Rev. D4 (1971) 2105.
[106] H. Terazawa, Phys. Rev. D5 (1972) 2259.
[107] T.F. Walsh and P. Zerwas, Nucl. Phys. B41 (1972) 551.
[108] Z. Kunszt, Phys. Lett. 40B (1972) 220;
Z. Kunszt and V.M. Ter-Antonyan, Dubna preprint E2-6257 (1972).
[109] V.L. Chernyak and V.G. Serbo, preprint Tp-79 Inst. of Math., Novosibirsk (1973); Nucl. Phys. B71 (1974) 395.
[110] R.L. Kingsley, Nucl. Phys. B36 (1972) 575.
[111] T. Walsh, Phys. Rev. D7 (1973) 2152.
[112] Yu.M. Shabelsky, Yad. Fiz. 14 (1971) 388.
[113] L.I. Perlovsky and E.P. Heifez, Yad. Fiz. 15 (1972) 776 (Sov. J. Nucl. Phys. 15 (1972) 435).
[114] G. Preparata, preprint IC/72/151.
[115] S.J. Brodsky, T. Kinoshita and H. Terazawa, Phys. Rev. Lett. 27 (1971) 280;
T.F. Walsh, Phys. Lett. 36B (1971) 121.
[116] J.J. Sakurai and D. Schildknecht, Phys. Lett. 40B (1972) 121.
[117] A. Bramon, E. Etim and M. Greco, Phys. Lett. 41B (1972) 609.
[118] J.J. Sakurai, Phys. Lett. 46B (1973) 207.
[119] F.E. Low, Phys. Rev. 120 (1960) 582.
[120] V.M. Budnev and A.K. Slivkov, Zh. Eksp. Teor. Fiz. Pis'ma 12 (1970) 523.
[121] B. Renner, Nucl. Phys. B30 (1971) 634.
[122] R. Van-Royen and V.F. Weisskopf, Nuovo Cim. 50A (1967) 617;
B.M. Struminsky and A.N. Tavkhelidze, High Energy Phys. and Theory of Elem. Part. Kiev, Naukova Dumka (1967).
[123] A.N. Zaslavsky, V.I. Ogievetsky and W. Tybor, Yad. Fiz. 9 (1969) 852.
[124] G. Kramer, J.L. Uretsky and T.F. Walsh, Phys. Rev. D3 (1971) 719;
A.M. Altukhov and I.B. Khriplovich, Yad. Fiz. 14 (1971) 783.
[125] J. Layssac and F.M. Renard, Nuovo Cim. 10A (1972) 407.
[126] J.L. Rosner, preprint CERN-TH-1632.
[127] B.J. Read, preprint DESY 73/23.
[128] A. Pais and S.B. Treiman, Phys. Rev. Lett. 25 (1970) 975.
[129] M.V. Terentjev, Usp. Fiz. Nauk. 112 (1974) 37.
[130] M.V. Terentjev, Zh. Eksp. Teor. Fiz. Pis'ma 13 (1971) 446 (JETP Lett. 13 (1971) 318).

[131] T.M. Yan, Phys. Rev. D4 (1971) 3523.
[132] H. Terazawa, Phys. Rev. Lett. 26 (1971) 1207.
[133] S. Weinberg, Phys. Rev. Lett. 18 (1967) 507.
[134] S.L. Adler, Phys. Rev. 177 (1969) 2426.
[135] M.V. Terentjev, Zh. Eksp. Teor. Fiz. Pis'ma 14 (1971) 140 (JETP Lett. 14 (1971) 94).
[136] S.L. Adler et al., Phys. Rev. D4 (1971) 3497.
[137] J. Wess and B. Zumino, Phys. Lett. 37B (1971) 95;
T.F. Wong, Phys. Rev. Lett. 27 (1971) 1617;
Yu.P. Malakyan, Yad. Fiz. 16 (1972) 1035;
N.D. Hari Dass, Phys. Rev. D5 (1972) 1542.
[138] E.S. Abers and S. Fels, Phys. Rev. Lett. 26 (1971) 1512.
[139] R.J. Crewther, Phys. Rev. Lett. 28 (1972) 1421.
[140] J.M. Cornwall, Phys. Rev. Lett. 16 (1966) 1174;
D.J. Gross and S.B. Treiman, Phys. Rev. D4 (1971) 2105.
[141] S. Ferrara, A.F. Grillo and G. Parisi, Phys. Lett. 45B (1973) 63.
[142] D.V. Shirkov, V.V. Serebryakov and V.A. Meshcheryakov, Dispersion theories of strong interaction at low energy (North-Holland, 1969).
[143] C.E. Carlson and W.K. Tung, Phys. Rev. D6 (1972) 147; Phys. Rev. D4 (1971) 2873.
[144] V.M. Budnev, A.N. Vall and V.V. Serebryakov, Submit. to Yad. Fiz.
[145] R.L. Goble and J.L. Rosner, Phys. Rev. D5 (1972) 2345.
[146] D.H. Lyth, Nucl. Phys. B48 (1972) 537.
[147] P.S. Isaev and V.I. Khleskov, Yad. Fiz. 19 (1974) 121.
[148] P.S. Isaev and V.I. Khleskov, Yad. Fiz. 16 (1972) 1012.
[149] G. Schierholz and K. Sundermeyer, Nucl. Phys. B40 (1972) 125.
[150] Y. Fujii and M. Kato, Nuovo Cim. 13A (1973) 311;
P.K. Williams, Phys. Rev. D6 (1972) 3178.
[151] M. Alston-Garnjost et al., Phys. Lett. B36 (1971) 152.
[152] M.S. Chanowitz and J. Ellis, Phys. Rev. D7 (1973) 2490.
[153] S.M. Berman, J.D. Bjorken and J.B. Kogut, Phys. Rev. D4 (1971) 3388.
[154] P. Roy, Phys. Lett. 39B (1972) 365.
[155] A. Pais, Proc. Element. Particles Conf., Amsterdam (1972).
[156] L.A. Khalfin, Zh. Eksp. Teor. Fiz. Pis'ma 15 (1972) 548;
V.N. Baier, Zh. Eksp. Teor. Fiz. Pis'ma 17 (1973) 446.
[157] H. Terazawa, Phys. Rev. D7 (1973) 3123.
[158] B.L. Ioffe and V.A. Khoze, Yad. Fiz. 13 (1971) 381.
[159] R. Gatto and G. Preparata, Lett. Nuovo Cim. 7 (1973) 507.
[160] H. Primakoff, Phys. Rev. 81 (1951) 889;
A. Halprin et al., Phys. Rev. 152 (1966) 1295.
[161] F. Calogero and C. Zemach, Phys. Rev. 120 (1960) 1860.
[162] P.C. De Celles and J.F. Goehl, Phys. Rev. 184 (1969) 1617.
[163] V.M. Budnev and I.F. Ginzburg, preprint TP-55, Inst. Math., Novosibirsk, (1970); Yad. Fiz. 13 (1971) 353 (Sov. J. Nucl. Phys. 13 (1971) 198).
[164] E.A. Choban and V.M. Shekhter, Yad. Fiz. 14 (1971) 190 (Sov. J. Nucl. Phys. 14 (1971) 105).
[165] V.N. Baier and V.S. Fadin, Phys. Lett. 35B (1971) 156.
[166] V.L. Chernyak and V.G. Serbo, Nucl. Phys. B67 (1973) 464; Yad. Fiz. 19 (1974) 127; E 20 (1974) 232.
[167] S.J. Brodsky, Proc. XVI Int. Conf. on High Energy Phys., Batavia, vol. 2 (1972).
[168] R.W. Brown and I.J. Muzinich, Phys. Rev. D4 (1971) 1496.
[169] V.N. Baier and V.S. Fadin, Zh. Eksp. Teor. Fiz. 63 (1972) 761.
[170] G. Bonneau, M. Gourdin and F. Martin, Nucl. Phys. B54 (1973) 573.
[171] M. Pratap, J. Smith and Z.E.S. Uy, Phys. Rev. D5 (1972) 269;
A. Zee, Phys. Rev. D6 (1972) 900.
[172] V.N. Baier and V.A. Khoze, Zh. Eksp. Teor. Fiz. 48 (1965) 708.
[173a] E.A. Choban, Yad. Fiz. 13 (1971) 624.
[173b] A.M. Altukhov, Yad. Fiz. 14 (1971) 391 (Sov. J. Nucl. Phys. 14 (1971) 220).
[174] Z. Kunszt, R.M. Muradyan and V.M. Ter-Antonyan, preprint JINR E2-5424 Dubna (1970).
[175] M.J. Creutz and M.B. Einhorn, Phys. Rev. Lett. 24 (1970) 341; Phys. Rev. D1 (1970) 2537.
[176] A.I. Vainstein and I.B. Khriplovich, Yad. Fiz. 13 (1971) 198.

[177] J. Parisi, preprint PA 73.02 Paris (1973), Talk given at the Int. Coll. on Phot.-Phot. Coll. on Elect.-Posit. Stor. Rings.
[178] Z. Kunszt and V.M. Ter-Antonyan, Lett. Nuovo Cim. 4 (1972) 940.
[179] E.A. Kuraev and L.N. Lipatov, Yad. Fiz. 16 (1972) 1060.
[180] V.M. Budnev, I.F. Ginzburg, G.V. Meledin and V.G. Serbo, Yad. Fiz. 16 (1972) 362.
[181] V.N. Baier and V.S. Fadin, Yad. Fiz. 15 (1972) 95 (Sov. J. Nucl. Phys. 15 (1972) 56).
[182] A.I. Akhiezer and V.B. Berestetsky, Quantum Electrodynamics (Inter. Pub., 1965);
V.B. Berestetsky, E.M. Lifshitz and L.P. Pitaevsky, Relativistic Quantum Theory, Part I (Nauka, Moscow, 1968).
[183] H.A. Bethe and W. Heitler, Proc. Roy. Soc. A 146 (1934) 85.
[184] S.J. Brodsky, Proc. Int. Symp. on Electron and Photon Inter. at High Energy, Liverpool (1969).
[185] I.Ya. Pomeranchuk and I.M. Shmushkevich, Nucl. Phys. 23 (1961) 1295.
[186] N. Jurisic and L. Stodolsky. Phys. Rev. D3 (1971) 724.
[187] E. Fermi, Z.Physik 29 (1924) 315.
[188] G. Nordheim et al., Phys. Rev. 51 (1937) 1037.
[189] R.H. Dalitz and D.R. Yennie, Phys. Rev. 105 (1957) 1598;
R.B. Curtis, Phys. Rev. 104 (1956) 211;
D. Kessler and P. Kessler, Compt. Rend. 242 (1956) 3045.
[190] V.N. Gribov et al., Zh. Eksp. Teor. Fiz. 41 (1961) 1834.
[191] P. Kessler, Talk given at the Int. Coll. on Phot.-Phot. Coll. in Elect.-Posit. Stor. Rings, College de France (1973).
[192] M. Greco, Nuovo Cim. 4A (1971) 689.
[193] V.N. Baier and V.S Fadin, Zh. ETF 61 (1971) 476.
[194] C.J. Brown and D.H. Lyth, Nucl. Phys. B53 (1973) 323.
[195] M. Gourdin, Nuovo Cim. 21 (1961) 1094;
L.N. Hand, Phys. Rev. 129 (1963) 1834.
[196] O.P. Sushkov and V.V. Flambaum, Yad. Fiz. 18 (1973) 159.
[197] V.N. Baier, V.M. Katkov and V.S. Fadin, Relativistic electron radiation (Moscow, Atomizdat, 1973);
V.G. Zima, Yad. Fiz. 16 (1972) 1051.
[198] E.A. Kuraev and V.G. Lasurik-Elzufin, Zh. Eksp. Teor. Fiz. Pis'ma 13 (1971) 391.
[199] E.A. Kuraev, L.N. Lipatov and M.I. Strikman, Yad. Fiz. 18 (1973) 1270.
[200] I.F. Ginzburg, Zh. Eksp. Teor. Fiz. Pis'ma 19 (1974) 413.
[201] S. Orito et al., Phys. Lett. 48B (1974) 380.
[202] H. Terazawa, Phys. Rev. Lett. 32 (1974) 694; Phys. Rev. D9 (1974) 1134.
[203] B. Richter, talk given at the Chicago APS Meeting (1974).
[204] F. Cooper, G. Frye and E. Schonberg, Phys. Rev. Lett. 32 (1974) 862;
J. Baacke, Phys. Lett. 49B (1974) 279.
[205] G. Bonneau and F. Martin, Nucl. Phys. B68 (1974) 367.